OFFICIAL USE ONLY

UNCLASSIFIED

MASTER

ANL-5730

AEC Research and Development Report

[redacted]

MASTER

Argonne National Laboratory

CHEMICAL ENGINEERING DIVISION

SUMMARY REPORT

January, February, and March, 1957

[redacted]

[redacted]

[redacted] defined in [redacted] 1954. Its transmittal or the disclosure of its contents in any manner to an unauthorized [redacted]

DO NOT PHOTOSTAT

[redacted]

UNCLASSIFIED

OFFICIAL USE ONLY

DISCLAIMER

This report was prepared as an account of work sponsored by an agency of the United States Government. Neither the United States Government nor any agency Thereof, nor any of their employees, makes any warranty, express or implied, or assumes any legal liability or responsibility for the accuracy, completeness, or usefulness of any information, apparatus, product, or process disclosed, or represents that its use would not infringe privately owned rights. Reference herein to any specific commercial product, process, or service by trade name, trademark, manufacturer, or otherwise does not necessarily constitute or imply its endorsement, recommendation, or favoring by the United States Government or any agency thereof. The views and opinions of authors expressed herein do not necessarily state or reflect those of the United States Government or any agency thereof.

DISCLAIMER

Portions of this document may be illegible in electronic image products. Images are produced from the best available original document.

[redacted]

OFFICIAL USE ONLY

UNCLASSIFIED

ANL-5730

CHEMISTRY-SEPARATION PROCESSES FOR PLUTONIUM AND URANIUM

LEGAL NOTICE

This report was prepared as an account of Government sponsored work. Neither the United States, nor the Commission, nor any person acting on behalf of the Commission:

A. Makes any warranty or representation, express or implied, with respect to the accuracy, completeness, or usefulness of the information contained in this report, or that the use of any information, apparatus, method, or process disclosed in this report may not infringe privately owned rights; or

B. Assumes any liabilities with respect to the use of, or for damages resulting from the use of any information, apparatus, method, or process disclosed in this report.

As used in the above, "person acting on behalf of the Commission" includes any employee or contractor of the Commission to the extent that such employee or contractor prepares, handles or distributes, or provides access to, any information pursuant to his employment or contract with the Commission.

UNITED STATES ATOMIC ENERGY COMMISSION

CHEMICAL ENGINEERING DIVISION SUMMARY REPORT FOR JANUARY, FEBRUARY, AND MARCH 1957

Price $2.20

for Access Permission

Available from
Technical Information Service Extension
P. O. Box 1001, Oak Ridge, Tennessee

July 1957

Argonne National Laboratory
Lemont, Illinois

Classification cancelled (or changed to Official Use Only)
Division Declassification
by authority of Br. dtd July 7, 1958
by J. L. Ridenour TISOR, date 3-11-60

Technical Information Service Extension, Oak Ridge, Tenn.

RESTRICTED DATA

This document contains restricted data as defined in the Atomic Energy Act of 1954. Its transmittal or the disclosure of its contents in any manner to an unauthorized person is prohibited.

This document contains Confidential Restricted Data relating to civilian applications of atomic energy.

[redacted]

AEC RESEARCH AND DEVELOPMENT REPORT

UNCLASSIFIED

OFFICIAL USE ONLY

CLASSIFICATION CANCELLED
DATE 3/21/60
For The Atomic Energy Commission
H. R. Carnell
Chief, Declassification Branch

OFFICIAL USE ONLY

[redacted]

UNCLASSIFIED

ANL-5730
Chemistry-Separation Processes
for Plutonium and Uranium
M-3679 (20th Ed.)
This document consists of 132 pages.
No. 128 of 242 copies. Series A .

ARGONNE NATIONAL LABORATORY
P. O. Box 299
Lemont, Illinois

CHEMICAL ENGINEERING DIVISION
SUMMARY REPORT

January, February, and March, 1957

Stephen Lawroski, Division Director

W. A. Rodger, Associate Division Director
R. C. Vogel, Associate Division Director
V. H. Munnecke, Assistant Division Director

July 1957

Preceding Quarterly Reports:

ANL-5668	October, November, December, 1956
ANL-5633	July, August, September, 1956
ANL-5602	April, May, June, 1956

Operated by The University of Chicago
under
Contract W-31-109-eng-38

UNCLASSIFIED
OFFICIAL USE ONLY

[redacted]

[redacted]

ANL-5730
Chemistry-Separation Processes
for Plutonium and Uranium

Distribution	Copy No.
Argonne National Laboratory	1- 58
Aeroprojects, Inc.	59
Air Technical Intelligence Center	60
Alco Products, Inc.	61
Armed Forces Special Weapons Project, Sandia	62
Armed Forces Special Weapons Project, Washington	63
Atomic Energy Commission, Washington	64- 67
Atomics International	68- 69
Battelle Memorial Institute	70
Bettis Plant (WAPD)	71
Brookhaven National Laboratory	72- 73
Bureau of Ships	74
Chicago Operations Office	75
Chicago Patent Group	76
Combustion Engineering, Inc.	77
Dow Chemical Company (Rocky Flats)	78
duPont Company, Aiken	79- 82
duPont Company, Wilmington	83
General Electric Company, Richland	84- 95
Goodyear Atomic Corporation	96
Hanford Operations Office	97
Iowa State College	98
Knolls Atomic Power Laboratory	99
Los Alamos Scientific Laboratory	100-101
Mallinckrodt Chemical Works	102
Mound Laboratory	103
National Advisory Committee for Aeronautics, Cleveland	104
National Lead Company of Ohio	105
Naval Research Laboratory	106
New York Operations Office	107
Patent Branch, Washington	108
Patterson-Moos	109
Phillips Petroleum Company (NRTS)	110-113
The Fluor Corporation	114
Union Carbide Nuclear Company (C-31 Plant)	115
Union Carbide Nuclear Company (K-25 Plant)	116-118
Union Carbide Nuclear Company (ORNL)	119-122
University of California Radiation Laboratory, Berkeley	123-124
University of California Radiation Laboratory, Livermore	125-126
Vitro Engineering Division	127
Technical Information Service Extension (For Official AEC Use)	128-242
TOTAL	242

DO NOT PHOTOSTAT [redacted]

TABLE OF CONTENTS

		Page
SUMMARY		9
I.	FLUORIDE VOLATILIZATION SEPARATIONS PROCESS	14
	A. Laboratory Investigations	15
	B. Pilot Plant Operations	31
II.	FLUIDIZATION	37
	A. Crude Green Salt from Uranium Ore Concentrates	37
	B. Waste Calcination	55
III.	REACTOR CHEMISTRY	59
	A. Metal Oxidation and Ignition	59
	B. Determination of Alpha, The Ratio of Capture to Fission Cross Sections, in EBR-I	78
IV.	CHEMICAL-METALLURGICAL SEPARATION PROCESSES	83
	A. Laboratory Studies	85
	B. Semi-Works Studies of High Temperature Processes	100
V.	ANALYTICAL RESEARCH	128
	A. An X-ray Spectrometric Method for Determining Plutonium in Solution	128
	B. Ascending Paper Chromatographic Analysis of Irradiated Uranium and Thorium in a Hydrofluoric Acid Medium	129
VI.	ROUTINE OPERATIONS	132
	A. Waste Processing	132
	B. Gamma Irradiation Facility	132

LIST OF FIGURES

No.	Title	Page
1	Equipment for Fused Fluoride Dissolution Experiments . . .	20
2	Flowsheet for Processing Zr-U Fuels by Volatility Methods: Fused Salt Process	31
3	Equipment Used in Preliminary Semi-Works Fused Salt Dissolver Tests.	32
4	Concentrations of Uranium in Fused Salt Dissolution	34
5	Schematic of Experimental Shielded Waste Calciner.	56
6	Reaction Chamber of Waste Calciner.	57
7	Top of Waste Calciner	57
8	Bottom of Waste Calciner	57
9	Waste Calciner Operating Panelboard	57
10	Arrhenius Plot of First Stage Rate vs Inverse Temperatures at 800 mm Oxygen Pressure	62
11	Arrhenius Plot of Second Stage Rate vs Inverse Temperatures at 800 mm Oxygen Pressure	62
12	First Stage Oxidation of Uranium at 200 C in 200 mm Oxygen Pressure	65
13	Second Stage Oxidation of Uranium at 200 C in 200 mm Hg Oxygen Pressure	65
14	First Stage Oxidation of Uranium at 150 C in 200 mm Hg Oxygen Pressure	66
15	Second Stage Oxidation of Uranium at 150 C in 200 mm Hg Oxygen Pressure	66
16	Reaction of Zirconium with Oxygen	70
17	Reaction of Zirconium with Oxygen	71
18	The Zirconium-Oxygen Reaction-Variation of Reaction Rate Constant with Temperature	72

LIST OF FIGURES

No.	Title	Page
19	Photomicrograph of Zirconium Specimen After Reaction with Oxygen at 900 C for 418 minutes	74
20	Selected Literature Data on Reaction of Thorium with Oxygen	77
21	Selected Literature Data on Reaction of Thorium Metal in Air	77
22	Schematic Diagram of EBR-I Showing Sample Positions	80
23	Horizontal Fission Pattern of U^{233} at Midplane of EBR-I	80
24	Vertical Fission Patterns of U^{233} and U^{238} in Central Rod of EBR-I	81
25	Horizontal Fission Pattern of U^{238} at Midplane of EBR-I	81
26	Horizontal Capture Pattern of U^{238} at Midplane of EBR-I	82
27	Vertical Capture Pattern of U^{238} in Central Rod of EBR-I	82
28	Assembly for Melting and Casting Plutonium Alloys	85
29	Iodine-131 Disintegration Rate Versus Temperature of Quartz Discs	92
30	Distribution Ratio of Plutonium Between Uranium-Chromium (4.5 w/o) and Magnesium	97
31	Flow System for Metal Retention Study on Sorbent Bed	103
32	Preliminary Flowsheet for Processing Five Per Cent Drag-Out Fuel Material	107
33	Mutual Equilibrium Solubilities of Ruthenium and Uranium in The System Ruthenium-Uranium-Zinc	108
34	Mutual Equilibrium Solubilities of Uranium and Ruthenium in The System Ruthenium-Uranium-[Zinc-3 w/o Magnesium]	109
35	Cerium, Barium, and Uranium Solubility as Single Components in Zinc	111

031 005

LIST OF FIGURES

No.	Title	Page
36	Mutual Solubilities of Barium and Uranium in The System Barium-Uranium-Zinc	112
37	Mutual Solubilities of Cerium and Uranium in The System	113
38	Zinc Filtration Apparatus	114
39	Uranium Recovery from UZn_9	115
40	Production of UZn_9	115
41	Magnesium Corrosion Test: Section of Steel Tank Containing Magnesium	122
42	Magnesium Corrosion Test Sample Coupons-Side View	123
43	Apparatus Used for Testing Model W Electrolytic Water Analyzer	125
44	Chromatograms of One Day and One Week Old Uranium	130
45	Chromatograms of Chalk River Uranium Irradiated to Approximately Ten Per Cent Total Atom Burn-up and Cooled Three Years	131

LIST OF TABLES

No.	Title	Page
1	Non-Impingement Corrosion Tests Made With Nickel in HF Sparged Fused Fluorides at 600 C	17
2	Analyses of High Melting Material from Corrosion Tests	18
3	Dissolution of Zirconium in Fused Zirconium Fluoride-Sodium Fluoride with Hydrogen Fluoride	21
4	Dissolution of Zirconium in Fused Equimolar ZrF_4-NaF with Hydrogen Fluoride and Helium	23
5	Hydrogen Fluoride Reaction with Sodium Fluoride-Zirconium Fluoride Fused Salt at 600 C	24
6	Hydrogen Fluoride Reaction with Sodium Fluoride-Zirconium Fluoride at 600 C	25
7	Fluorination of Crude Uranium Tetrafluoride in a Fluidized Bed	26
8	Bulk Densities and Screen Analyses of the Crude Uranium Tetrafluorides Produced from Various Types of Ore Concentrates	27
9	Vapor Pressure of Vanadium Pentafluoride	30
10	Volatilization of Uranium in Fused Salt Dissolution	33
11	Overall Material Balance on Volatile Material in Uranium Dissolution	34
12	Dissolution of Zirconium-Uranium Alloy Plates in Fused Salt	35
13	Chemical Analyses of Ore Concentrates Studied in Green Salt Pilot Plant	38
14	Summary of Batch Fluid-Bed Conversion of Acid-Leach Ore Concentrate to Crude Green Salt	40
15	Operating Conditions for Green Salt Pilot Plant Runs on Uranium Ore Concentrates	42

001 007

LIST OF TABLES

No.	Title	Page
16	Effect of Reduction and Hydrofluorination on Particle Size and Density of Acid-Leach Concentrate	44
17	Composition of Crude Green Salt Product from Pilot Plant Runs on Acid-Leach Ore Concentrate	46
18	Composition of Crude Green Salt in Stages of Hydrofluorination Reactor	46
19	Summary of Minor Constituent Analyses on Acid-Leach Concentrate Before and After Treatment	47
20	Results of Batch Fluid-Bed Run of Carbonate-Leach Concentrate	49
21	Particle Size and Density of Carbonate-Leach Ore Concentrate Before and After Reduction and Hydrofluorination in Pilot Plant	51
22	Chemical Analyses on Product Pilot Plant Run on Carbonate-Leach Ore Concentrate	52
23	Results of Corrosion Tests in Pilot Plant Runs on Uranium Ore Concentrate	53
24	Oxidation of Uranium in 800 mm Oxygen Pressure	61
25	Activation Energies for the Oxidation of Uranium at 125 through 295 C in 20, 50, 200 and 800 mm Oxygen	63
26	Spectrographic Analysis of Dr. D. Cubicciotti's Uranium Bed	64
27	Comparison of Rod and Cube Oxidations in 200 mm Oxygen Pressure	67
28	Analysis of Zirconium	69
29	Cubic Rate Constants for the Reaction of Zirconium with Oxygen	70
30	Dependence of Reaction Rate on Sample Pretreatment at 700 C and 200 mm of Oxygen	73

LIST OF TABLES

No.	Title	Page
31	Kinetic Data for Reactions of Thorium in Air, Oxygen and Nitrogen	76
32	Corrosion of Thorium and a Thorium-Beryllium Alloy in Air at Various Temperatures	78
33	Melt Refining of Plutonium-Uranium Alloy	87
34	Effect of Inert Atmosphere on Dross Formation	88
35	Distribution of Iodine-131 in Melt Refining Experiment	91
36	The Solubility of Uranium Alloys in Magnesium	99
37	The Distribution of Fission Product Elements Between Magnesium and Uranium - 5 w/o Chromium	100
38	Cerium Removal in Magnesia Crucibles	101
39	Removal of Metal Vapor from Carrier Gas with Surface Active Materials	104
40	Successive Batch Extractions of Plutonium in Small Scale Batch Extraction Unit	117
41	Materials Tested as Sampling Tube	120
42	Corrosion Rate of Metal Samples in 950 C Magnesium	124
43	Calibration Tests on Model W Electrolytic Water Analyzer	126
44	Summary of the Behavior of Radioactive Nuclides with Hydrogen Fluoride and Hydrogen Fluoride-Methyl Ethyl Ketone Medium in Ascending Paper Chromatograms	129
45	Samples Irradiated During Period January-March, 1957	132

CHEMICAL ENGINEERING DIVISION

SUMMARY REPORT

For January, February, March, 1957

SUMMARY

I. Fluoride Volatilization Separations Process (pages 14 to 36)

A fused fluoride process for dissolution of zirconium-uranium fuel alloys is being developed. The alloy is dissolved in an equimolar sodium fluoride-zirconium fluoride melt at 600 C by sparging the system with hydrogen fluoride. The uranium is volatilized from the melt as the hexafluoride by a sparging operation with fluorine or bromine pentafluoride vapor. This product is then decontaminated and purified by fractional distillation.

Additional corrosion tests were conducted in an effort to find metals suitable for service as a dissolver in the fused fluoride process. Nickel was found to be susceptible to a sulfur-type attack. High melting solids also collected in the vessels. Hastelloy B appeared to show some promise as a structural material for the dissolver. Graphite has shown excellent chemical resistance; its principal limitation appears to be its lack of mechanical strength. Thermal cycling tests of graphite in contact with the salt did not result in any degradation of the graphite.

Studies of the dissolution rate of zirconium in sodium fluoride-zirconium fluoride melts indicate that the dissolution rate was not affected appreciably by the degree of impingement of the hydrogen fluoride sparge gas upon the zirconium sample. It was observed that a limited amount of dissolution occurs in the absence of hydrogen fluoride. Dilution of the hydrogen fluoride with helium did not affect the dissolution rate.

Studies were made of the production of uranium hexafluoride by fluorination in fluidized beds of uranium tetrafluoride produced by the reduction and hydrofluorination of ore concentrates. It was found that the uranium tetrafluoride from carbonate-leach ore concentrates might require the addition of an inert solid diluent for satisfactory fluidization during the fluorination.

Vanadium pentafluoride was prepared from the elements, and its melting point, vapor pressure and vapor density were measured.

Two preliminary dissolution and uranium recovery runs were made in the present semi-works scale fused salt process equipment for dissolution of fuel alloys using un-irradiated material. The first run made to

test the rate of volatilization of uranium (added as uranium tetrafluoride) from a sodium fluoride-zirconium fluoride melt by means of a bromine pentafluoride sparge showed that greater than 99 per cent of the uranium volatilized from the melt in the first 1 1/2 hr of sparging. The second run made to test the rate of dissolution of zirconium-uranium alloy plates in sodium fluoride-zirconium fluoride fused salt sparged with hydrogen fluoride showed 90 per cent of the 14-lb plate charge dissolved in 6 hr.

Design and construction of a test unit for studying the production of uranium hexafluoride from uranium tetrafluoride in a fluidized-bed reactor was begun.

II. Fluidization (pages 37 to 58)

A fluidized-bed technique has been applied to the conversion of uranyl nitrate to uranium tetrafluoride by calcination, reduction and hydrofluorination reactions. The technique has also been applied to the conversion of uranium trioxide (or uranium ore concentrates) to uranium tetrafluoride (green salt) in the multi-stage reduction and hydrofluorination reactors which form the Green Salt Pilot Plant.

Activities in the Green Salt Pilot Plant were directed toward the processing of uranium ore concentrates to crude uranium tetrafluoride. Two runs were made with acid-leach concentrate and one with carbonate-leach concentrate. Operability of the equipment was satisfactory, and excellent conversion of the uranium to green salt was obtained. Of the two types of ore concentrates tested, best results were obtained with the acid-leach material. The carbonate-leach concentrate showed a tendency to break up into fines during the reduction step, but this tendency was greatly reduced by drying the ore concentrate before hydrogen reduction. The presence of sodium fluoride in the hydrofluorinated carbonate-leach material considerably reduced its melting and sintering temperatures, and necessitated very careful start-up conditions to avoid caking.

Fluidization has been applied to the calcination of radioactive liquid wastes to solids in a shielded waste calciner.

Inactive shakedown runs were made to test the shielded waste calciner; one run using highly diluted (1 part ICPP IAW* solution to 1000 parts inactive aluminum nitrate solution) radioactive waste solution was successfully completed. A small amount of equipment installation remains to be done preparatory to operations at higher activity levels.

---

*ICPP IAW is liquid, first cycle aqueous waste from the Idaho Chemical Processing Plant.

III. Reactor Chemistry (pages 59 to 82)

The program to elucidate the factors governing the pyrophoric characteristics of uranium, zirconium, thorium and plutonium is being pursued by means of a study of the kinetics and mechanism of oxidation of these metals.

The base-line data for uranium oxidation have been completed. Oxidations were conducted at temperatures of 125 to 295 C in 20 to 800 mm oxygen pressures. Activation energies have been calculated from an Arrhenius equation and were found to be surprisingly pressure dependent. Work is in progress to determine the effect of low concentrations of certain alloying agents and contaminants. Direct observation of accelerated oxidations or ignitions has been initiated. The influence of gas concentrations and contaminants will be studied with the Stanton thermobalance.

The base-line runs for arc-melted Grade I crystal bar zirconium have been completed in the temperature range of 400 to 900 C in oxygen at 200 mm oxygen pressure. The zirconium oxidation seems to obey the cubic rate law $W^3 = kt$; an activation energy of 42.5 kcal/mole has been found on the basis of this rate law.

A literature survey of the oxidation of thorium has been completed. The disagreement of various investigators in observed rate laws, activation energies and in experimental rate constants is similar to the case for uranium.

A study of the variation of alpha as a function of position in EBR-I has been made for uranium-238 and uranium-233. The uranium-233 fission patterns are similar to those of uranium-235 and plutonium-239, as would be expected. The uranium-238 capture patterns have the same general shape as the capture patterns of the other nuclides.

IV. Chemical-Metallurgical Separations Processes (pages 83 to 127)

Pyrometallurgical methods of processing discharged reactor fuels are being developed. Melt refining processes have shown considerable promise for decontamination of metallic fuel elements.

The suitability of the Stokes furnace (described in ANL-5466, pages 32 to 39) for melt refining and casting of plutonium-bearing materials has been tested in an experiment employing uranium alloyed with approximately 1 w/o plutonium. Alpha contamination was confined to the interior of the furnace and the plastic bag used as a plutonium dust box for unloading the furnace after the melting operation. A preferential concentration of alpha activity in the dross was found in this experiment. A 3500-g master "fissium" alloy containing 20 w/o plutonium is being prepared.

Studies have been made of the amount of radioactive iodine volatilized in melt refining of discharged reactor fuel. Under the conditions proposed for EBR-II fuel processing (inert atmosphere at 1200 to 1300 C) negligible iodine was volatilized (less than one per cent).

X-ray analysis has shown tantalum monoboride (TaB) is the most stable boride formed in the ternary system uranium-boron-tantalum (U-B-Ta). This indicates tantalum monoboride may be a satisfactory container material for melting uranium.

Equipment to measure vapor pressures is being assembled and tested by an effusion method in the range 400 K to 2500 K.

Re-examination of the analytical method for determination of beryllia and lime ratios in mixtures (considered as a flux in melt refining) showed the analysis to be satisfactory for beryllia but poor for lime.

Determinations of the distribution coefficient of plutonium between magnesium and uranium or uranium-chromium alloys have been made over the range 930 to 1190 C. The distribution coefficients of plutonium are 0.19 (+0.01,-0.005) at 1190 C and 0.37 at 930 C. The heat of transfer of plutonium from the uranium-chromium phase (4.5 w/o chromium alloy) to the magnesium is $\Delta H = -9.2 \pm 1.6$ kcal/g atom.

Additional runs have been made to study the extraction of plutonium from powdered uranium-1 w/o plutonium alloy by liquid magnesium. The partition of zirconium, niobium, molybdenum, ruthenium, rhodium, palladium, silver and cadmium between uranium-iron alloys (5 and 10 weight per cent iron) or uranium-5 w/o chromium alloy has been studied.

Experiments to determine the extent of cerium removal by dross refining (3 hr at 1200 C) showed poor removal of cerium (20 to 45 per cent) in slip-cast magnesia crucibles. Effective removal (greater than 98 per cent) of cerium was obtained by the addition of zirconia chips.

The adsorption of metals volatilized during melt refining of discharged fuel material by the surface active materials, "Molecular Sieves," activated carbon, and activated alumina was further examined to determine the capacity and efficiency of the adsorbents under various flow and temperature conditions. Sodium has been used to test removal efficiency; high removal capacity (20 to 40 wt per cent of adsorber) and efficiency were shown by all three adsorbents (at rates to 500 ml/min equivalent to 145 ml/(min)(sq cm) calculated for room temperatures and atmospheric pressure).

Fractional crystallization of uranium with zinc or other low-melting metals provides a pyrometallurgical process for the removal of fission products from spent reactor fuels. A preliminary flowsheet for removal of

noble metals by this method has been developed and demonstrated on a small scale. Individual and multicomponent fission product solubilities in zinc and zinc-magnesium alloys have been determined for the following systems: (a) uranium-ruthenium-zinc, (b) uranium-ruthenium-(zinc-3 w/o magnesium), (c) barium-zinc and barium-uranium-zinc, and (d) cerium-zinc and cerium-uranium-zinc. The reduction of uranium compounds with magnesium in zinc-magnesium alloy has been demonstrated; this may have important applications in pyrometallurgical processing of nuclear fuel materials and in the preparation of uranium feed materials. Apparatus has been designed and tested for the separation of zinc from UZn_9 and the recovery of uranium from UZn_9.

Semi-works studies on the extraction of plutonium from uranium-5 w/o chromium alloys with molten magnesium and the subsequent magnesium distillation have shown good plutonium extraction (98 per cent), but distillation runs to date have shown poor recovery of plutonium from the magnesium phase. Corrosion testing of materials for handling molten magnesium has shown tantalum to be the only metal to show promise as a container material.

An electrolytic water analyzer under consideration for continuous monitoring of EBR-II fuel processing cell gas for oxygen has been tested for accuracy and response times over a wide range of water content (up to 840 ppm).

V. Analytical Research (pages 128 to 131)

An X-ray spectrophotometric method for determining plutonium in solution has been developed.

An ascending paper chromatographic analysis of irradiated uranium and thorium targets in a hydrofluoric acid medium has been developed. The analyses of these targets are being used for determination of various reactor cross sections.

VI. Routine Operations (page 132)

The operation of the radioactive liquid waste facility and the gamma-irradiation facility continued without incident.

I. FLUORIDE VOLATILIZATION SEPARATIONS PROCESS

Development work was continued on a fused fluoride process for zirconium-uranium fuel alloys. The alloy is dissolved in a sodium fluoride-zirconium fluoride melt at 600 C by sparging the system with hydrogen fluoride. The uranium is volatilized from the melt as the hexafluoride by a sparging operation with fluorine or bromine pentafluoride vapor. This product is then decontaminated and purified by fractional distillation.

Additional corrosion tests were conducted in an effort to find metals suitable for service as a dissolver in the fused fluoride process. Nickel was found to be susceptible to a sulfur-type attack. High-melting solids also collected in the vessels. Hastelloy B appeared to show some promise as a structural material for the dissolver. Graphite has shown excellent chemical resistance. Its principal limitation appears to be its lack of mechanical strength. Thermal cycling tests of graphite in contact with the salt did not result in any degradation of the graphite.

Further laboratory studies were made on the dissolution rate of zirconium in sodium fluoride-zirconium fluoride melts. It was found that the dissolution rate was not affected appreciably by the degree of impingement of the hydrogen fluoride sparge gas upon the zirconium sample. It was also observed that a limited amount of dissolution occurs in the absence of hydrogen fluoride. Dilution of the hydrogen fluoride with helium did not affect the dissolution rate.

An attempt was made to determine the extent to which hydrogen fluoride dissolves in or reacts with molten sodium fluoride-zirconium fluoride.

Work was continued on the fluorination in fluidized beds of uranium tetrafluoride produced by the reduction and hydrofluorination or ore concentrates. It was found that the uranium tetrafluoride from carbonate-leach ore concentrates might require the addition of an inert solid diluent for satisfactory fluidization during the fluorination.

Vanadium pentafluoride was prepared from the elements, and its melting point, vapor pressure and vapor density were measured.

Two preliminary dissolution and uranium recovery runs were made in the present semi-works scale fused salt process equipment using unirradiated material. The first run made to test the rate of volatilization of uranium (added as uranium tetrafluoride) from a sodium fluoride-zirconium fluoride melt by means of a bromine pentafluoride sparge showed greater than 99 per cent of the uranium volatilized from the melt in the first $1\frac{1}{2}$ hr of sparging. The second run made to test the rate of dissolution of zirconium-uranium alloy plates in sodium fluoride-zirconium fluoride fused salt sparged with hydrogen fluoride showed 90 per cent of the 14-lb plate charge dissolved in 6 hr.

Design and construction of a test unit for studying the production of uranium hexafluoride from uranium tetrafluoride in a fluidized-bed reactor was begun.

Work of the volatility group was discussed with representatives of ORNL, Horizons, Inc. and Union Carbide and Carbon.

A. Laboratory Investigations
(R. K. Steunenberg)

1. Fused Salt Processing of Enriched Reactor Fuels

a. Corrosion Investigations
(W. B. Seefeldt, S. Vogler, L. Hays, R. L. Breyne, G. Redding)

Corrosion testing of several materials in fused fluoride melts sparged with hydrogen fluoride and bromine pentafluoride has been continued. Unless otherwise indicated all tests were made at 600 C in equimolar sodium fluoride-zirconium fluoride melts sparged with hydrogen fluoride.

(1) Metal Tests: Nickel

A series of five non-impingement tests was made with "A" nickel liners. In non-impingement tests the liner wall was subjected only to gas-saturated melt. This was accomplished by using a draft tube to isolate the incoming gas from the liner wall. A tabulation of these runs follows:

93 No grain growth in liner or sparger; scattered growth in draft tube and thermocouple well. Most surfaces roughened in intergranular fashion, but no intergranular effects were observed at 400X.

94 Severe grain growth in liner, general growth in thermocouple well, little growth in sparger and draft tube. Sulfurous deposits extending through entire liner wall evident at 100X. Large sulfurous deposits in great quantity visible in sparger and draft tube at 35X; at 400X, globular deposit present in thermocouple well.

95 Little grain growth in liner and sparger. Globular deposits visible in sparger at 400X, but no sulfur-type deposits. Such deposits absent in liner. Carburization evident in sparger but not in liner.

96 Grain growth in outer liner wall and scattered locations. Scattered grain growth in other components. Bottom of liner had sulfur-type deposits at and within one grain of the surface; also wall of liner

near point of fracture. Other wall locations contained globular deposits. At one location of draft tube (1 in. from bottom) severe sulfur-type attack was evident; at other locations globular deposits were evident, with a greater concentration on outer wall.

97 Little grain growth in any component. No sulfur-type deposits evident. Globular deposits present in liner through wall but at somewhat greater concentration within first two grains, and also in the upper sections of the draft tube; none seen in sparger or thermocouple well.

Runs 96 and 97 were repetitions of Runs 93 and 94, respectively. The hydrogen fluoride for runs 95 through 97 was supplied from a common hydrogen fluoride manifold. The purpose of these runs was to determine whether there was any difference in metallurgical susceptibility between metals subjected to one-phase and two-phase attack.

The degree of metallurgical deterioration of the "A" nickel was determined by one of two methods: (1) metallographic examination, with particular emphasis placed on sulfur-type deposits, and (2) bend tests on liner walls in the vicinity of maximum expected attack. The results of liner bend tests are shown in Table 1; the results of metallographic examination have been previously discussed. Run 93 was conducted in greater part with recycled hydrogen fluoride from 6-lb cylinders. Most of this hydrogen fluoride probably had a low sulfur content, but in one or two instances the sulfur content of the vapor reached 30 ppm. The hydrogen fluoride for Run 94 was taken from a 100-lb cylinder and the sulfur content was more likely to be constant. In Runs 95 through 97 the sulfur content of the hydrogen fluoride at no time exceeded 4 ppm. Even with this low sulfur content the liner from Run 96 was badly embrittled. The result from Run 95 would seem to indicate that the presence of graphite reduced the reaction of sulfurous materials with the nickel liner. From Run 97 it might be concluded that the hydrogen dilution of the hydrogen fluoride had a beneficial effect relative to sulfur attack; however, this does not check the results from Run 94. The data of these runs indicate relatively low rates of change of dimensions. Typical rates were 0.11 to 0.14 mil per day. This may be compared with 0.3 to 2 mils per day under impinging conditions.

(2) Metal Tests: Hastelloy B

A test with Hastelloy B was made under impinging conditions. This was terminated after 1,000 hr. Hastelloy B has an age-hardening characteristic. The micro structures of liner samples after the run revealed that little, if any, age hardening had occurred.

The metal in the vicinity of the interface was subjected to a bend test; the resulting fracture was brittle in nature. A similar test on liner metal from the upper portions of the liner resulted in a ductile fracture.

Table 1

NON-IMPINGEMENT CORROSION TESTS MADE WITH NICKEL IN HF-SPARGED FUSED FLUORIDES AT 600 C

300 g equimolar $NaF-ZrF_4$ in 1 7/16-in. ID nickel liner, 0.032-in. wall, sparged with HF at rate of 20 g/hr; sparge gas isolated from liner by 1/2-in. OD draft tube

Run	Draft Tube	10% H_2 dilution	Time of Test (hr)	Bend Test on Liner	Sulfur Content of HF (ppm)
93	"A" Nickel	No	1000	Material ductile; no fracture or surface cracks	1.2 to 37
94	"A" Nickel	Yes	419	Severely embrittled	No reliable results
95	Graphite	No	1000	Reasonably ductile; microscopic cracks on inside	Consistently less than 4 ppm in 14 samples taken[a]
96	"A" Nickel	No	594	Severely embrittled, but not as badly as in Run 94	
97	"A" Nickel	Yes	1000	Reasonably ductile; microscopic cracks on inside	

[a]HF for runs 95 to 97 was supplied from a common manifold.

Preliminary metallographic examination revealed no intergranular effects, although there was some preferential metal depletion within one or two mils of the interior surface. Dimensional change reached a maximum of about two mils. This corresponded to 0.04 mil per day.

(3) Melt Tests: High-Melting Sludge

In longer term tests involving nickel a high-melting material collected in two portions of the liner: in the bottom, and in the vicinity of the interface. Three samples of this high-melting material were taken together with one of clean melt that was in contact with this high-melting material. The complete chemical analysis of these melts is reported in Table 2. Two things can be observed: (1) The nickel fluoride contents of the high-melting material range from 12.8 to 15.1 mol per cent. (2) There is an enrichment of zirconium in the same three samples. In addition to causing a problem of removal it is possible that uranium could be absorbed irreversibly in the material. The amount of nickel found corresponded quite well to the corrosion rates observed.

(4) Tests: Graphite

No additional tests were made during the quarter to get additional data on graphite corrosion. However, the graphite draft tube from Run 95 was checked for corrosive attack. Total dimensional changes

of up to 10 mils were observed after 240 hr on the first draft tube used; in the second draft tube the maximum observed attack was 12 mils over a period of 756 hr. The former corresponds to one mil per day, the latter to 0.38 mil per day. These are higher by a factor of 5 to 15 over rates previously observed. However, the hydrogen fluoride velocity from Run 95 was 2 to $3\frac{1}{2}$ ft per sec compared to a maximum of 0.15 ft per sec from graphite tests.

Table 2

ANALYSES OF HIGH-MELTING MATERIAL FROM CORROSION TESTS

		Clean Melt, First Half FF-93	High-Melting Bottom Residue: Second Half FF-93	High-Melting Bottom Residue: First Half FF-93	High-Melting Residue From FF-95[a]
Sample Reported Analyses, Wt %	Na	12.0	7.0	8.22	4.3
	Zr	39.0	38.4	39.6	41.4
	Ni	0.325	7.46	6.82	6.48
	F	45.0	43.4	44.2	43.9
		96.3	96.3	98.8	96.1
F Calculated from Na, Zr, Ni, Wt %		42.6	42.6	44.2	42.2
Calculated Mol %	NaF	54.7	35.7	39.3	25.6
	ZrF_4	44.8	49.4	47.9	59.3
	NiF_2	0.6	14.9	12.8	15.1
Calculated Zr to Na Mol Ratio		0.82 to 1	1.38 to 1	1.22 to 1	2.3 to 1

[a]High-melting material from 4 to 6 in. above bottom of liner.

A thermal-cycling test of graphite in contact with molten fluoride was made to determine whether or not there is any degradation of the graphite due to a combination of melt penetration into the pores and subsequent expansion and contraction from the cycling. The test was made with a CS grade graphite crucible, 6 in. outside diameter, and having $1\frac{1}{2}$-in. walls. One heat cycle per day, consisting of 10 hr heating and 14 hr cooling, was used. Salt was added to a depth of 4 in. and was agitated with a helium stream. The first test was terminated at the end of one week. There was no degradation of the graphite observed nor was there any gross penetration of melt into the graphite pores.

(5) Conclusions

Nickel appears to have two limitations: (1) its susceptibility to sulfur-type materials, and (2) the high-melting solid that collects in the vessel. In Run 96 failure of the nickel occurred although

the sulfur content of the hydrogen fluoride did not exceed 4 ppm. The effects of sulfur are accumulative and there is no way in which damaged metal can be restored to the original condition. It is felt at this time that nickel is not likely to be a satisfactory material of construction for the hydrofluorination step. The results from the Hastelloy B tests indicate that this may be a satisfactory metal. The indicated low rates of dimensional change may mean that the accumulation of high-melting material will be at a low rate. Its other limitation is its age-hardening characteristic. The Metallurgy Division of ORNL is working on alloy modification to eliminate or reduce this characteristic.

The mechanical strength of graphite is its greatest limitation. The Chemical Engineering Division is sub-contracting the development and construction of a graphite dissolver. This work is to be done by Horizons, Inc. The design concept includes the utilization of a cold-wall technique together with central heat induction.

(6) Program

Hastelloy B, copper, and cupro-nickel will be explored in a limited manner. The latter two will be subjected to draft-tube tests, while Hastelloy B will be given sulfur-susceptibility tests. In order to clarify the usefulness of graphite, tests will be started on bonding materials, perhaps baked-on carbons, and upon the effect of hydrogen fluoride impurities, such as water on corrosiveness.

The fluorination step will also be reconsidered. Nickel liners from the early bromine pentafluoride tests will be re-evaluated in the light of better metallographic techniques acquired since the tests were made. Several longer term tests using "L" nickel are also indicated.

b. Dissolution of Zircaloy with Hydrogen Fluoride in Equimolar Zirconium Fluoride-Sodium Fluoride Salt (S. Vogler, H. Griffin)

Previous ANL data (ANL-5422, pages 24 to 27) had demonstrated that hydrogen fluoride was a satisfactory reagent for the dissolution of zirconium metal in fused zirconium fluoride-sodium fluoride systems. The following conclusions were obtained from these data:

1. The rate of dissolution decreased slightly as the time of exposure was increased.
2. The rate of dissolution was proportional to the 0.25 power of the hydrogen fluoride sparge rate. Thus the dissolution was increased only to a small extent by an increased hydrogen fluoride addition rate.

3. The temperature coefficient for the dissolution rate corresponded to an activation energy of approximately 6 kcal/mole.

More recent data had indicated that, in the dissolution of zirconium by hydrogen fluoride in a fused fluoride salt, the proximity of the dissolving material to the gas stream was not an important variable, that is, material further removed from the gas stream dissolved at about the same rate as the material directly in the hydrogen fluoride path.

This seemed contrary to data which had indicated more severe corrosion when test specimens were in the path of the hydrogen fluoride sparge stream. Thus, it seemed desirable to examine this point.

A series of dissolutions of Zircaloy-2 (97.5 w/o zirconium, 2.5 w/o tin) metal were conducted in equimolar zirconium fluoride-sodium fluoride with hydrogen fluoride passing through the melt. The experiments were performed in the two-inch tube furnace used previously (see ANL-5422, page 25). A schematic representation of the apparatus is given in Figure 1.

FIGURE 1.
EQUIPMENT FOR FUSED
FLUORIDE DISSOLUTION EXPERIMENTS.

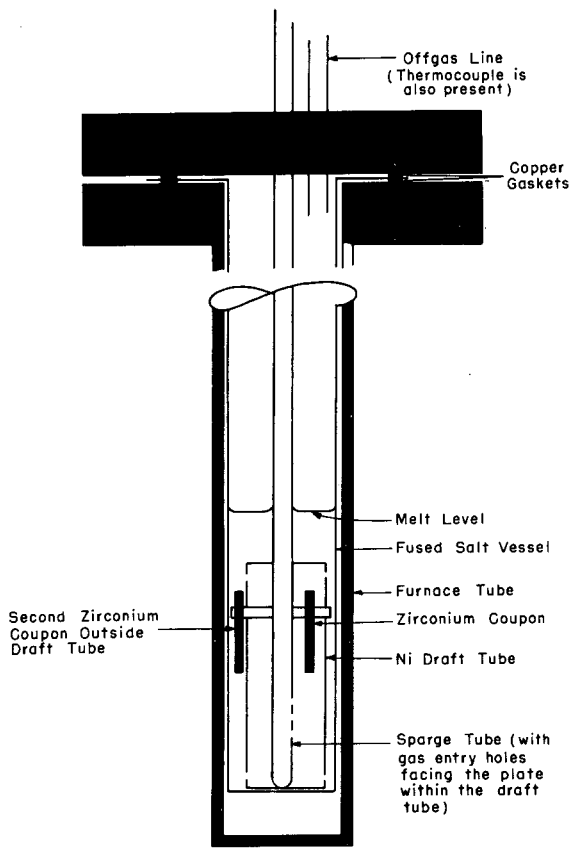

In each experiment, two pieces of Zircaloy (1 x 1/2 x 3/32 in.) were used, one suspended inside the draft tube and the second outside the draft tube. The configuration was such that the Zircaloy within the draft tube was directly over the point of gas entry. The second piece of Zircaloy was outside the draft tube and opposite the first. The dissolutions were carried out at different hydrogen fluoride flow rates. For each experiment the weight losses of the Zircaloy pieces were used as a measure of the Zircaloy dissolved. The data are given in Table 3.

Table 3

DISSOLUTION OF ZIRCONIUM IN FUSED ZIRCONIUM FLUORIDE-SODIUM FLUORIDE WITH HYDROGEN FLUORIDE

Temp: 600 ± 10 C
Time: 70 min
Sample: Zircaloy Plate[a], 1 x 1/2 x 3/32 in.

Gas Flow (g/min)	Per Cent Dissolved		Penetration Rate (mm/hr)	
	Within Tube	Outside Tube	Within Tube	Outside Tube
1.0	61	50	0.50	0.41
0.87	55	48	0.45	0.39
0.69	41	41	0.34	0.34
0.23	37	37	0.30	0.30
0.10	28	28	0.23	0.23
0.60	49	44	0.40	0.37
0.34	43	31	0.36	0.26
0.54	41	29	0.34	0.24

[a]Zircaloy-2 (97.5 w/o zirconium, 2.5 w/o tin)

The data indicate that there are probably slight differences in the dissolution rates for the two coupons, with the coupon directly in the gas stream dissolving at a slightly faster rate. Further evaluation is difficult without a determination of the mixing pattern within the tube.

If the logarithm of the per cent dissolved is plotted against the logarithm of the hydrogen fluoride flow rate, a power dependence of approximately 0.3 is obtained, which is in essential agreement with the earlier result of 0.25.

(1) Dissolution Rate in the Absence of Hydrogen Fluoride

Examination of the dissolution rate data suggests that at zero hydrogen fluoride flow, zirconium should dissolve in the melt alone. This was confirmed by carrying out a dissolution experiment with only helium bubbling (450 cc/min*) through the melt. The temperature and the time intervals were the same as previously. At the end of the experiment, 15 per cent of the zirconium had dissolved.

In a slightly different experiment, a Zircaloy coupon was suspended in molten equimolar sodium fluoride-zirconium fluoride, prefluorinated by passing bromine pentafluoride through it at 600 C. After the prefluorination, helium was bubbled through the melt for one hour at 200 cc/min. The Zircaloy coupon was immersed for 70 min in 100 ml of melt at 600 C. At the end of this exposure, the coupon had lost 20 per cent of its weight. A second coupon exposed to the same melt under the same conditions lost 4 per cent of the original weight.

After the second dissolution, hydrogen fluoride was bubbled through the melt at 600 C for one hour at a rate of 20 g/hr. Then the melt was sparged with helium at 200 cc/min for one hour. In this melt, a Zircaloy coupon exposed for 70 min at 600 C in 100 ml of melt lost 11 per cent of its weight.

The experiments indicate that fused sodium fluoride-zirconium fluoride is capable of dissolving a zirconium coupon to the extent of approximately 15-20 per cent in 70 min at 600 C. Because a subsequent dissolution produced a much lower dissolution rate, it appears that the amount of zirconium dissolved depends upon the amount of melt present. It could also be due to a reduced form of zirconium or an increased zirconium concentration. The amounts of zirconium dissolved were probably too small to show a concentration effect. These results agree quite well with similar results obtained at Oak Ridge.[1]

(2) Dissolution of Zircaloy in Fused Sodium Fluoride-Zirconium Fluoride with Hydrogen Fluoride Plus Helium

The purpose of these experiments was to attempt to separate the variables of hydrogen fluoride saturation of the melt and mixing of the melt produced by the gas sparging during dissolution. This was done by mixing helium with the hydrogen fluoride sparge gas. Several such experiments were performed and the results are tabulated in Table 4.

---

*Measured at room temperature.

[1]R. G. Wymer, "Dissolution of Uranium-Zirconium Fuel Elements in Fused $NaF-ZrF_4$," ORNL-2183, 18 (1957).

Within the reproducibility of the results, it appears that dilution of the hydrogen fluoride gas does not greatly change the dissolution rate obtained with hydrogen fluoride alone.

Table 4

DISSOLUTION OF ZIRCONIUM IN FUSED EQUIMOLAR ZrF_4-NaF WITH HYDROGEN FLUORIDE AND HELIUM

Temp: 600 C
Time: 70 min
Sample: Zircaloy Plate[a], 1 x 1/2 x 3/4 in

Experiment	HF Flow (g/min)	Helium Flow (cc/min)	HF/He[b]	Per Cent Dissolved: Within Draft Tube	Per Cent Dissolved: Outside Draft Tube
5	0.23	-	-	37	37
11	0.34	-	-	43	31
14	0.24	225	1.3	30	29
15	0.24	335	0.88	40	39
17	0.29	335	1.1	32	31
16	0.33	450	0.9	38	33

[a] Zircaloy-2 (97.5 w/o zirconium, 2.5 w/o tin)

[b] 0.2 g HF/min is equivalent to 224 cc/min at standard conditions. With the temperature correction (room temperature) this would be 244 cc/min.

c. Hydrogen Fluoride Solubility in and Reaction With Molten Sodium Fluoride-Zirconium Fluoride Salt

(J. Fischer, W. Gunther)

Experiments were conducted to measure the solubility of hydrogen fluoride in approximately equimolar sodium fluoride-zirconium fluoride melts. At the same time an attempt was made to measure the degree of reaction of hydrogen fluoride with the fused salt mixture. No significant solubility data were obtained in these experiments. Essentially all the hydrogen fluoride added was consumed in these experiments. The fluorine content of the hydrofluorinated salt was nearly the same as that of the original salt (43.8 w/o vs 44.3 w/o), while the nickel content rose sharply (from 15 ppm to 8.28 w/o), indicating the chief reason for hydrogen fluoride consumption was reaction with the nickel vessel.

The experiments were carried out in a reaction vessel consisting of a Monel cylinder, of approximately 125-ml capacity, heated by a large table furnace controlled by a Capacitrol-thermoregulator. The molten salt contained 51.1 mole per cent sodium fluoride and 48.9 mole per cent zirconium fluoride.

The salt was first pretreated with hydrogen fluoride at 100 C. Following removal of excess hydrogen fluoride by heating the salt above its melting point and evacuating to one micron pressure, hydrogen fluoride was added to the salt in the furnace tube and the tube heated to about 600 C. The pressure in the tube dropped steadily with time (see Table 5). After cooling the furnace overnight, no hydrogen fluoride was recovered by heating the salt above its melting point and then condensing the vapor.

Table 5

HYDROGEN FLUORIDE REACTION WITH SODIUM FLUORIDE-ZIRCONIUM FLUORIDE FUSED SALT AT 600 C

Salt Charge = 100 g
125-ml Monel Furnace Tube
51.1 mole per cent NaF, 48.9 mole per cent ZrF_4[a]

Pressure (mm Hg)	Expired Time After 600 C Reached (hr)	HF Consumed (moles)
610	0	
505	1	
428	2	
373	3	
297	4.7	
30	20[b]	0.0032[c]

[a]Salt pretreated with HF at 100 C

[b]Furnace turned off overnight after 4.7-hr operation.

[c]HF added--negligible HF recovery after run.

A similar experiment with a new charge of salt and a new reaction tube gave a similar result (see Table 6). Analysis of the salt removed from the vessel showed little change in fluorine content (original 44.3 w/o, final 43.8 w/o) but a marked increase in nickel content (15 ppm

to 8.28 w/o). This indicates that hydrogen fluoride did not react with the salt but was consumed by reaction with the nickel vessel. It was concluded that significant data for the solubility of hydrogen fluoride in the melt could not be obtained by this method.

Table 6

HYDROGEN FLUORIDE REACTION WITH SODIUM FLUORIDE-ZIRCONIUM FLUORIDE AT 600 C

Salt Charge = 1.055 g
125-ml Monel Furnace Tube
51.1 mole per cent NaF, 48.9 mole per cent ZrF_4[a]

Pressure (mm Hg)	Expired Time After 600 C Reached (hr)	HF Consumed (moles)
830	0	
789	0.8	
729	1.7	
692	2.1	
178	17	0.0144

[a]Salt pretreated with HF at 100 C.

2. Feed Materials Processing - The Conversion of Uranium Tetrafluoride to the Hexafluoride
(O. Sandus, W. A. Shinn)

Studies were continued on the fluorination of crude uranium tetrafluoride in a fluidized bed. This material was produced by the reduction and hydrofluorination of South African and domestic ore concentrates in fluidized-bed reactors.

Preliminary work described in the previous quarterly report, ANL-5668, page 24, had demonstrated in the laboratory that the crude uranium tetrafluoride could be fluorinated satisfactorily in the absence of a solid diluent. Table 7 gives the results of four experiments in which crude uranium tetrafluoride alone was fluorinated in a fluidized bed with fluorine-nitrogen mixtures of various compositions. Two of these runs, which were reported previously, are given in their final form. The results indicate, as stated in the previous report, that the fluorine concentration did not affect the fluorine efficiency appreciably, but it did have a strong influence on the rate of uranium hexafluoride production. This concluded the laboratory work with the crude uranium tetrafluoride produced from South African Rand ore concentrate.

Table 7

FLUORINATION OF CRUDE URANIUM TETRAFLUORIDE IN A FLUIDIZED BED

Charge: 75 g crude UF_4 (71.8% U) produced from South African Rand ore concentrate
Fluorine: 1 stoichiometric equivalent
Temperature: 450 C
Linear Flow Rate: 0.5 ft/sec

Run No.	Flow Rate (cc/min) N_2	Flow Rate (cc/min) F_2	Mole Ratio F_2/N_2	Time of Run (min)	Fluorine[a] Efficiency (per cent)	Uranium Balance (per cent)
20	2665	481	0.18	30	83.3	93.6
21	2310	836	0.36	17.3	77.5	96.0
22	1825	1321	0.72	10.9	69.6[b]	96.9
23	0	~3146[c]	pure F_2	4.0	80.9	97.3

[a]Fluorine Efficiency = UF_6 collected/UF_6 theoretical.

[b]Operational difficulties due to a plugged filter.

[c]Difficulty in maintaining a constant flow rate.

Samples of crude uranium tetrafluoride produced by the reduction and hydrofluorination of Anaconda acid and carbonate leach ore concentrates were obtained for fluorination. The bulk densities and screen analyses of these two samples are given in Table 8. Data on the South African material are included for comparison.

The uranium tetrafluoride produced from the acid leach material fluidized with or without calcium fluoride diluent almost as well as the -40 mesh samples from the Rand material. The crude uranium tetrafluoride produced from the carbonate leach ore concentrates did not fluidize as well as the other two, nor did the addition of calcium fluoride diluent improve the fluidization substantially. When a -60 mesh fraction of this material was taken, its fluidization was improved, and the addition of calcium fluoride to this fraction resulted in a mixture with good fluidizing properties.

A fluorination run was performed with the crude uranium tetrafluoride from the acid leach ore concentrate. Three successive 75-g portions were fluorinated with approximate stoichiometric equivalents of fluorine at 450 C. The mole ratio of fluorine to nitrogen was 0.36, and the flow rate was 0.5 ft/sec. Pure fluorine was then passed through

the reactor to fluorinate any remaining material as thoroughly as possible. The purpose of this procedure was to determine the gangue elements present in the residue and in the volatilized uranium hexafluoride. The analytical results are not available at present.

Table 8

BULK DENSITIES AND SCREEN ANALYSES OF THE CRUDE URANIUM TETRAFLUORIDES PRODUCED FROM VARIOUS TYPES OF ORE CONCENTRATES

Crude uranium tetrafluoride samples produced by reduction and hydrofluorination of the ore concentrates in fluidized beds.

	Anaconda Acid Leach	Anaconda Carbonate Leach	Rand
Tapped Bulk Density (g/ml)	2.7	2.7	1.6
Sieve No.	(per cent)	(per cent)	(per cent)
+ 20	0.02	0.05	0.1
-20 + 40	0.1	6.4	46.1
-40 + 60	7.6	27.7	29.0
-60 + 100	25.0	30.5	14.0
-100 + 200	36.3	31.9	8.0
-200 + 325	24.1	12.4	1.3
-325	6.8	0.9	1.5

A similar run was attempted with the -60 mesh fraction of crude uranium tetrafluoride from the carbonate leach material. When fluorine was passed into the 75-g charge of uranium tetrafluoride the reactor became plugged, and little uranium hexafluoride was produced. When the reactor was opened, a hard plug of sintered green material was found to extend for some length in the 1-in. pipe.

The tendency of the carbonate-leach uranium tetrafluoride to form plugs may arise from sodium introduced into the material during the leaching operation. There is a sufficient amount of sodium fluoride present in this crude green salt to complex most of the uranium as a sodium fluoride-uranium tetrafluoride compound. X-ray evidence indicated that little, if any, uranium tetrafluoride was present as such in this material. The major constituent present was the compound $7\ NaF \cdot 6\ UF_4$. Thus it is this compound, and not uranium tetrafluoride, that is being fluorinated in the fluidized bed.

Since the carbonate leach ore concentrate consisted largely of sodium diuranate, the hydrogenation and hydrofluorination procedures may be expected to produce various mixtures of sodium fluoride and uranium tetrafluoride. This binary system forms several compounds and eutectics with much lower melting points than either of the pure components. This would also tend to lower the sintering temperature of this system. An experimental determination of the melting point of this green salt gave a value of 670 ± 15 C. The addition of some sodium fluoride lowered the melting point to about 610 C. This crude green salt also contains other impurities, including potassium, which lead to a very complicated chemical system. These factors are probably responsible for the fact that the crude green salt was found to sinter at 500 C, and possibly even lower temperatures.

3. Vanadium Fluoride Studies - The Preparation and Properties of Vanadium Pentafluoride

(L. E. Trevorrow, J. Fischer, H. D. Tyler)

Vanadium is found in varying amounts in uranium ores, primarily in the form of vanadates. A knowledge of the chemistry of vanadium is important in feed material processing schemes in order to show that the uranium product will not exceed the vanadium specification.

There is a lack of information on the behavior of vanadium during the reduction, hydrofluorination and fluorination of ore concentrates. The physical and chemical properties of vanadium oxides, oxyfluorides and fluorides are therefore of particular interest. The work described in this report is concerned with vanadium pentafluoride.

Previous distillation experiments in this laboratory had indicated that vanadium pentafluoride must be much more volatile than the reported data of Ruff and Lickfett had indicated.[2] They erroneously described vanadium pentafluoride as a white solid at room temperature which sublimed at 111.2 C (758 mm Hg), and which melted somewhere above 200 C.

Vanadium metal was obtained from the Vanadium Corporation of America, who supplied an analysis indicating 99.5 per cent purity. The fluorine used in this preparation had been shown previously to have a purity in excess of 99 per cent.[3]

The apparatus used to prepare and to measure the physical properties of vanadium pentafluoride was constructed of nickel and Monel. The components were joined by welding or by flare connectors with Teflon gaskets. Since preliminary experiments had indicated that silver solder and Fluorothene were attacked by vanadium pentafluoride, their use was

---

[2] O. Ruff and H. Lickfett, Ber., 44, 2439 (1911).

[3] J. Fischer, J. Bingle and R. C. Vogel, J. Am. Chem. Soc., 78, 902 (1956).

avoided in the final purification and in the physical measurements. The apparatus was joined to a manifold which was equipped with a vacuum source, liquid nitrogen cold traps, and helium and fluorine gas supplies. Monel diaphragm and Teflon-seated bellows valves were used.

That portion of the apparatus used to measure the vapor pressure and vapor density was housed in a thermostatted air bath. Care was taken to insure that no portion of this apparatus was at a lower temperature than the liquid during the vapor pressure measurements. The temperatures were measured to 0.1 C with thermocouples which had been calibrated with a platinum resistance thermometer. A recording potentiometer was used to determine the melting point by means of time-temperature curves.

The pressures were measured with a mercury manometer in conjunction with a Booth-Cromer pressure transmitter and self-balancing relay,[4] which isolated the fluorine compound from the manometer. The pressures were measured to the nearest 0.1 mm Hg.

The vanadium pentafluoride was prepared by passing fluorine over granulated vanadium metal in a 3/4-in. nickel reaction tube at 300 C. Chemical analyses of the product indicated 34.2 per cent vanadium and 66.5 per cent fluorine. The theoretical values are 34.9 and 65.1 per cent. Since vanadium pentafluoride is extremely hygroscopic, it was necessary to exclude atmospheric moisture from the compound. Transfers were therefore made by vacuum distillation.

The melting point and vapor pressure determination were made on a 15-ml sample of vanadium pentafluoride, which was distilled into a 25-ml nickel tube with a thermocouple well. Traces of hydrogen fluoride and fluorine were removed from the sample by freezing it with dry ice and evacuating the system. The sample was then melted, and this cycle was repeated several times. Fractions of the sample were removed by distillation until a constant vapor pressure was observed.

The vapor density of vanadium pentafluoride was determined by weighing a given volume in a nickel vessel at a known temperature and pressure. The average value of several measurements was 146.1 ± 0.2 g/GMV. The formula weight is 145.95 g/mole. The values obtained at 24 C and 76 C were identical, within the experimental error. It was found that the vapor density did not change during a 36-hr exposure to the nickel system, indicating that vanadium pentafluoride is stable under these conditions.

In the melting point determinations, the purified liquid exhibited severe supercooling tendencies. As a result, it was necessary to use thaw curves for the thermal analysis. Since the vapor pressure of the

[4] S. Cromer, "The Electronic Pressure Transmitter and Self-Balancing Relay," MDDC-803 (1947).

compound at the melting point is appreciable, it was also necessary to maintain a pressure of vanadium pentafluoride from another vessel in order to repress cooling effects due to vaporization. The melting points obtained in this fashion averaged almost a degree higher than those obtained by the usual method. The average value of several determinations was 19.0 ± 0.9 C. This may be compared with another recently reported value of 19.5 ± 0.5 C.[5]

The vapor pressure measurements were made in such a way that the equilibrium was approached from both higher and lower temperatures. The vapor pressure measurements from 24 C to 86 C are listed in Table 9. Interpolation of these data gives a normal boiling point of 48.5 C. Emeleus and Clark,[5] who measured the vapor pressure from 23 C to 45 C reported a boiling point of 48.3 C.

Table 9

VAPOR PRESSURE OF VANADIUM PENTAFLUORIDE

Temperature (C)	Pressure (mm Hg)	Temperature (C)	Pressure (mm Hg)
24.1	203.2	58.2	1281.4
24.6	214.6	58.3	1289.8
24.9	222.6	64.5	1697.2
25.0	225.1	64.5	1708.1
25.4	222.1	69.9	2158.8
25.7	225.1	70.0	2154.5
34.6	372.5	70.0	2155.0
34.7	377.3	73.7	2523.9
44.4	633.2	74.1	2528.8
44.4	639.9	78.4	2971.1
44.6	636.9	78.4	2972.1
50.5	871.5	83.0	3467.6
50.5	880.4	83.0	3467.6
55.6	1123.9	85.4	3734.5
55.6	1123.9	85.5	3734.0

The general agreement of this work with that of Emeleus and Clark which was done in quartz equipment indicates that the material can be handled equally satisfactorily in nickel or quartz systems.

[5]H. J. Emeleus and H. C. Clark, Private Communication of material soon to be published.

4. Plutonium Hexafluoride Studies
(M Steindler, M. D. Adams, D. V. Steidl)

Study of the rate of fluorination of plutonium tetrafluoride has been continued. A complete report on the plutonium hexafluoride program will be issued in the near future.

B. Pilot Plant Operations
(R. Kessie, R. Liimatainen, G. J. Vogel, G. Goring,* W. J. Mecham)

1. Fused Salt Process for Dissolution of Fuel Alloys

a. Equipment and Flowsheet

A flowsheet for a fused salt volatility process to recover decontaminated uranium hexafluoride from uranium-zirconium alloys is shown in Figure 2. The fuel elements are dissolved in a molten fluoride bath with a hydrogen fluoride sparge and then the uranium hexafluoride is volatilized from the melt with a bromine pentafluoride or fluorine sparge. The use of fractional distillation to provide a high degree of decontamination of uranium hexafluoride from fission products and from bromine fluorides has been shown to be feasible in studies reported previously in quarterly reports of this Division.

FIGURE 2.

FLOWSHEET FOR PROCESSING Zr-U FUELS BY VOLATILITY METHODS; FUSED SALT PROCESS.

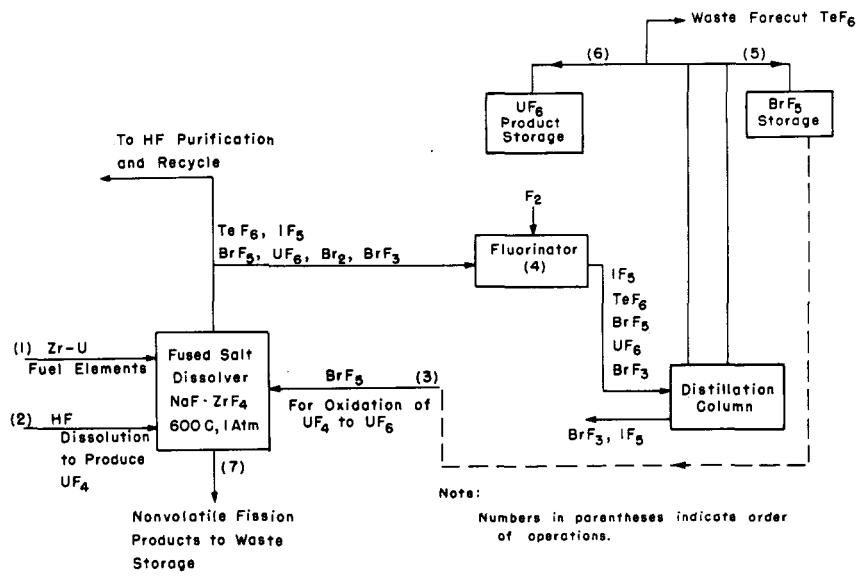

*Special scientific employee on loan from Union Carbide Nuclear Company.

The equipment used in the present tests is shown in Figure 3. Electrically heated weigh tanks produce vapor which is conducted through heated lines to the sparge gas distributor in the dissolver vessel, which is located within a furnace in a shielded pit. The off-gas system consists of a solids trap packed with nickel and held at about 150 C, a condensate receiver (water-cooled and mounted on a scale) and a caustic sparge tower for disposal of fluoride wastes. In these tests the uranium hexafluoride-bromine pentafluoride mixture was collected as condensate.

FIGURE 3.

EQUIPMENT USED IN PRELIMINARY SEMI-WORKS FUSED SALT DISSOLVER TESTS.

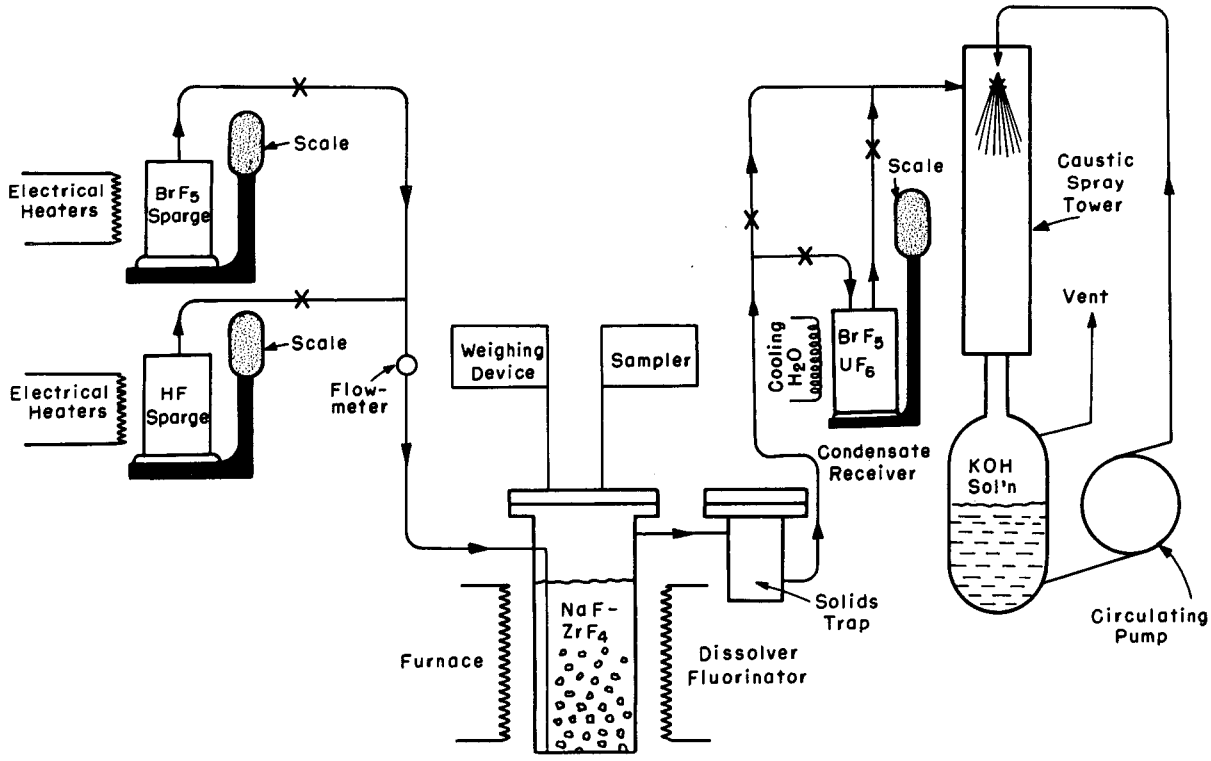

The dissolver is eight inches in diameter and seven feet long, with a flanged top for charging solids. The sparge gas distributor consists of a bottom plate with five 3/16-in. diameter holes. A connection at the top is provided for (1) a weighing device and (2) a spoon-type sampler from which a portion of the melt can be removed. All components are made of nickel or Monel. This dissolver is a temporary piece of equipment designed for preliminary experiments. The permanent dissolver is now being constructed.

b. Dissolution and Uranium Recovery Tests

Run 1 The purpose of this test was to measure on the semiworks scale the rate of removal of uranium from a sodium fluoride-zirconium fluoride melt by means of a bromine pentafluoride sparge. Two hundred pounds of salt were charged to the dissolver and prefluorinated with bromine pentafluoride. Then solid uranium tetrafluoride was charged to the dissolver and the molten mixture sparged four hours with helium to form a homogeneous solution. This was followed with a four-hour sparge with bromine pentafluoride, during which time overhead material containing uranium hexafluoride was condensed in a weigh tank cooled with tap water (14 C). Samples of salt and of overhead vapor were taken.

In Table 10 is given a summary of run conditions and in Figure 4 the results of the salt and overhead vapor samples are given. During the helium sparge period the uranium concentration of the salt rose to that calculated on the basis of the quantities of materials charged. At the beginning of the sparge period relatively high concentrations of uranium in both the salt and the overhead were detected, then the values rapidly decreased. After 1.5 hr of sparging the uranium concentration in the salt dropped to the concentration reported on a salt blank. The scattering of the values of the salt samples is believed due to analytical difficulties with the very low levels of uranium in the salt and to sampling problems. A fluorophotometric determination of uranium was used.

Table 10

VOLATILIZATION OF URANIUM IN FUSED SALT DISSOLUTION

(Run 1)

Run Conditions

1. Initial salt charge:

   200 lb salt; 40 mole per cent ZrF_4, 60 mole per cent NaF

2. Uranium charge:

   400 g UF_4

3. Sparge conditions:

   (a) 650 C

   (b) 15 psia

   (c) 17.25 lb BrF_5 added in 4-hr sparge period

FIGURE 4.

CONCENTRATIONS OF URANIUM IN FUSED SALT DISSOLUTION. Run I.

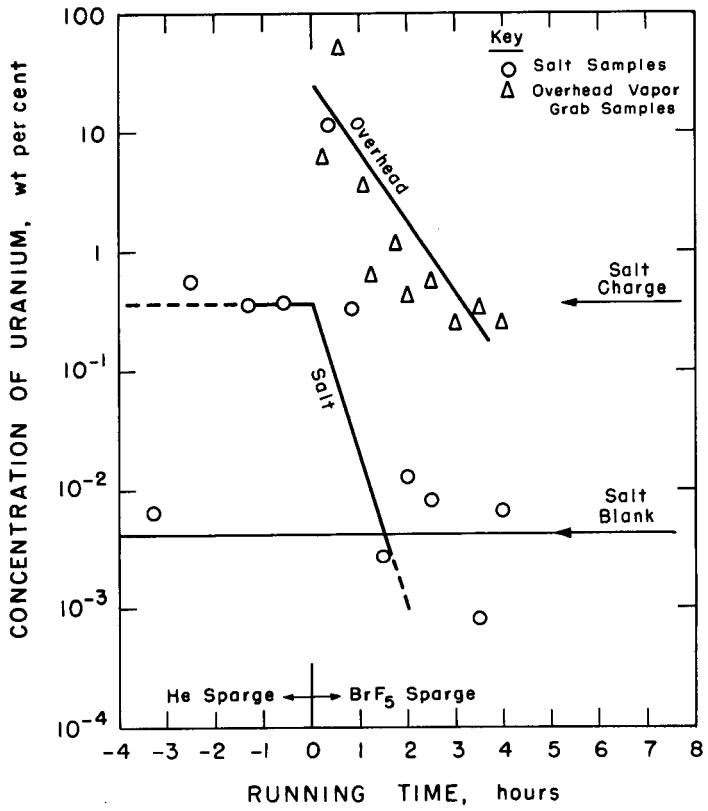

The rate of decrease in the uranium concentration of the overhead vapor as shown in Figure 4 is believed to be determined by vapor hold-up in the dissolver and solids trap. The overall material balance on volatile material is given in Table 11.

Table 11

OVERALL MATERIAL BALANCE ON VOLATILE MATERIAL IN URANIUM DISSOLUTION

(Run 1)

Total Material	Charge	Collection	Material Balance Per Cent
(BrF_5, UF_6)	17.25 lb	13.7 lb	80
Uranium (as UF_4)	303 g	310 g	102

The more favorable material balance on uranium compared to total condensible material is probably due to the fact that uranium hexafluoride is less volatile than bromine trifluoride.

From the salt samples (Figure 4) it appears that the bulk of the uranium left the melt very quickly and that at least 99 per cent of the uranium had been volatilized from the melt in the first $1\frac{1}{2}$ hr of sparging.

Run 2 The purpose of this experiment was to obtain preliminary dissolution rate data in the equipment.

Four zirconium-uranium alloy plates were suspended in the melt from a hook on a weighing device and sparged with hydrogen fluoride vapor. The run conditions are given in Table 12. During the run appreciable heat was released by the reaction, as noted by reduced power requirements on the furnace.

Table 12

DISSOLUTION OF ZIRCONIUM-URANIUM ALLOY PLATES IN FUSED SALT

(Run 2)

Four alloy plates: 1 per cent uranium, 99 per cent zirconium.
Plate dimensions: 4 ft long, 2-17/32 in. wide, 3/32 in. thick.

Charge Weight (lb)		Sparge Conditions				
Salt[a]	Metal	Temp (C)	Dissolver Pressure (psia)	Total HF (lb)	Addition[b] (hr)	Per Cent Dissolved[c]
200	14	600	17	21.8	6	90

[a]40 mole per cent ZrF_4, 60 mole per cent NaF (remaining from Run 1).

[b]Average sparge rate: 11 lb HF/(hr)(sq ft).

[c]Average penetration rate: 7 mils/hr.

The weighing device consisted essentially of a Monel bellows functioning as a spring, the movement of which was detected by an induction coil. Changes of position of the weighing rod attached to the bellows were calibrated against an electrical output, which was continuously recorded. The device operated to give a relative weight record. However, because in

this test the plates were suspended from the top rather than contained in a basket, the record showed a dropping off of the plates rather than a dissolution rate. One alternative method* of following dissolution rate is by hydrogen evolution, which is to be used subsequently.

In six hours, 90 per cent of the metal had dissolved, as determined by removing remaining pieces from the dissolver and weighing them.

The hydrogen fluoride efficiency was 50 per cent. The average sparge was 11 lb hydrogen fluoride/(hr)(sq ft), based on the inside cross-sectional area of the dissolver. The average calculated penetration rate was 7 mils/hr.

2. Design and Construction of a Fluidized-Bed Unit for Uranium Hexafluoride Production

During this period, design and construction was begun on a unit to study the production of uranium hexafluoride in a fluidized bed of uranium tetrafluoride. The effects of temperature, fluorine concentration, and dilution of the bed with other fluorides are variables to be considered. Such a process may be applicable to the fluorination of impure uranium tetrafluoride made from ore concentrates.

The reactor is a single-stage unit with an internal diameter of 2.5 in. and a maximum bed height of 2 ft. Other components of the system include an exit gas filter and a uranium hexafluoride cold trap.

The equipment installation is about 60 per cent completed.

*Another method proposed is to obtain rate of dissolution data by weighing the hydrogen fluoride charge tank and hydrogen fluoride receiver.

II. FLUIDIZATION

(A. A. Jonke)

Activities in the Green Salt Pilot Plant were directed toward the processing of uranium ore concentrates to crude uranium tetrafluoride. Two runs were made with acid-leach concentrate, and one run with carbonate-leach concentrate. Operability of the equipment was satisfactory, and excellent conversion of the uranium to green salt was obtained. Of the two types of ore concentrates tested, best results were obtained with the acid-leach material. The carbonate-leach concentrate showed a tendency to break up into fines during the reduction step, but this tendency was greatly reduced by drying the ore concentrate before hydrogen reduction. The presence of sodium fluoride in the hydrofluorinated carbonate-leach material considerably reduced its melting and sintering temperatures, and necessitated very careful start-up conditions to avoid caking.

Inactive shakedown runs were made to test the shielded waste calciner; one run using highly diluted (1 part ICPP* IAW solution to 1000 parts) radioactive waste solution was completed. Operation was satisfactory, but no analytical data have been completed. A small amount of equipment installation remains to be done preparatory to operations at higher activity levels.

Mr. W. Ruch and Mr. E. Gaskill of General Chemical Division, Allied Chemical and Dye Corporation, were present to observe the processing of uranium ore concentrates in the pilot plant. Waste calcination work was discussed with Mr. C. E. Stevenson of Phillips Petroleum Company (Idaho Division). Mr. J. D. Cotter of Phillips Petroleum Company (Idaho Division) joined the waste calcination group for a six-week period to assist in operation of the pilot plant.

A. Crude Green Salt from Uranium Ore Concentrates

(N. Levitz, E. Petkus, M. Jones, T. Cannon, D. Raue)

Because considerable interest has been expressed in the production of refined uranium hexafluoride from uranium ore by a process involving fractional distillation of crude uranium hexafluoride, the green salt pilot plant was temporarily diverted from the processing of refined uranium salts to the processing of ore concentrates. The objective of these experiments was to demonstrate that the multi-stage, fluidized-bed reactors could be used for the production of crude green salt by reduction and hydrofluorination of uranium ore concentrates.

---

*Idaho Chemical Processing Plant

Two types of ore concentrates were studied. One was produced by an acid-leach process, which resulted in a concentrate consisting primarily of uranium trioxide and U_3O_8. The second was produced by a carbonate-leach process, which resulted in a product consisting primarily of sodium diuranate. These are the two major types of ore concentrate production processes used in this country. The acid-leach process is considerably more predominant than the carbonate-leach process.

1. Feed Preparation

To prepare the concentrates for fluid bed operation it was necessary to aggregate the finely powdered material to a particle size suitable for fluidization. This was done in a high-capacity pellet mill. The pelleted concentrates were crushed and sieved through a 30-mesh screen to produce the feed to the fluid bed process.

The chemical analyses of the ore concentrate feeds are given in Table 13.

Table 13

CHEMICAL ANALYSES OF ORE CONCENTRATES STUDIED IN GREEN SALT PILOT PLANT

Constituent	Acid-Leach Concentrate (%)	Carbonate-Leach Concentrate (%)
U	67	59
Loss at 110 C	5.9	4.2
P_2O_5	0.17	0.23
V	0.025	0.63
Mo	0.0015	0.0005
Fe	0.53	0.075
SO_4	2.35	0.13
CO_3	0.22	2.02
SiO_2	0.5	a
Mg	0.4	-
Na	0.093	7.3
K	-	0.6
NH_3	2.32	0.05

[a]Si content 1 to 10% by spectrochemical analysis.

2. Equipment Modifications

For the reasons given in the previous report (ANL-5668, p. 48) the operation of the multi-stage reactors with solids of low bulk density necessitated a reduction in the pressure drop for gas flow through the gas distributor plates in order to reduce the solids level in the downcomers. For processing ore concentrates (bulk density about 2 g/cc) the holes in the gas distributor plates were enlarged from 5/64 in. to 3/32 in. in diameter. This reduced the pressure drop across the plate from 16 in. to 7 in. of water at 0.6 ft/sec. A preliminary test using acid-leach concentrate showed that the solids flow through the reactor was satisfactory.

An additional modification was found to be necessary after initial attempts were made to process the ore concentrates. After a short period of operation it was found that the line which carried the combined off-gases from both the reduction and hydrofluorination reactors became plugged with a white, powdered solid. The solid was identified as ammonium fluoride, which resulted from the reaction of ammonia (given off from the ore concentrate feed) with the excess hydrogen fluoride from the hydrofluorination reactor. This difficulty was easily corrected by treating the off-gases from the two reactors separately before exhausting them to the ventilating system.

At the completion of the first run with uranium ore concentrate, it was found that the sintered Monel plate used as a gas distributor on the bottom stage of the hydrofluorination reactor had badly deteriorated from heat and corrosion. The plate had cracked and weakened to the point where it could be easily broken with the fingers. This sintered metal had been in contact with hydrogen fluoride gas at 600 C for a period of about 30 hr. Since the sintered Monel is apparently unsatisfactory under these conditions, it was decided to operate the bottom stage at a lower temperature (400 C) temporarily until the bottom flange could be redesigned to accommodate a perforated plate similar to those in the upper stages. Since the bottom stage at 400 C probably had little effect on the reaction, the hydrofluorination reactor was, in effect, operated as a four-stage rather than a five-stage unit.

3. Acid-Leach Ore Concentrate - Batch Experiment

In order to establish a base line with which to compare the results of the pilot plant runs, a batch run was made in the 3-in. diameter reactor. Samples were taken at intervals during the run to determine the nearness to completion of the reaction. The run conditions and results are given in Table 14.

Due to sampling and analytical difficulties only one of three samples of the reduced product was satisfactorily analyzed. The results on this sample, as well as on the hydrofluorinated product, indicated that at

Table 14

SUMMARY OF BATCH FLUID-BED CONVERSION OF ACID-LEACH ORE CONCENTRATE TO CRUDE GREEN SALT

Equipment:	3-in. diameter Monel reactor
Starting Material:	7.5 lb acid-leach ore concentrate
Particle Size:	minus 30-mesh
Bed Depth:	18 in. (static)
Reduction Temp:	575 C
Hydrofluorination Temo:	450 C

Sample Designation	Duration of Treatment (hr)	Total U (%)	U (+4) (%)	AOI (%)	U Content of AOI (%)	Water Soluble U (%)	Fluoride (%)	Sulfur (%)
Reduction Product	6.3	82	82					
Hydro-fluorination Product	1.6	72	70	1.2	79	-	24	0.03
Hydro-fluorination Product	3.4	73	70	1.2	60	0.9	22	0.03
Hydro-fluorination Product	4.4	73	71	1.0	67	1.2	26	0.01

least 97 per cent reduction was achieved. This was confirmed by the low water-soluble uranium content, which indicated a maximum uranyl fluoride content of 1.5 per cent (assuming all of the water soluble uranium to be uranyl fluoride).

The hydrofluorination reaction was essentially complete after only 1.6 hr of treatment, indicating that the reactivity of this material is very high indeed. Continued hydrofluorination had almost no further effect, the AOI (ammonium oxalate insoluble) dropping from 1.2 per cent after 1.6 hr of hydrofluorination to 1.0 per cent after 4.4 hr. The uranium content of the AOI (about 70 per cent) was lower than the theoretical value for uranium dioxide (88.2 per cent), indicating that the AOI was either a mixture of uranium dioxide and impurities or another uranium compound. The fluoride content of the hydrofluorinated product averaged 24 per cent, which is near the theoretical value for uranium tetrafluoride (24.2 per cent fluoride).

The sulfur content was reduced about 40-fold, from 0.8 per cent in the concentrate to about 0.02 per cent in the crude uranium tetrafluoride.

4. Pilot Plant Start-Up

In starting up the multi-stage reactors it was necessary to have each stage at least partially filled with solids in order to provide a seal for the lower end of the downcomers. Ore concentrate was therefore charged into each stage through a fill line provided for this purpose. It was considered advisable that the starting bed material be converted to the reaction product before continuous operation was begun. It was necessary, therefore, first to reduce the ore concentrate in both reactors, then to hydrofluorinate the material in the Monel reactor. To avoid having the stages become partially emptied due to solids carry-over through the downcomers, a continuous flow of solids at a low rate was fed into the reactors during the bed conversion operation. The entire operation was intentially prolonged in order to gain operating experience without the use of large amounts of feed. The following procedure was used:

The reduction and hydrofluorination reactors were brought to temperature using nitrogen gas for fluidization. Ore concentrate was fed to the reduction reactor at a low rate (about 3 lb/hr), and the product from both reactors was recycled back to the top of the hydrofluorination reactor. Hydrogen was then introduced into the nitrogen stream of both reactors in the ratio of two parts hydrogen to one part nitrogen. This operation was continued for 14 hr, during which time essentially no net product was removed. The small amount of feed served merely to counteract the volume decrease of the solids brought about by the increase in bulk density during reduction.

At the end of this period the hydrogen flow to the hydrofluorination reactor was stopped, and hydrogen fluoride was introduced into the nitrogen stream. The rate of hydrogen fluoride introduction was controlled to keep the heat of reaction from raising the bed temperatures above 450 C. By observing the temperature behavior it was noted that reaction occurred in one stage at a time, proceeding from the bottom stage to the top. When the reaction was nearly complete in all stages, the hydrogen fluoride flow rate was gradually increased until the gas stream contained essentially 100 per cent hydrogen fluoride. After seven hours of hydrofluorination both reactors were brought on stream and a run was started. The start-up operation and the run which followed represented 30 hr of continuous operation.

In subsequent runs this start-up procedure was not necessary, since the reactors were started with the bed material from the previous run. However, a small flow of feed was maintained to keep the stages filled during the period in which the reactors were being heated.

5. Acid-Leach Concentrate - Pilot Plant Runs

a. Operating Conditions

Two pilot plant runs were made with acid leach ore concentrate. The first run was discontinued after nine hours because of the failure of the sintered metal plate at the bottom of the hydrofluorination reactor (see page 39). The second run was arbitrarily stopped after 20 hr of operation. As shown in Table 15, the operating conditions used for the two runs were substantially the same, the principal difference being a somewhat higher feed rate in Run 2 (10.4 lb U/hr) than in Run 1 (7.4 lb U/hr).

Table 15

OPERATING CONDITIONS FOR GREEN SALT PILOT PLANT RUNS ON URANIUM ORE CONCENTRATES

(Pilot plant described in ANL-5668, p. 43)

	Acid-Leach Concentrate		Carbonate-Leach
Reduction Conditions	Run OCP-1	Run OCP-2	Run OCP-3
Bed Temperatures, C	520 - Stg 1 565 - Stg 2 575 - Stg 3 575 - Stg 4	400 - Stg 1 575 - Stg 2 575 - Stg 3 575 - Stg 4	300 - Stg 1 575 - Stg 2 575 - Stg 3 575 - Stg 4
Inlet Gas Velocity, ft/sec	0.3	0.35	0.49
Inlet Gas Composition	74% H_2, 26% N_2	76% H_2, 24% N_2	79% H_2, 21% N_2
Feed Rate, lb solids/hr	11.0	15.5	12.6
Feed Rate, lb U/hr	7.4	10.4	7.5
Avg Solids Residence Time, hr	7	5	6
Hydrofluorination Conditions			
Bed Temperatures, C	350 - Stg 1 400 - Stg 2 450 - Stg 3 500 - Stg 4 600 - Stg 5	400 - Stg 1 450 - Stg 2 500 - Stg 3 550 - Stg 4 400 - Stg 5	350 - Stg 1 400 - Stg 2 450 - Stg 3 500 - Stg 4 400 - Stg 5
Inlet Gas Velocity, ft/sec	0.42	0.33	0.3
Inlet Gas Composition	82% HF, 18% N_2	100% HF	100% HF
Avg HF Rate, lb/hr	6.0	8.1	6.5
HF/U Stoichiometric Ratio	2.7	2.6	2.0[a]
Avg Solids Residence Time, hr	10	8	7
Run Duration, hr	9.0	20.3	13.5 (reduction) 9.4 (hydrofluorination)

[a]Based on sodium and uranium.

It was intended that all stages in the reduction column be operated at 575 C. However, the heat required for the evaporation of water and other volatiles from the ore concentrate limited the maximum temperature of the top stage to 520 C in the first run and 400 C in the second. In the hydrofluorination reactor a temperature gradient from 350 C on the top stage to 600 C on the bottom was used in Run 1. In Run 2, however, the bottom stage temperature was reduced to 400 C to limit corrosion of the sintered Monel plate. At this temperature the bottom stage was probably ineffective, except for preheating the gas.

A moderately large excess of hydrogen fluoride was used - 2.6 times the stoichiometric ratio of hydrogen fluoride to uranium. A portion of the excess reagent was used in reaction with silica, iron, and other impurities.

The gas velocity used was about the minimum which would produce fluidization with a moderate amount of solids agitation (about 0.3 ft/sec. The gas velocity varied slightly from top to bottom of the reactor because of the differences in pressure and temperature and because of the volume change in the reaction (hydrofluorination). In addition, some variation in velocity occurred as a result of the change in reactor pressure as the off-gas filters became coated with solids. The reactor pressure was kept below 5 psig by occasional blowback of the filters.

b. Equipment Operability

No caking or sintering of the solids was observed in either the reduction reactor or the hydrofluorination reactor. However, on very infrequent occasions the solids appeared to cease flowing momentarily through one or another of the downcomers in either reactor. This evidenced itself by a small increase in stage differential pressure, which was assumed to indicate an increase in solids level in the bed. When this occurred (generally at widely spaced intervals of four to eight hours), the vibration produced by a few blows of a rubber-covered mallet was sufficient to resume solids flow. The use of the mallet is aesthetically displeasing, and it is hoped that further experimentation will uncover the source of this annoyance.

c. Particle Size Effects

The effect of the fluid-bed operations on the particle size of the feed material was studied to determine if there was a tendency for the solids to disintegrate by mechanical attrition or chemical reaction. Excessive production of fines is undesirable, since fine particles tend to be entrained in the gas and carried over into the filters. Table 16 gives the sieve analyses of the solids at various stages of treatment from ore concentrate to crude green salt. The results show a slight decrease in particle size. For example, the fraction larger than 60 mesh decreased from 33 per cent in the

Table 16

EFFECT OF REDUCTION AND HYDROFLUORINATION ON PARTICLE SIZE AND DENSITY OF ACID-LEACH CONCENTRATE

(Run OCP-2; see Table 15 for conditions)

	Percentage in Each Size Range				
Mesh Size	Ore Concentrate Feed	Top Reduction Stage	Reduction Product	Top Hydro-fluorination Stage	Hydro-fluorination Product
+40	8	0.7	0.9	0.2	0.4
-40, +60	24	15	20	8.5	7.9
-60, +100	23	26	28	29	24
-100, +200	19	27	24	36	36
-200, +325	19	20	17	19	24
-325	5	12	10	7.2	7.3
Bulk Density (g/cc)					
Untapped	1.6		2.9		2.5
Tapped	2.0		3.0		2.8

feed to 8.3 per cent in the hydrofluorinated product, while the fraction in the 100 to 200 mesh range increased from 19 to 36 per cent. Tests in a glass column showed that the fluidization quality of the reduced and hydrofluorinated products was better than that of the feed, probably because the free-flow characteristics were improved by removal of moisture.

A comparison of the product and top-stage sieve analyses for both columns showed very little difference in particle size, indicating no tendency for the fines to accumulate in the upper part of the reactor. Instead, the fines tended to be removed by the off-gas and carried into the filters. In both runs about 14 per cent by weight of the feed was carried out of the reduction reactor into the filter chamber, and an additional 3 to 12 per cent was carried into the hydrofluorination filters. Sieve analyses showed that the particle size of the solids in the reduction filters was almost identical to that of the solids in the reactor. This means that additional disengaging space is needed above the top stage to allow the coarser particles to separate from the gas.

The fines which collected in the hydrofluorination filters were smaller in size, being chiefly in the range from 200 to 325 mesh. Calculations based on Stokes Law showed that particles having a diameter of about 40 microns (325 mesh) or less would have a free-fall velocity less than the gas velocity at the top of the reactor, and would therefore tend to be removed from the fluid bed. Larger particles should not become entrained provided that sufficient disengaging space is furnished.

As shown in Table 16 the bulk density of the ore concentrate increased considerably in the reduction step, going from a tapped density of 2.0 g/cc to 3.0 g/cc. A slight decrease occurred in the hydrofluorination step, the product having a tapped density of 2.8 g/cc.

d. Chemical Conversion

The composition of the crude uranium tetrafluoride samples taken at intervals during the runs is listed in Table 17. Samples of the reduced product were also taken, but due to sampling and analytical difficulties the results are not reliable. These samples oxidize readily in air, and analysis is complicated by the presence of impurities. The data in Table 17 indicate that nearly complete conversion was obtained in both the reduction and hydrofluorination steps. Moreover, the analyses of samples taken from the stages of the hydrofluorination reactor at the completion of the runs (Table 18) show that the reaction was essentially completed in the top stage of the reactor, and that the remaining stages were unnecessary at the feed rates employed in these runs. This means that the reaction went virtually to completion at temperatures of 350 to 400 C with residence times of two to three hours. These pilot plant runs confirm the results obtained in the batch experiment (page 44), which showed that the ore concentrate has a very high chemical reactivity. It is likely, therefore, that the feed rate could be considerably increased above that used in Run 2, and that the excess of hydrogen fluoride could be substantially reduced without affecting the conversion.

As shown in Table 18, the fines which collected in the off-gas filters were highly converted to uranium tetrafluoride, the AOI being eight per cent in the first run and one per cent in the second. This material could, therefore, be blended with the product. As shown in Table 17 the sulfur was reduced to a very low value in the crude green salt (0.01 per cent or less), a decrease of about 80-fold from the ore concentrate. Analyses of the product from the reduction reactor showed that all of the sulfur removal occurred in the reaction step.

A summary of the impurity concentrations in the ore concentrate and hydrofluorinated product is given in Table 19. In addition to sulfur, a number of other elements, such as silicon, molybdenum, and vanadium, were considerably reduced in concentration by the treatment. The only impurities observed to have concentrations above 1000 ppm in the crude green salt are calcium, magnesium, and iron. Because of the relatively high purity of this uranium tetrafluoride, the final purification of this material by fluorination and distillation would appear to be highly practicable.

Table 17

COMPOSITION OF CRUDE GREEN SALT PRODUCT FROM PILOT PLANT RUNS ON ACID LEACH ORE CONCENTRATE

(For Run Conditions see Table 15)

Run OCP-1

Hours After Start	Total U (%)	U (+4) (%)	AOI (%)	Water Soluble U (%)	Sulfur (%)
2.5	72	70	4.4		0.01
3.5	74	71	1.6		
4.5	71	71	0.9		
5.5	73	70	1.6	0.9	0.01

Run OCP-2

Hours After Start	Total U (%)	U (+4) (%)	AOI (%)	Water Soluble U (%)	Fluoride (%)	Sulfur (%)
1.8	73	72	0.4			
5.8	72	70	0.2			
7.8	71	70	0.4		24	0.01
10.3	72	71	0.2		24	
12.3	73	70	0.4	0.9		
14.3	73	70	0.6		23	0.002
16.8	72	71	0.2	0.7		
18.8	72	71	0.9			
20.3	71	70	0.5	0.8	25	0.007

Table 18

COMPOSITION OF CRUDE GREEN SALT IN STAGES OF HYDROFLUORINATION REACTOR

(Samples taken at end of runs; see Table 15 for conditions.)

	Run OCP-1			Run OCP-2
Stage	Total U (%)	U (+4) (%)	AOI (%)	AOI (%)
1 (top)	71	71	2.6	0.4
2	72	70	0.8	0.3
3	72	71	1.0	0.3
4	72	70	1.1	0.4
5 (bottom)	70	70	0.6	0.4
Filters	69	69	8.1	1.0

Table 19

SUMMARY OF MINOR CONSTITUENT ANALYSES ON ACID-LEACH CONCENTRATE BEFORE AND AFTER TREATMENT

(Run OCP-2; see Table 15 for conditions)

	Analysis (ppm)			
	Ore Concentrate		Crude Green Salt	
Element	Spectrochemical[a]	Chemical	Spectrochemical[a]	Chemical
Al	3000		400	
As			< 10	
B			< 0.1	
Ca	2000		>1000	
Cu			200	
Fe	10,000	5300	>1000	
K	400		100	
Mg	2000	4000	>1000	
Mo		15	< 20	4
Na	1000	930	500	
Ni			70	
P		750	< 50	
Pb	1000		70	
Si	>1000	2300	15	
S		7800		70
V		250	< 10	

[a]Estimated accuracy of spectrochemical analyses is an order of magnitude.

6. Carbonate-Leach Concentrate

Processing of the carbonate-leach ore concentrate (primarily sodium diuranate) in the pilot plant was attempted, using the material which remained in the reactors after the completion of the acid-leach runs as the starting bed. As the solids in the reduction reactor were displaced by the carbonate-leach feed, the fluidization in the stages became progressively poorer and the solids flow became very erratic. The reduced product was observed to contain a substantial quantity of fines, some of which had aggregated into small balls. After 10 hr of operation it was necessary to discontinue the run. During this time the hydrofluorination unit operated well, but the feed entering this reactor was primarily acid leach material from the starting bed of the reduction column.

On dismantling the reduction reactor, the gas-distributor plates and downcomers were found to be partially plugged with fines. A sieve analysis of the bed of the top stage showed that the minus 200 mesh fraction had increased from 11 per cent to 36 per cent. Apparently the strength of the carbonate-leach particles is much less than that of the acid-leach particles. This might be expected since uranium trioxide, the major constituent of the acid-leach ore concentrate, is known to form hydrates which are capable of cementing into hard particles. Sodium diuranate, the major constituent of carbonate-leach ore concentrate, apparently does not have this property.

Despite the lower strength of the diuranate particles, it was felt that the amount of fines produced in the reduction reactor was more than might be expected from mechanical attrition. It seemed possible that disintegration might have occurred as a result of rapid vaporization of moisture from the particles in the top stage. It was therefore decided to dry the concentrate, remove the minus 200 mesh fraction, and use the oversize as feed to the pilot plant. Drying was performed in a batch-operated fluidized bed at 400 C, and the fines were removed in a continuous Sweco classifier. Removal of the fines was difficult due to frequent clogging of the 200 mesh screen.

a. Batch Experiment

Before resuming pilot plant operations, a batch run was made in the 3-in. diameter reactor to determine whether or not there was any further tendency for the dried and screened concentrate to disintegrate. The usual operating conditions were used, the reduction being three hours in duration and the hydrofluorination 5.4 hr. To avoid rapid initial reaction during hydrofluorination, a dilute mixture of hydrogen fluoride in nitrogen was introduced at 350 C; then, as the reaction progressed, the concentration and temperature were increased up to 60 per cent hydrogen fluoride at 500 C.

Samples were taken at $1\frac{1}{2}$-hr intervals and sieve analyses made. The results, listed in Table 20, show that there was no apparent change in the particle size during the run. Evidently the particles after drying had sufficient strength to withstand the reduction and hydrofluorination treatment without breakup.

In attempting to obtain reliable chemical analyses of the carbonate-leach hydrofluorinated product, difficulties were encountered because of the relatively high concentration of impurities, such as sodium and vanadium. The results obtained are listed in Table 20, but it should be pointed out that these are subject to potential error, since not all of the possible interferences by impurities have been checked. Moreover, the proper interpretation of the AOI and water-soluble uranium results is not well

understood, since the chemical behavior of the double salts of uranium and sodium in these analytical tests has not been studied. Although it appears that the AOI may represent an unhydrofluorinated uranium compound analogous to uranium dioxide in refined green salt, and that the water-soluble uranium may represent a hexavalent uranium oxyfluoride compound, analogous to uranyl fluoride, this is by no means known with assurance. To be safe the extent of hydrofluorination is best judged by the fluoride content, which in this run reached a maximum value of 26 per cent after 3.5 hr of hydrofluorination.

Table 20

RESULTS OF BATCH FLUID-BED RUN OF CARBONATE-LEACH CONCENTRATE

(Concentrate dried at 400 C before treatment.)

Reduction: 3 hr at 560 C
Hydrofluorination: 5.4 hr at 350 to 500 C
Gas Velocity: 0.6 ft/sec

Particle Size Analyses

		Percentage in Indicated Size Range						
		Reduction		Hydrofluorination				
Mesh Size	Ore Feed	1.5 hr	3.0 hr	1.5 hr	3.0 hr	4.5 hr	5.4 hr	Final Bed
+40	2.1	1.2	1.3	1.3	2.1	1.7	2.2	4.3
-40, +60	24	24	23	24	31	21	25	24
-60, +100	37	37	36	36	37	36	39	39
-100, +200	27	32	31	23	22	29	25	25
-200, +325	9.4	6.0	8.6	16	7.6	12	8.6	7.6
-325	0.3	0.3	0.1	0.1	0.0	0.1	0.1	2.4

Chemical Analyses - Hydrofluorination

Hours of Hydrofluorination	Total U (%)	U (+4) (%)	AOI (%)	U Content of AOI (%)	Water Soluble U (%)	Fluoride (%)
1	63	57	42	74		16
2	62	57	14	74		23
3.5	61	55	6.4	53	4.0	26
5.4	63	59	5.4	-	3.3	26

b. Pilot-Plant Operation - Carbonate-Leach Ore Concentrate

Since the batch experiment showed that particle disintegration could be diminished by prior drying of the carbonate-leach concentrate, a second attempt was made to operate the pilot plant using dried and screened concentrate. On this occasion difficulties of a different nature were encountered in the hydrofluorination reactor on start-up. While the reactors were heating up, a small flow of feed was introduced into the reduction reactor and the reduced-product overflow was fed to the hydrofluorination reactor. The top two stages of the latter reactor thus acquired a large percentage of unreacted solids by the time the hydrogen fluoride flow was started. When the hydrogen fluoride reached the upper stages, a temperature surge of over 100 C occurred in stages 1 and 2. Caking resulted in these stages and in the downcomers. The hydrofluorination reactor was therefore shut down, but the reduction reactor was maintained in operation for 13.5 hr until the feed was exhausted. The reduced product was collected in sealed containers for later use in hydrofluorination.

It was apparent that the hydrofluorination reactor would have to be started under conditions which would produce a less rapid initial reaction. Consequently, when the hydrofluorination reactor was again started up, hydrogen fluoride was slowly fed into the nitrogen stream as soon as the top stage temperature reached 250 C. The temperature and reagent concentration were then gradually increased to the desired values. With this procedure no difficulties were encountered, and the hydrofluorination reactor was operated for a period of 9.2 hr using the previously produced reduction product as feed. The operating conditions used in the reduction and hydrofluorination runs are given in Table 15.

c. Pilot Plant Results

Sieve analyses on the products (Table 21) confirmed the results of the batch experiment, which showed that little degradation of the particles occurred after the concentrate was pretreated by drying and screening. As with the acid-leach concentrate, the bulk density increased substantially, going from 2.2 g/cc in the concentrate to 2.9 in the hydrofluorinated product.

Prior to this run the hydrofluorination reactor was equipped with a disengaging chamber above the top stage to reduce the amount of solids carried over into the filters. The chamber was 12 in. in diameter and 12 in. long with the lower end flanged to mate to the top of the reactor. In this run the amount of fines collected in the filters was only 3.7 per cent by weight of the material fed to the reactor as compared to 12 per cent in the previous run (OCP-2) with acid-leach concentrate. The reduction column had not yet been equipped with an enlarged disengaging section for this run, and the solids collected in the filters amounted to 12 per cent of the feed.

Table 21

PARTICLE SIZE AND DENSITY OF CARBONATE-LEACH ORE CONCENTRATE BEFORE AND AFTER REDUCTION AND HYDROFLUORINATION IN PILOT PLANT

(Run OCP-3; see Table 15 for conditions.)

		Percentage in Indicated Size Range	
Mesh Size	Ore Feed	Reduction Product	Hydrofluorination Product
+40	1.2	8.5	1.8
-40, +60	24	24	12
-60, +100	37	30	25
-100, +200	32	26	41
-200, +325	6.0	10.2	17
-325	0.3	1.1	2.4
Bulk Density, g/cc			
Untapped	1.8	2.4	2.7
Tapped	2.2	2.5	2.9

The products of reduction and hydrofluorination of the diuranate ore concentrate were examined by X-ray diffraction to determine the nature of the compounds. The reduction product has not yet been characterized, since no pattern has yet been found to correspond to the one obtained with this material. The major constituent of the hydrofluorinated product has been identified as the compound 7 NaF · 6 UF_4. A melting point determination showed that this material melts at approximately 675 C, considerably lower than uranium tetrafluoride (960 C).*

The low melting point accounts for the ease with which the carbonate-leach concentrate cakes during rapid reaction. Sintering occurs at temperatures much below the melting point unless the solids are agitated. In the pilot plant reactor the agitation of the fluidized bed prevented caking even at a bed temperature of 500 C (lower stage).

The results of chemical analyses of the product samples are given in Table 22. These are subject to the reservations previously mentioned. The fluoride analysis is believed to be reliable, and an estimation of the extent of conversion should probably be based on this element. The fluoride content attained a value of about 25 per cent, which is somewhat lower than that obtained in the batch experiment (about 26 per cent). The theoretical fluoride content of 7 NaF · 6 UF_4 is 27 per cent.

*X-ray studies performed by S. Flikkema; melting point by O. Sandus.

Table 22

CHEMICAL ANALYSES ON PRODUCT PILOT PLANT RUN ON CARBONATE-LEACH ORE CONCENTRATE

(Run OCP-3; see Table 15 for conditions.)

Product Samples

Hours After Start	Total U (%)	U (+4) (%)	AOI (%)	U Content of AOI (%)	Water Soluble U (%)	Fluoride (%)	Sulfur (%)
3	67	60	3.4	44		21	0.01
4	66	58	3.3	47			
5	66	58	3.3	40	8.6	26	0.02
6	66	60	2.5	43			
7	65	55	5.2	50	9.5	24	0.02
8	63	54	5.9	57			
9	65	59	5.0	55		25	0.02

Stage Samples - (end of run)

Stage	AOI (%)	U Content of AOI (%)
1	16	73
2	8.1	59
3	8.3	55
4	6.6	56
5	6.9	50
Filters	9.3	63

The sulfur content of the carbonate-leach concentrate was already low (0.04 per cent), and this was reduced about twofold to 0.02 per cent in the hydrofluorinated product.

7. Corrosion Tests - Ore Concentrate Runs

In order to obtain preliminary corrosion data on materials of construction for the processing of uranium ore concentrates to crude green salt, metal coupons were placed in each bed of each reactor. Three types of stainless steel, 304, 309 and 347, were tested in the reduction column, and Monel, Inconel and Hastelloy B in the hydrofluorination column. The coupons were wired to rods with nichrome wire and inserted into the fluidized-solids phase through a 1/2-in. pipe opening. After about 80 hr of exposure under process conditions, one complete set of samples were removed. The

other set was placed back in the columns for additional exposure. Due to the short exposure period only a preliminary comparison of the metals can be made at this time. The results listed in Table 23 are reported as weight change for the exposure period, since extrapolation of the data to mils per year would be presumptuous.

Table 23

RESULTS OF CORROSION TESTS IN PILOT PLANT RUNS ON URANIUM ORE CONCENTRATE

(Total exposure time about 80 hr; see Table 15 for run conditions.)

Reduction Reactor

Location in Reactor	Temp of Stage, C	Dimensional Change, mils		
		304 SS	309 SS	347 SS
Stage 1	a	0.009	0.008	0.028
Stage 2	575	0.053	0.022	0.017
Stage 3	575	0.011	0.033	0.049
Stage 4	575	0.021	0.016	0.031

Hydrofluorination Reactor[b]

Location in Reactor	Temp of Stage, C	Dimensional Change, mils		
		Monel	Inconel	Hastelloy B
Stage 1	350 to 400	4.1	0.17	0.18
Stage 2	400 to 450	0.48	0.087	0.13
Stage 3	450 to 500	0.38	0.059	0.093
Stage 4	500 to 550	0.030	0.053	0.022
Stage 5	400 & 600[c]	0.018	0.094	0.11

[a]Temperature varied depending upon feed rate from 350 to 575 C.

[b]Includes 14 hr of hydrogen reduction in this reactor during start-up.

[c]Includes about 30 hr at 600 C, the remaining 50 hr at 400 C.

The stainless steel coupons were washed in boiling distilled water and hot 10 per cent nitric acid solutions to remove the uranium oxide film before drying and weighing. The coupons from the hydrofluorination column were subjected to a more vigorous cleaning procedure to remove

the adhering uranium fluoride films. These were washed in boiling water, then 10 percent nitric acid at 60 C for three minutes, then three times in boiling saturated ammonium oxalate solution with hand brushing between solutions. Blanks were tested in these solutions to make sure weight loss would not be high enough to distort the data. Blank losses for the Hastelloy B, Inconel, and Monel in the 10 per cent nitric bath were 2.7, 0.2, and 2.2 mg, respectively. After three ammonium oxalate baths, only the blank Hastelloy B coupon showed weight loss, 0.6 mg.

From the data, it is apparent that there were about equal and small weight losses for all the stainless steels tested, the highest being 0.053 mil for the 347 coupon in stage 2, and the majority being below 0.030 mil for the exposure time of 80 hr. There were no gross changes in the appearance of any of the metals, except for a darker appearance for all of the coupons from stage 1.

The coupons in the hydrofluorination reactor clearly showed a greater corrosion rate in the upper stages than in the lower. This may be due to the presence of higher water concentration and/or higher gaseous impurity concentrations of the upper stages. Corrosion rates were low for all three metals in the lower stages, but Inconel and Hastelloy B were clearly superior to Monel in the upper stage. It is possible, however, that much of the Monel corrosion occurred during the start-up hydrogen-reduction period in this reactor (see page 50), since the sulfur concentration in the gas would be high in this operation.

8. Direct Preparation of Uranium Metal from Crude Green Salt

The moderately high purity of the crude uranium tetrafluoride produced from acid-leach ore concentrate prompted academic interest in determining whether or not uranium metal of moderate purity could be prepared directly from this material. Accordingly, a mixture of the crude green salt and magnesium metal, totaling about 1200 g, was allowed to react in a graphite crucible inside a stainless steel bomb. The uranium button was removed and separated from the slag. A sample of the metal was mounted in plastic, polished, etched, and examined microscopically. The metal appeared to consist of uranium crystals occupying about 90 to 95 per cent of the area in a matrix which probably contained uranium, iron, and aluminum. A spectrochemical analysis of the uranium showed iron and aluminum to be less than 1000 ppm each, copper 200 ppm, nickel 70 ppm, calcium, potassium and magnesium less than 50 ppm each, and molybdenum less than 20 ppm. The boron content was 0.5 ppm. Though the uranium metal appears to be moderately pure, it is substantially below nuclear reactor grade as would be expected.

B. Waste Calcination

(J. Loeding, W. Pehl, C. Schoffstoff, H. Brown)

Several shakedown runs, with inactive solutions were completed to test the operation of the shielded waste calciner. One run with low activity level (1 to 1000 dilution of ICPP IAW solution) was also made. A small amount of installation work remains to be completed before runs of higher activity level can be made. This involves primarily the installation of equipment for remotely removing the solid product from the calciner into a storage area.

1. Equipment Description

A schematic layout of the calcination equipment is shown in Figure 5. The calciner itself is similar in design to the one used in previous studies (see ANL-5290, pages 114 to 118); however, some alterations and improvements have been made. The tubular electric heaters on the outside wall are bonded to the stainless steel shell with sprayed copper metal to improve heat conduction and reduce the heater sheath temperatures. A number of thermocouples are installed on the heater sheaths and in the reactor wall.

Two spray nozzles are installed in the calciner, the second unit being a spare in the event that the first becomes inoperative. Both nozzles are equipped with clean-out needles, which are sealed by flexible bellows. Waste solution is pumped to the spray nozzle by a Lapp Pulsafeeder having a remote, shielded head. The flow rate is measured by a calibrated, automatic rate bulb.

The number of porous filters for dust removal has been increased to ten in this unit. The filters are divided into five banks of two filters each, four banks being in operation while one is blown back. To reduce the possibility of leakage of radioactive gases and dust, a slight vacuum is maintained in the calciner by means of a steam jet exhauster. The off-gases and the steam from the steam-jet pass through two condensers and an entrainment separator before being exhausted to the vent duct.

Both the top and the bottom of the calciner are flanged to permit access to the filters and the porous gas distributor, if this becomes necessary. The top flange is provided with quick-opening clamps to reduce the time required for flange removal.

Solids may be removed from the calciner either through an overflow pipe at the top of the bed or from the bottom through a slide valve. The solids are temporarily retained and cooled in a chamber equipped with a cooling coil, then discharged through a plug valve into an expendable container.

FIGURE 5.

SCHEMATIC OF EXPERIMENTAL SHIELDED WASTE CALCINER.

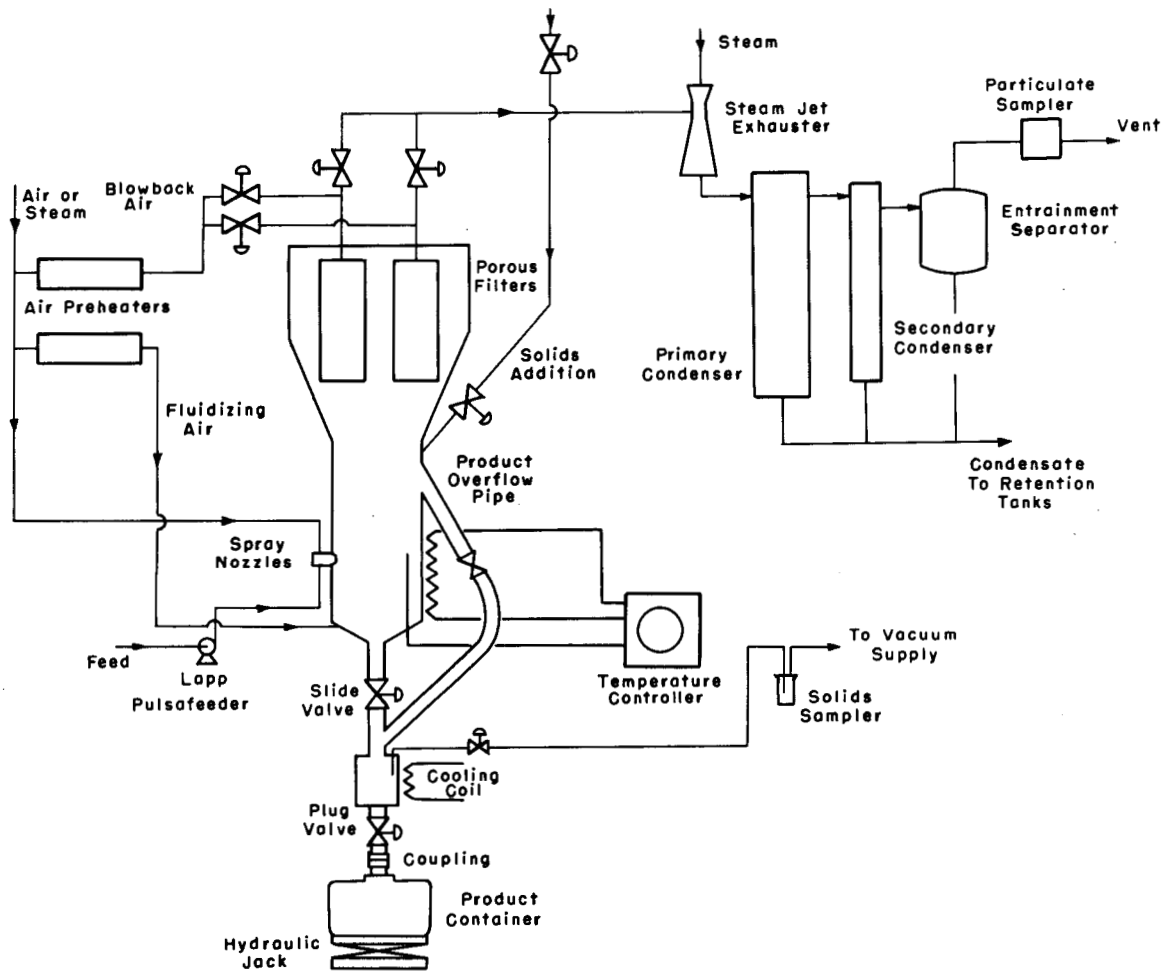

The latter will be remotely uncoupled and transferred to a shielded cask for removal to the burial grounds or other disposal. Samples of the solids may be removed from the cooling chamber by vacuum transport into an evacuated bottle.

Photographs showing various portions of the experimental, shielded calciner are shown in Figures 6 to 9.

2. Shakedown Runs

Four shakedown runs, totaling 20 hr of operation, were made with inactive solutions to test the equipment. These were followed by a run with radioactive solution prepared by dilution of three-year old Idaho CPP waste with aluminum nitrate-nitric acid solution in the ratio of one part active waste to 1000 parts of inactive solution. A feed rate of about five liters per hour

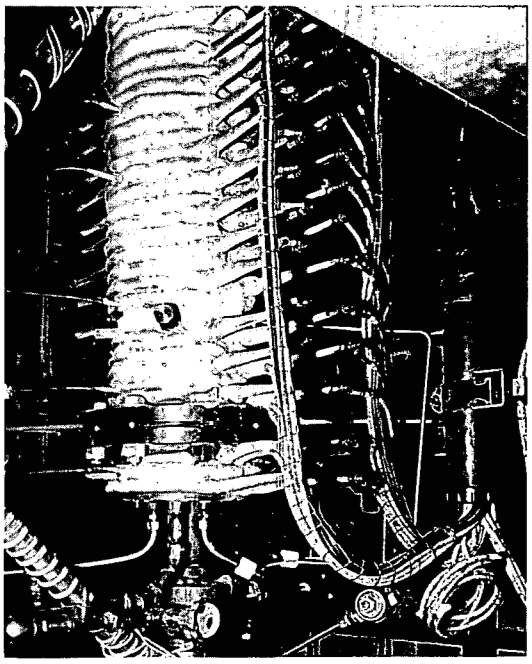

Figure 6

REACTION CHAMBER OF WASTE CALCINER, SHOWING ELECTRIC HEATERS COVERED WITH SPRAYED COPPER METAL. SOLID PRODUCT OVERFLOW PIPE IS AT THE LEFT.

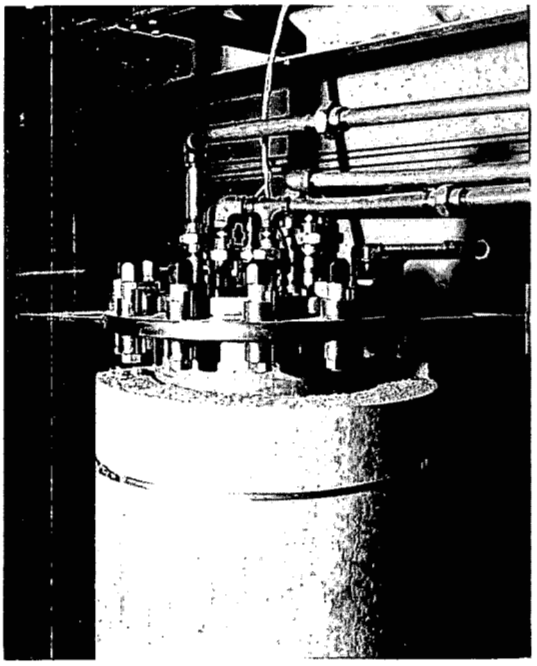

Figure 7

TOP OF WASTE CALCINER, SHOWING QUICK-OPENING CLAMPS ON COVER FLANGE.

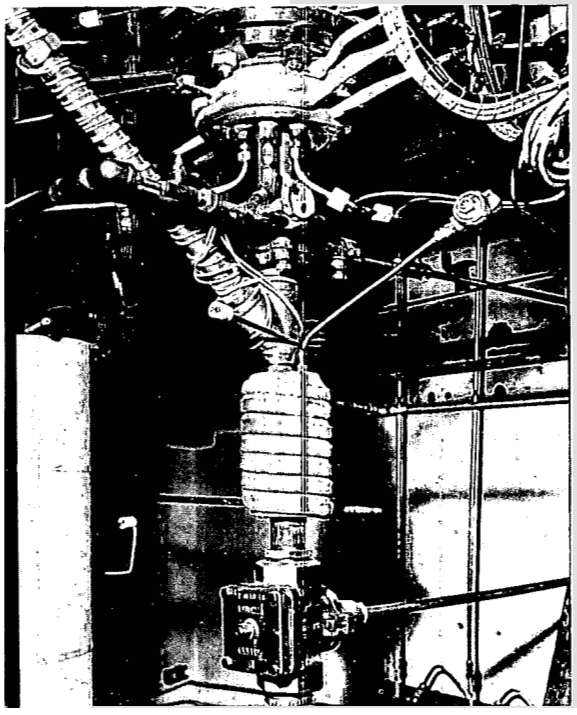

Figure 8

BOTTOM OF WASTE CALCINER, SHOWING PRODUCT REMOVAL VALVES AND SOLIDS COOLING CHAMBER.

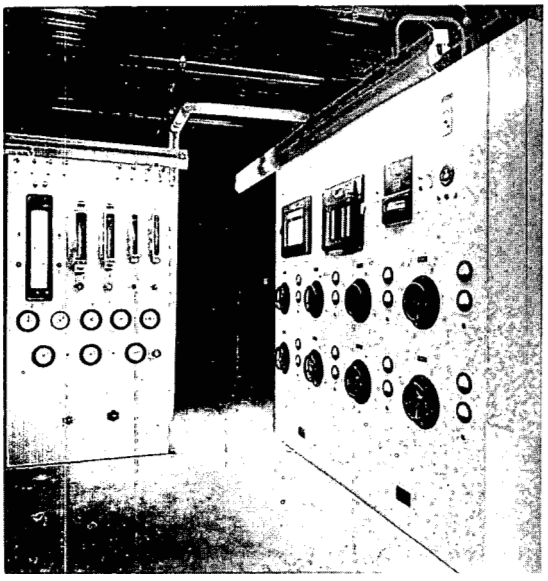

Figure 9

WASTE CALCINER OPERATING PANELBOARD.

was used, and the calcination temperature was 400 C. Duration of the run was 7.5 hr. Analytical data from this run are not yet available, and results will be reported in the next Quarterly Report. The solids reached an activity level of 225 mr/hr at the exterior surface of the glass container.

The shakedown runs showed that the sprayed copper metal on the electric heaters considerably improved the heat transfer characteristics. The temperature of the heater sheaths seldom exceeded the fluidized bed temperature by more than 100 C. The use of five filter banks for the off-gas resulted in a more constant pressure in the reactor than was possible in the first calciner, which used two filter banks. During operation the calciner pressure varied from 0 to 5 in. of mercury vacuum between filter changes.

The shakedown experiments also showed that the entrainment separator, which consists of a chamber packed with stainless steel wool, did not adequately remove entrained condensate droplets. Other de-entrainment devices, including a cyclone separator, will be tested.

During the next quarter it is planned to continue runs with active solutions, gradually increasing the radiation level of the feed to the maximum which can be safely tolerated.

III. REACTOR CHEMISTRY

A. Metal Oxidation and Ignition

(P. J. Pizzolato, H. A. Porte, J. G. Schnizlein, R. C. Vogel, J. Bingle, D. Fischer, L. Mishler, A. Porter, R. F. Testin*)

The program to elucidate the factors governing the pyrophoric characteristics of uranium, zirconium, thorium and plutonium is being pursued by means of a study of the kinetics and mechanism of oxidation of these metals. Previous pertinent reports from this laboratory are as follows: Program approach and uranium oxidation literature survey, ANL-5494, pages 104 to 109; apparatus, uranium analysis, surface preparation and preliminary rate data, ANL-5602, pages 65 to 77; preliminary pressure dependence and preliminary electron micrographs, ANL-5633, pages 81 to 90; base-line uranium oxidation data, pressure and temperature dependence and metallurgical variables, ANL-5668, pages 51 to 62; zirconium oxidation literature survey, ANL-5602, pages 77 to 86.

The base-line data for uranium oxidation have been completed. Oxidations were conducted at temperatures of 125 to 295 C in 20 to 800 mm oxygen pressures. Activation energies have been calculated from an Arrhenius equation and were found to be surprisingly pressure dependent. Work is underway to determine the influence of low concentrations of certain alloying agents and contaminants. Direct observation of accelerated oxidations or ignitions has been initiated. The influence of gas concentrations and contaminants will be studied with the Stanton thermobalance.

The base-line runs for arc-melted Grade I crystal bar zirconium available at ANL have been completed in the temperature range of 400 to 900 C in oxygen at 200 mm oxygen pressure. The zirconium oxidation seems to obey the cubic rate law $W^3 = kt$; an activation energy of 42.5 kcal/mole has been found on the basis of this rate law.

A literature survey of the oxidation of thorium has been completed. The disagreement of various investigators in observed rate laws, activation energies and in experimental rate constants is similar to the case for uranium.

1. Uranium

The base-line data have been completed with oxidations of uranium at temperatures of 125 through 295 C and in pressures of oxygen of 20, 50, 200 and 800 mm. Efforts are now being devoted to experiments which may elucidate the mechanism of reaction, study of the influence of certain alloying agents and common contaminants, and direct observation of ignition temperatures.

*Cooperating institution student from Detroit University.

a. Base-Line Oxidation Data

Additional runs have been completed in 800 mm oxygen pressure at 150, 200 and 250 C to complete the base-line data. The rate data are presented in Table 24. These data supersede those presented in Table 18 in ANL-5668. In conjunction with Tables 15, 16, and 17 of ANL-5668, this report constitutes the entire base-line data on the oxidation of uranium at temperatures 125 through 295 C in pressures of 20, 50, 200 and 800 mm oxygen.

An Arrhenius plot of the first stage rates in 800 mm oxygen pressure is shown in Figure 10, the second stage rates in 800 mm in Figure 11.

The data for the first stage rates (125 through 295 C) and for the second stage rates (125 through 200 C) were fitted to an Arrhenius equation of the type

$$\log K = \log A - \frac{\Delta E}{2.303\ RT}$$

by the method of least squares. The resulting equations, in which K_I is the first stage linear rate constant and K_{II} is the second stage linear rate constant, are as follows:

$$\log K_I = 8.4940 - 4.096\ (1/T)$$

$$\log K_{II} = 10.3214 - 4.476\ (1/T).$$

From these data the activation energies with their standard deviations and the constant, A, are the following:

$$\Delta E_I = 18.7 \pm 2.4 \text{ kcal/mole}$$

$$A_I = 3 \times 10^8$$

$$\Delta E_{II} = 20.5 \pm 0.9 \text{ kcal/mole}$$

$$A_{II} = 2 \times 10^{10}$$

The standard deviation is larger than those calculated at other pressures because of the reduced precision in determination of rates at this higher pressure.

Comparisons in Table 25 with the activation energies for 20, 50, and 200 mm (previously reported in ANL-5668, pages 52 and 54) show a pressure dependence. The theoretical significance of this is not clear at this time.

Table 24

OXIDATION OF URANIUM IN 800 mm OXYGEN PRESSURE

Analytical, metallurgical and surface preparation data given in ANL-5602 pages 67 to 71.
Oxidation data at 20, 50 and 200 mm given in ANL-5668, pages 53 to 54.

	First Stage Rate			Second Stage Rate			Break Weight[a]			Break Time[a]		
Temp (C)	μg/(sq cm)(min)	Avg Dev Mean %	No. Runs	μg/(sq cm)(min)	Avg Dev Mean %	No. Runs	μg/(sq cm)(min)	Avg Dev Mean %	No. Runs	min	Avg Dev Mean %	No. Runs
150	0.088	-	1	0.56	12.5	4	48	-	1	549	-	1
200	0.66	36	5	7.4	15.	6	61	15	5	108	27	5
250	5.8	25	2	40.[c]	1.8	2	83	48	2	15	33	2
295	-[b]	-	-	225.[c]	-	1	-[b]	-	-	-[b]	-	-

[a] Intersection of extrapolated first and second stage rates.

[b] Unable to distinguish satisfactorily to date.

[c] Rate decreases.

FIGURE 10.

ARRHENIUS PLOT OF FIRST STAGE RATE vs INVERSE TEMPERATURE 800 mm OXYGEN PRESSURE.
(Average deviation from the mean indicated by the bar above and below the average point)
ΔE_{act} = 18.7 ± 2.4 kcal/mole

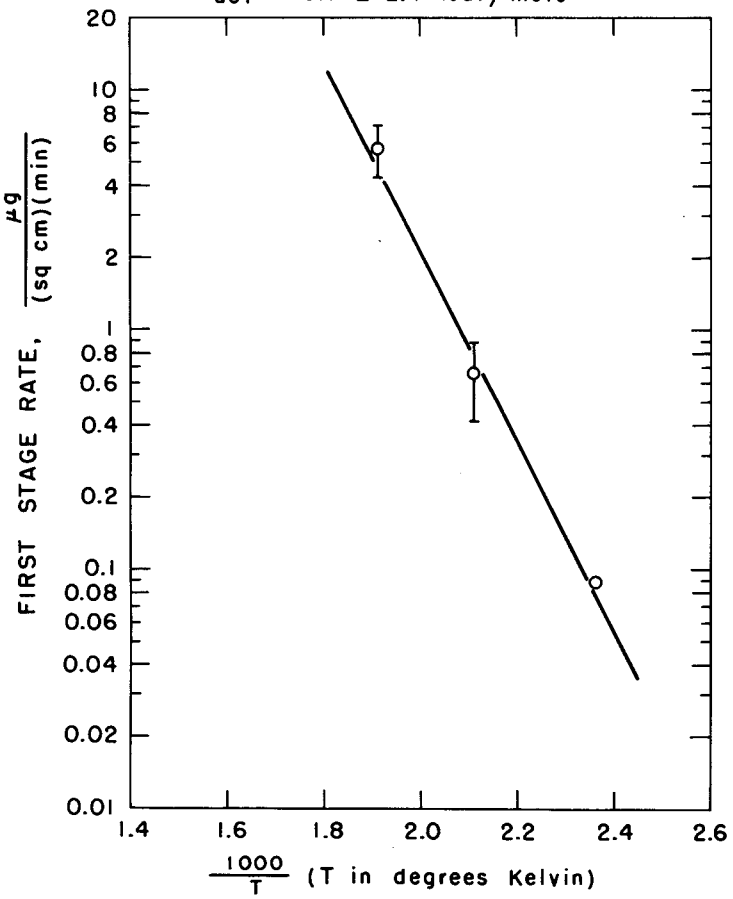

FIGURE 11.

ARRHENIUS PLOT OF SECOND STAGE RATE vs INVERSE TEMPERATURE 800 mm O_2 PRESSURE.
(Average deviation from the mean indicated by the bar above and below the average point)
ΔE_{act} = 20.5 ± 0.9 kcal/mole

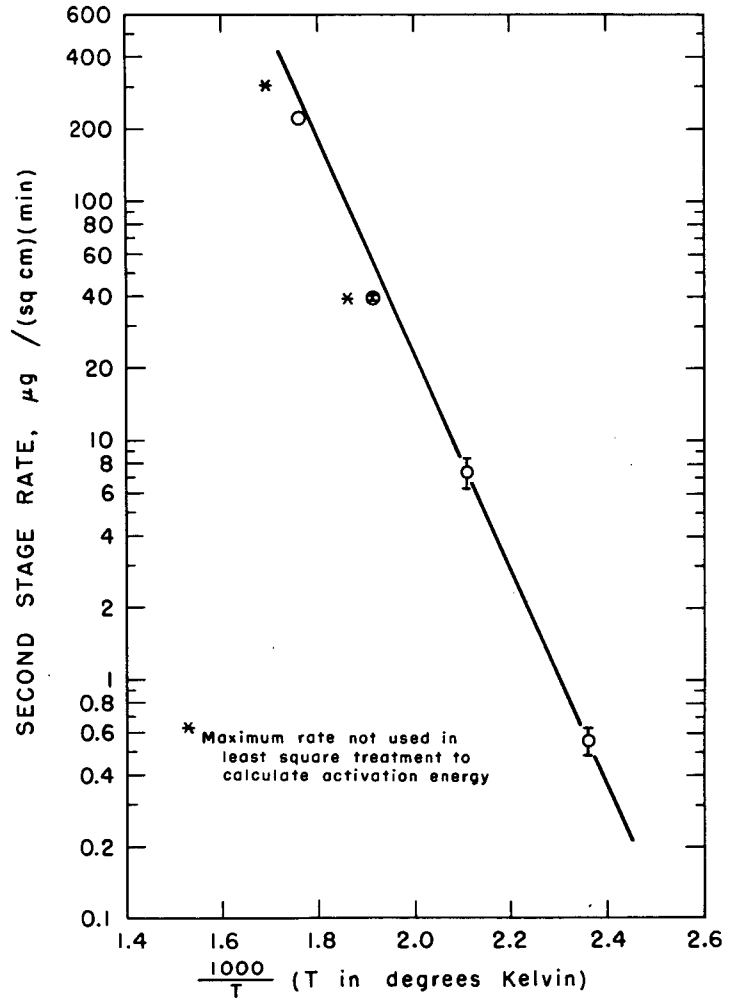

Table 25

ACTIVATION ENERGIES FOR THE OXIDATION OF URANIUM AT 125 THROUGH 295 C IN 20, 50, 200 AND 800 mm OXYGEN

(Constants determined by the method of least squares.)

Oxygen Pressure (mm)	ΔE (kcal/mole)[a]	A, μg/(sq cm)(min)
	FIRST STAGE	
20	12.4 ± 0.9	1.7×10^5
50	12.6 ± 0.7	2.4×10^5
200	15.0 ± 0.6	5.3×10^6
800	18.7 ± 2.4	3×10^8
	SECOND STAGE[b]	
20	16.8 ± 0.7	2.0×10^8
50	18.2 ± 0.3	1.4×10^9
200	19.9 ± 0.5	1.0×10^{10}
800	20.5 ± 0.9	2×10^{10}

[a]The accuracies expressed are standard deviations.

[b]Based on rate data for 125 to 200 C only.

b. Dr. D. Cubicciotti's Uranium Sample

The opportunity to observe the oxidation rates of the sample of uranium that Dr. D. Cubicciotti used in his study[6] was graciously offered to us. Oxidation studies of his sample in our apparatus therefore offer the unusual opportunity to reconcile the results of two independent investigations.

The apparatus used in his work was similar to ours in that it utilized volumetric measurement of oxygen consumption. His sample was in the form of a 1-cm diameter rod, 8.3 cm long (approximately 25 sq cm surface), whereas we have used 1-cm cubes (approximately 6 sq cm surface). No specific analysis of his sample was reported by Dr. Cubicciotti other than 99.5 per cent purity. Recent analysis has shown a total of more than 1500 ppm impurities (see Table 26). Analysis of representative cubes have shown a total of about 300 ppm impurities (reported in ANL-5602, pages 65 to 86).

[6]D. Cubbicciotti, "The Reaction Between Uranium and Oxygen," J. Am. Chem. Soc. 74, 1079 (1952).

Table 26

SPECTROGRAPHIC ANALYSIS OF
DR. D. CUBICCIOTTI'S URANIUM ROD

Element	ppm
Si	80
Fe	>1000
Ni	100
Al	10
Cr	200
Mn	80
Mg	3
Cu	15
Na	40
Pb	2

The following elements less than their listed limit of detection: Ag 1, As 10, B 0.1, Be 0.5, Bi 1, Ca 20, Co 5, K 20, Li 1, Mo 20, P 50, Sb 1, Sn 5, Ti 50, Zn 50.

The surface preparation reported for the uranium rod was by abrasion with 400 emery cloth. The usual surface preparation for the cubes had been electropolish, although other surface preparations were tested (ANL-5602, pages 69 to 74).

Oxidations of the rod have been done at 150 C and 200 C with both a 600 grit silicon carbide (dry) polished surface and electropolished surface. The first and second stage rates observed are compared with observations from runs on our cubes with similar conditions in Table 27. Graphic comparisons are presented in Figures 12, 13, 14, and 15.

The following observations are noted.

(1) Comparison of the first stage data for D. Cubicciotti's sample with surface prepared by 600 grit and electropolish (Figure 12) at 200 C suggest that his data (J. Am. Chem. Soc. 74, 1078 (1952)) are based on a surface polish closer to our electropolish. The reported "400 grit emery" may be erroneous. A likely polishing agent would be 4/0 emery.

(2) At 200 C the first stage rates for our cube and D. Cubicciotti's sample are essentially alike when polished with 600 grit (Figure 12). Both show linear rates of similar values. However, with electropolished surfaces our cubes oxidize more slowly. Examination of

FIGURE 12.
FIRST STAGE OXIDATION OF URANIUM
AT 200 C IN 200 mm OXYGEN PRESSURE.

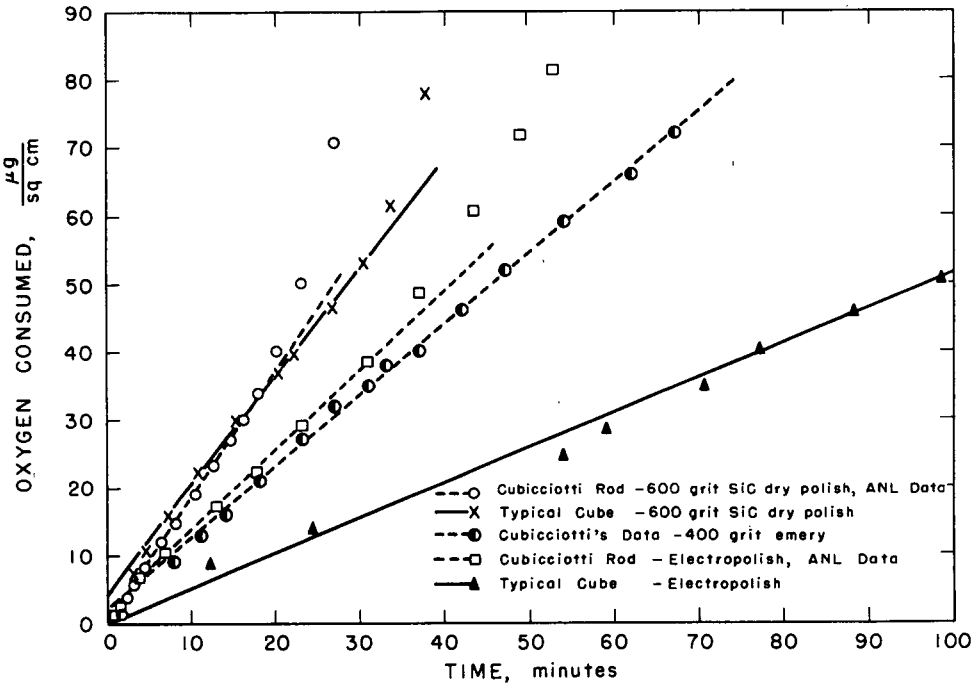

FIGURE 13.
SECOND STAGE OXIDATION OF URANIUM
AT 200 C IN 200 mm Hg OXYGEN PRESSURE.
ANL DATA

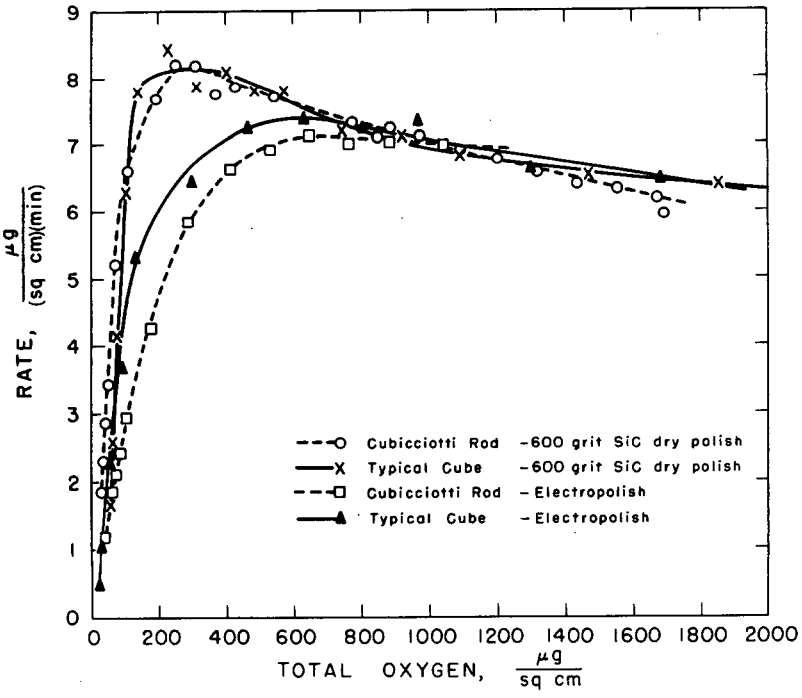

FIGURE 14.
FIRST STAGE OXIDATION OF URANIUM
AT 150 C IN 200 mm Hg OXYGEN PRESSURE.

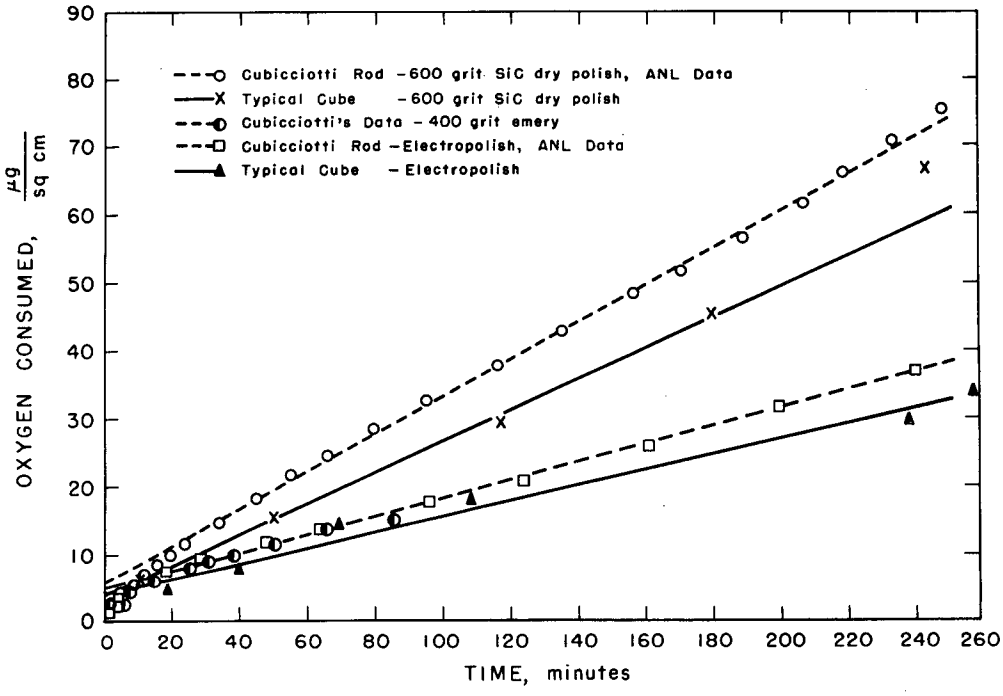

FIGURE 15.
SECOND STAGE OXIDATION OF URANIUM
AT 150 C IN 200 mm Hg OXYGEN PRESSURE.
ANL DATA

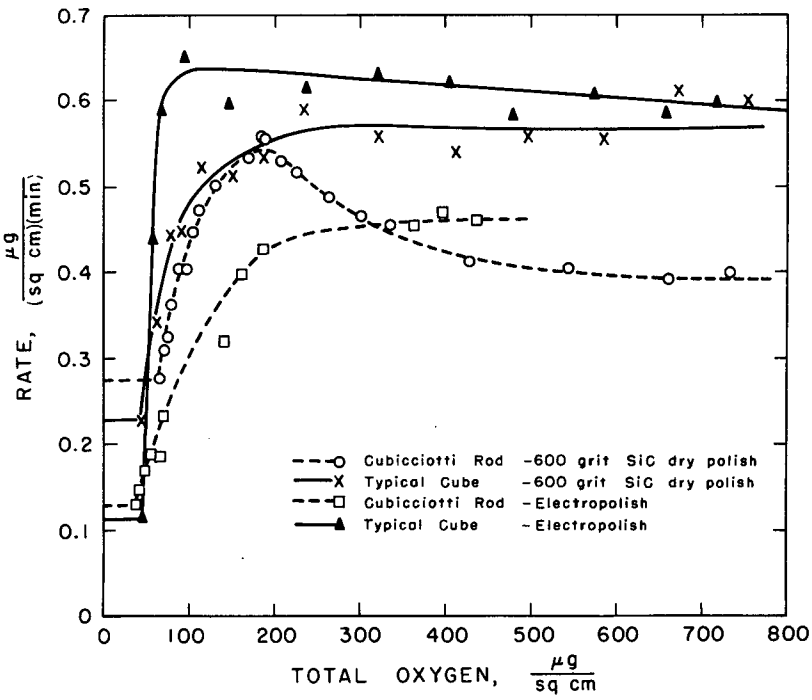

Table 27

COMPARISON OF ROD AND CUBE OXIDATIONS IN 200 mm OXYGEN PRESSURE

(Rates in $\mu g/(sq\ cm)(min)$)

Sample	Surface Preparation	150 C First Stage	150 C Second Stage	200 C First Stage	200 C Second Stage
Cube	600 Grit Dry	0.23	0.56	1.65	8.2
Rod	600 Grit Dry	0.28	0.54	1.86	8.2
Rod	400 Grit Emery[b]	0.13[a]	-	1.05[a]	-
Rod	Electropolish	0.13	0.47	1.17	7.0
Cube[c]	Electropolish	0.11 ± 0.2	0.60 ± 0.05	0.49 ± 0.03	6.6 ± 0.6

[a]Our estimation of linear type rate from reported 150 C parabolic data (J. Am. Chem. Soc. 74, 1079 (1952)). At 200 C the first stage is reported by Cubicciotti as linear.

[b]It is suspected that 4/0 emery, which produces a smoother surface than 600 grit, was actually used instead of 400 grit emery.

[c]Avg base-line data.

the rod showed a fair number of pin holes and voids in the casting. Measurement of weight and volume give density of the rod as 18.2, as compared to the density of a cube of 18.8 and the theoretical density of 19.0. This would make the true area greater than the measured area and therefore the rates might appear higher.

(3) The second stage oxidation at 200 C (Figure 13) shows remarkable agreement. The dry abraded surfaces show somewhat higher maximum rates, but the rates fall to the same value as those for electropolished samples. This figure indicates quite clearly good agreement for uranium from two different sources if the surfaces are prepared in the same manner.

(4) At 150 C the first stage oxidation data (Figure 14) shows the influence of surface treatment as discussed above (1).

(5) Dr. Cubicciotti suggested that a parabolic rate law was the proper interpretation of his data. His runs were generally of about 100 min or less. If only the first 100 min of our runs at 150 C are considered, the agreement with the parabolic rate law is satisfactory. However, continuation for longer periods of time causes closer agreement to the

linear rate law. We have selected the rate law which fits the data over the long period and have chosen to call the early parabolic-type behavior a deviation from the linear rate law. A fact that supports the linear rate law interpretation of long duration data is that at 125 C and at both 125 or 150 C in lower pressures (where the volume measurements yield somewhat greater precision in rates) the fit to linear is better than to parabolic rate law. The rate law selected for the first stage at 150 C is definitely dependent, however, on the length of time considered.

Since there is some tendency toward a parabolic rate, it is suspected that the fit to a parabolic law might become better at lower temperatures.

(6) The second stage rate curve at 150 C (Figure 15) illustrates agreements similar to that observed at 200 C.

c. Oxidation of Alloys

Alloys of iron, silicon, aluminum, carbon, nitrogen, molybdenum, copper, ruthenium, zirconium, beryllium and niobium in concentrations of 0.5, 1 and 2 atom per cent are being oxidized. We will determine if these elements (the first five are common impurities) in low concentrations influence the oxidation rate of uranium.

Analysis of 35 castings obtained from Battelle Memorial Institute is underway for carbon, nitrogen, oxygen, hydrogen, the specific alloying agent, and trace elements. Metallographic examination is being undertaken by A. Porter and M. D. Odie.* Testing of homogeneity has been completed for the heavy metals by means of X-ray emission by D. S. Flikkema and R. Schablaske.

d. Direct Ignition

An attempt to determine directly an "ignition temperature" for uranium metal has been initiated. Although a clear definition of "ignition" has not been formulated, the oxidation behavior under conditions which are expected to produce accelerated reactions will be observed.

e. Proposed Studies

The Stanton thermobalance is being calibrated and prepared for use in the study of uranium oxidation by gravimetric means in slowly flowing gas streams. The influence of such gas variables as oxygen concentration, air, water vapor and other gas contaminants will be observed.

---

*Metallography Section of Metallurgy Division, Argonne National Laboratory

2. Zirconium

A number of runs have been made on zirconium in the temperature range 400 to 900 C at an oxygen pressure of 200 mm. A chemical and spectrochemical analysis was made on the arc-melted, grade I crystal bar zirconium used in this series of runs. These data are given in Table 28. The oxygen used was taken directly from the tank without further purification. Mass spectrographic analysis showed the following impurities: A, 0.09 per cent; CO_2, 0.08 per cent; H_2O, 0.1 per cent; N, 0.56 per cent.

Table 28

ANALYSIS OF ZIRCONIUM

Element[b]	ppm	Element	ppm
Al	10	N[a]	23
C[a]	79	Ni	100
Cu	5	O[a]	185
Fe	800	Pb	4
Mn	1	Si	50

[a]Chemical analysis for C, N, O; all other elements analyzed by spectrochemical analysis.

[b]Following elements less than their listed limit of detection: Ag 1, As 10, B .1, Ba 10, Be .5, Bi 1, Ca 100, Ce 1000, Co 5, Cr 1, Dy 200, Er 100, Eu 50, Gd 1000, Hf 1000, Ho 500, K 20, La 50, Li 1, Lu 10, Mg 1, Mo 20, Na 10, Nd 500, P 50, Pr 500, Tb 500, Th 1000, Ti 50, Tm 500, V 20, W 200, Y 10, Yb 10, Zn 50.

The zirconium specimens were machined parallelepipeds, 1 x $1\frac{1}{2}$ x 2 cm. The reaction rate was found to obey the expression $W^n = kt$, since a plot of log W (log weight gain/sq cm) versus log t (log time) produced a straight line at all temperatures as illustrated by typical runs in Figure 16. The slope of the line in this type of plot is 1/n, where n is the exponent of W in the above rate expression.

From the values of 1/n listed in Table 29 it is seen that the reaction rate is best expressed by the cubic rate law, $W^3 = kt$. The cubic rate law constants were obtained from plots of W versus $t^{1/3}$. Typical runs at different temperatures are shown plotted in this manner in Figure 17.

FIGURE 16.

REACTION OF ZIRCONIUM WITH OXYGEN

(O_2 Consumed / sq cm vs Time)

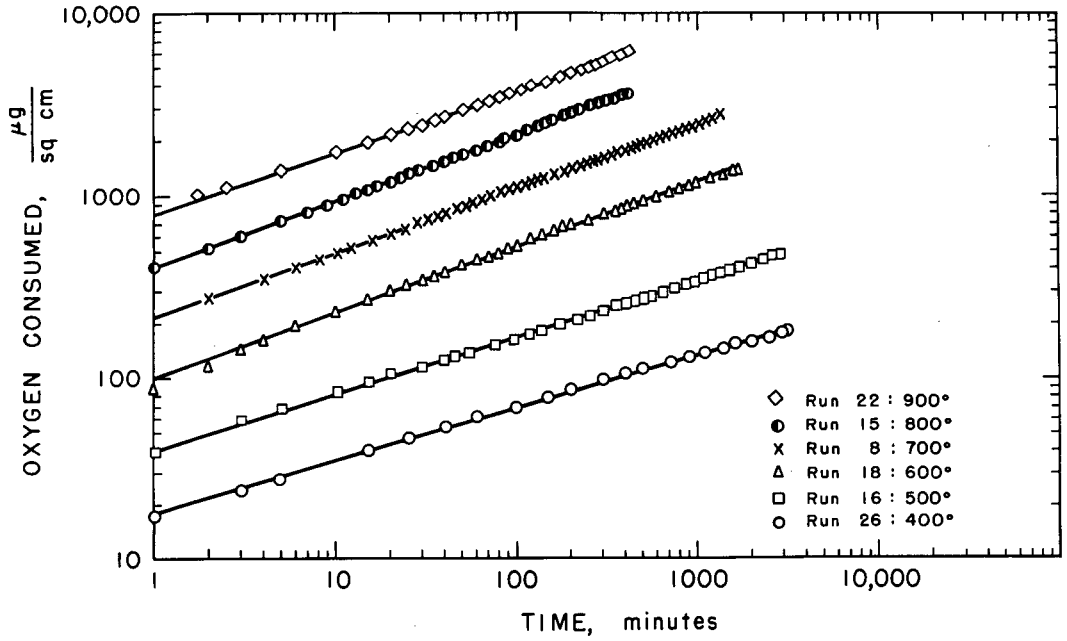

Table 29

CUBIC RATE CONSTANTS FOR THE REACTION OF ZIRCONIUM WITH OXYGEN

Temperature (C)	Length of Run, min	Slope of Log-Log Plot, 1/n	Rate Constant (K), $(\mu g)^3$ $cm^{-6}min^{-1}$
400	3235	0.29	1.6×10^3
400	4275	0.29	5.6×10^2
500	2860	0.32	3.6×10^4
500	4238	0.30	3.5×10^4
600	1660	0.33	1.6×10^6
600	4250	0.34	8.9×10^5
700	1323	0.35	1.7×10^7
700	1345	0.36	1.3×10^7
700	400	0.36	1.6×10^7
700	1408	0.36	1.4×10^7
800	413	0.38	1.3×10^8
800	415	0.39	1.3×10^8
800	400	0.37	1.3×10^8
900	400	0.31	5.3×10^8
900	418	0.34	5.3×10^8

FIGURE 17.
REACTION OF ZIRCONIUM WITH OXYGEN.
(μg O_2 consumed per sq cm vs (TIME)$^{1/3}$)

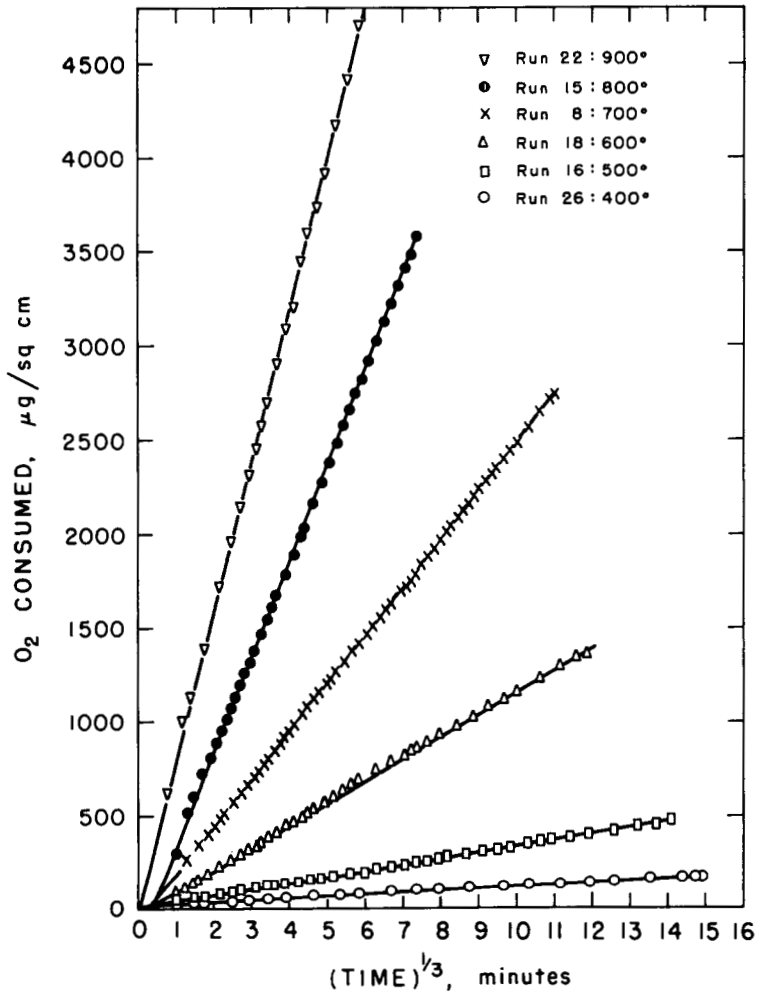

The value of 1/n increases slightly from 400 to 800 C and then drops a bit at 900 C. There is no apparent reason for the increasing trend in the value of 1/n; however, the drop from 800 to 900 C may be attributed to the transformation from α to β zirconium, which occurs at 862 C.

Figure 18 represents a plot of the log of the cubic rate constants versus 1/T. From the slope of the best straight line that could be drawn through all of the points, the activation energy was determined to be 42.5 kcal/mole.

FIGURE 18.

THE ZIRCONIUM-OXYGEN REACTION—VARIATION OF REACTION RATE CONSTANT WITH TEMPERATURE.

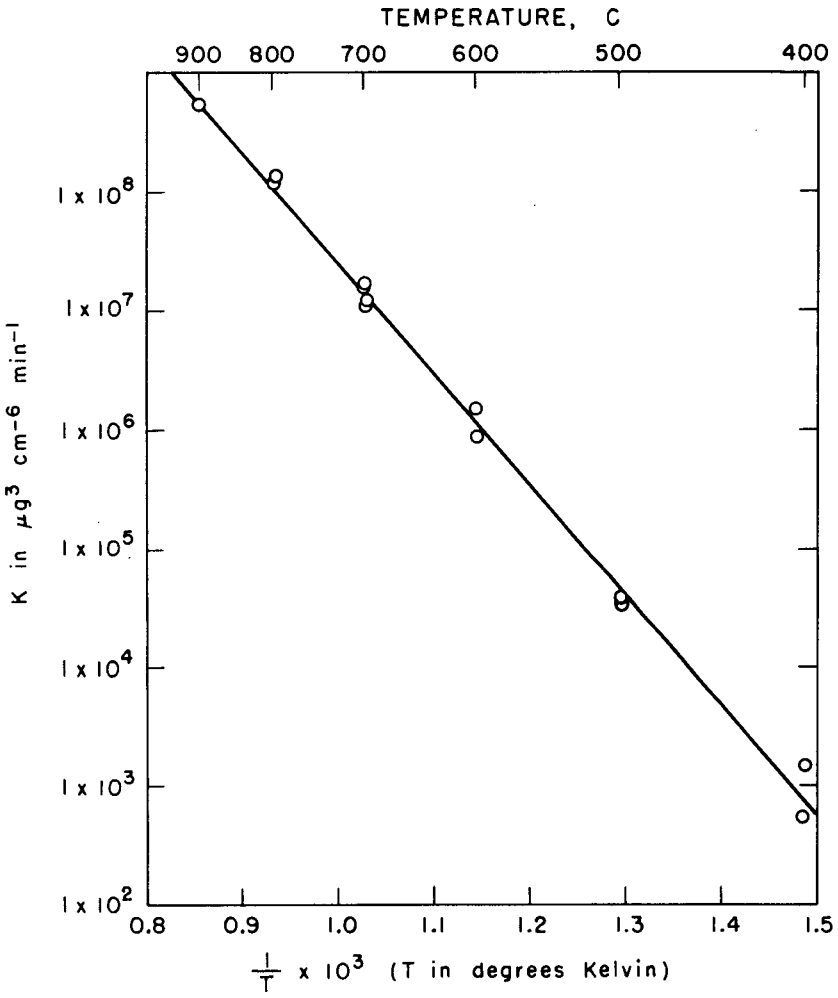

To determine the effect of surface preparation on reaction rate, a number of runs were made in which the samples were polished in different ways. The results of these runs, made at 700 C and at an oxygen presure of 200 mm, are reported in Table 30.

The 600 grit mechanical polish was accomplished by grinding the zirconium down with different grades of silicon carbide paper and finally finishing with the 600 grit paper. The lubricant was water. The 0.5-μ mechanical polish was simply an extension of the 600 grit polish with Linde A aluminum oxide abrasive on a Miracloth lap. The polishing was continued until all of the visible 600 grit scratches were removed.

00_ 073

Table 30

DEPENDENCE OF REACTION RATE ON SAMPLE PRETREATMENT AT 700 C AND 200 mm OF O_2

Method of Polishing	Slope of Log-Log Plot	Rate Constant (k), $(\mu g)^3\ cm^{-6}\ min^{-1}$
Mech. Pol. - 600 Grit, Average 4 Runs	0.36 ± 0.00	$1.5 \pm 0.1 \times 10^7$
Mech. Pol. - 0.5μ , Average 2 Runs	0.36 ± 0.01	$1.5 \pm 0.1 \times 10^7$
Attack Pol., Average 3 Runs	0.36 ± 0.02	$1.3 \pm 0.1 \times 10^7$
Chemical Pol., Average 3 Runs	0.35 ± 0.01	$1.5 \pm 0.2 \times 10^7$

The attack polishing technique was a variation of the 0.5-μ mechanical polishing method in which 1 ml hydrofluoric and 1/2 ml nitric acid are added to 98.5 ml of the Linde A abrasive.

The preparation utilizing a chemical polish consisted of grinding the zirconium down to 600 grit and subsequently immersing the metal in a solution of 10 parts hydrofluoric acid, 45 parts nitric acid and 45 parts water by volume. After a few seconds the metal was removed from the solution, dipped into water, and finally rinsed with alcohol.

From the data presented in Table 30 it appears that the reaction rate is relatively insensitive to sample pretreatment. The slopes obtained from the chemically polished runs were a trifle lower than those from the other methods, and the rate constants calculated from the attack polished runs were slightly less than those obtained from the other polishing methods. However, the reproducibility in all of the methods was excellent. Since the 600 grit mechanical polish was found to be the quickest and simplest, it was adopted as the standard method of preparing samples. Therefore, all of the data reported in this section have been taken from runs in which the samples were prepared by a 600 grit mechanical polish, unless otherwise specifically noted.

The reaction produced a shiny blue-black colored oxide at all temperatures. A few white specks were observed at 900 C.

Because of the large solubility of oxygen in zirconium (29 atom per cent), the reaction is somewhat complicated. A sample which had been run at 900 C was mounted in Bakelite, polished, and then photomicrographs were taken (see Figure 19). The thickness of zirconium dioxide, as measured from the photomicrograph, was found to be 22 microns; the thickness calculated from the amount of oxygen consumed was 41 microns, based on the assumptions that (1) the ratio of the real to measured surface area was

Figure 19

PHOTOMICROGRAPH OF ZIRCONIUM SPECIMEN AFTER REACTION WITH OXYGEN AT 900 C FOR 418 MINUTES

Polarized Light, Magnification 250 x

one and (2) the only product formed was zirconium dioxide having a density of 5.73 g/cc. Evidently solution of zirconium dioxide in zirconium takes place at 900 C.

Two runs were made with foils to determine the dependence of reaction rate on sample shape. The foil from which the samples were cut was a 10-mil thick sheet which had been rolled from sponge zirconium. The foil samples were polished through 600 grit and run at 700 C and 200 mm of oxygen pressure. The slopes of the log-log plots were 0.35 in both cases, in good agreement with parallelepiped samples. The cubic rate constants were found to be 2.3×10^7 and 2.8×10^7 $(\mu g)^3$ cm^{-6} min^{-1}, slightly larger than values obtained from parallelepiped samples. Examination of the product immediately after one of the foil runs revealed an adherent black oxide film similar to those formed on the parallelepiped samples.

3. Literature Survey of Thorium Oxidation

A survey of the literature on thorium reveals that comparatively few studies have been made of the reactions of this metal with air, oxygen,

nitrogen, and water vapor. The oxidation of thorium in air and oxygen has received the attention of a number of investigators, but comparisons of their results are limited by wide differences in the temperature ranges studied and in the durations of their experiments. The disagreement in observed rate laws, values for the activation energy, and in selected values of experimental rate constants can be seen in Table 31, which summarizes the results together with some of the more important experimental details. The extent of the spread in the experimental data is shown in Figures 20 and 21, in which sample weight gain in μg/sq cm is plotted against time in minutes. The reaction in air in the range 100 to 900 C studied by Mallett and Albrecht[7] was believed to be principally an oxidation process, although some evidence of reaction with nitrogen was observed at 400 and 500 C.

Rates of reaction of nitrogen with thorium were determined by Gerds and Mallett[8] for the temperature range from 670 to 1490 C at 1 atmosphere pressure. The reaction occurs at a slower rate than with oxygen and follows a parabolic law. The value of the energy of activation, 24,300 ± 1300 cal/mole, is lower than the activation energies reported in the literature for the reaction of nitrogen with other metals.

The reaction between thorium and water vapor was examined by Deal and Svec[9] in the temperature range 200 to 600 C and at water vapor pressures between 40 and 100 mm Hg. Thorium dioxide and hydrogen were identified as the main species formed during the reaction, with thorium dihydride believed to be a possible side-reaction product. The reaction data were found to follow the logarithmic rate law $W = k \log (1 + 0.45\ t)$, where W is the weight of water reacted per unit area of thorium surface, t is time, and k is the rate constant. An average value of 6.44 ± 0.75 kcal/mole was calculated for the activation energy of the reaction.

Information in the literature on the effect of alloying additions on these reactions is limited to a few observations, mainly qualitative in nature, on the reaction in air. Feibig[10] found that a 2 w/o beryllium alloy corroded at a somewhat lower rate in air than unalloyed thorium at temperatures from 425 to 500 C (see Table 32). Alloys of thorium with aluminum (10 w/o) and with copper (5 to 10 w/o) were found to have poor resistance to oxidation, disintegrating to fine powders on standing in air.[11]

---

[7]Mallett, M. W., and Albrecht, W. M., BMI-819 (1953).

[8]Gerds, A. F. and Mallett, M. W., J. Electrochem. Soc. 101, 175 (1954).

[9]Deal, B. E., and Svec, H. J., J. Electrochem. Soc. 103, 421 (1956).

[10]Feibig, J. G., CT-2400 (1945).

[11]Carlson, O. N., Et al., Proc. Int. Conf. Peaceful Uses of Atomic Energy (Geneva) 9 74 (1956).

Table 31

KINETIC DATA FOR REACTIONS OF THORIUM IN AIR, OXYGEN AND NITROGEN

Metal Source	Gas	Temp Range Studied (C)	Pressure (mm)	Max Time of Run (min)	Rate Law	Rate Constants (K), $\mu g^2/cm^4/min$ (P),[a] or $\mu g/sq\ cm/min$ (L)[b]		Energy of Activation (kcal/mole)	Remarks	Reference
Westinghouse (Ca reduction of ThO_2)	O_2	250-350	450	80	Parabolic	5.0	(300 C)	31	Metal contained 1.0-1.5% ThO_2, 0.04% Ca, 0.03% Fe	(4)
		350-450	210	30	Linear	3.6	(400 C)	22		
		450	Non-isothermal conditions							
Iodide Crystal Bar	O_2	840-1415	760	180	Parabolic	4.1×10^3	(850 C)	63	Below 1100 C discarded early stages data (non-isothermal conditions)	(5)
						8.6×10^7	(1415 C)			
Ames	Air	200-500	760	300	Linear	10	(400 C)			(6)
Ames	Air	100-900	760	From ~4000 hr at 100 C to 1 hr at 900 C	Linear	0.43	(100 C)	13(100-200 C)		(2)
						2.8	(400 C)	18(400-900 C)		
						560.	(900 C)			
Iodide Crystal Bar	N_2	670-1490	760	200	Parabolic	1.0×10^3	(670 C)	24		(3)
						1.0×10^6	(1490 C)			

(2) Mallett, M. W., and Albrecht, W. M., BMI-819 (1953).
(3) Gerds, A. F. and Mallett, M. W., J. Electrochem, Soc. 101, 175 (1954).
(4) Levesque, P. and Cubicciotti, D., J. Am. Chem. Soc. 73, 2028 (1951).
(5) Gerds, A. F. and Mallett, M. W., J. Electrochem, Soc. 101, 171 (1954).
(6) Feibig, J. G., CT-2400 (1945).

[a]Parabolic rate law.

[b]Linear rate law.

FIGURE 20.

SELECTED LITERATURE DATA ON REACTION OF THORIUM WITH OXYGEN.

(1) Levesque and Cubicciotti, J. Amer. Chem. Soc. 73, 2028 (1951)

(2) Geros and Mallett, J. Electrochem. Soc. 101, 171 (1954)

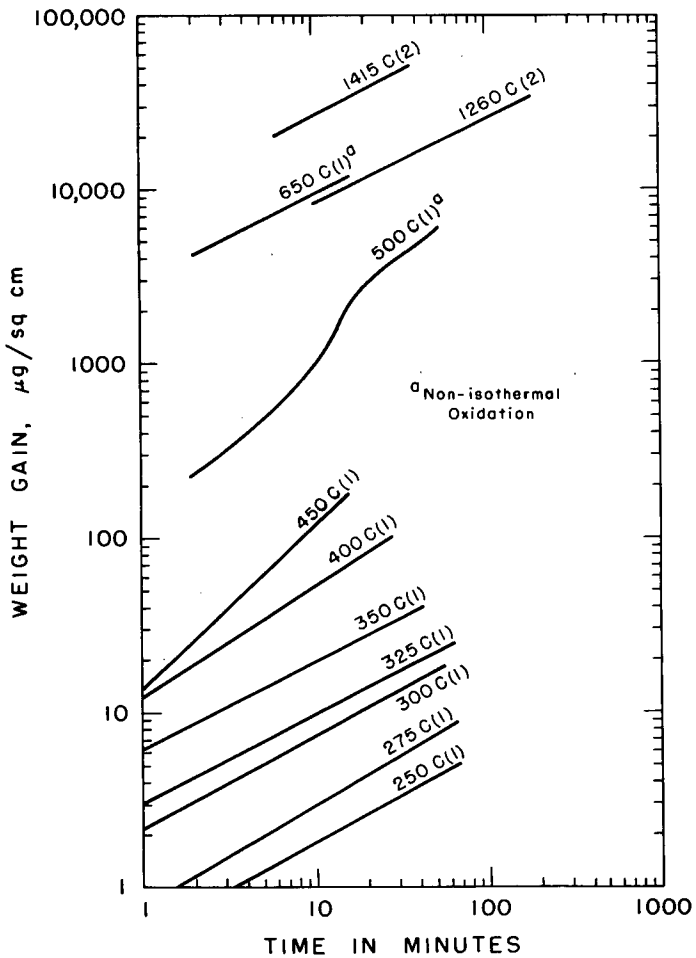

FIGURE 21.

SELECTED LITERATURE DATA ON REACTION OF THORIUM METAL IN AIR.

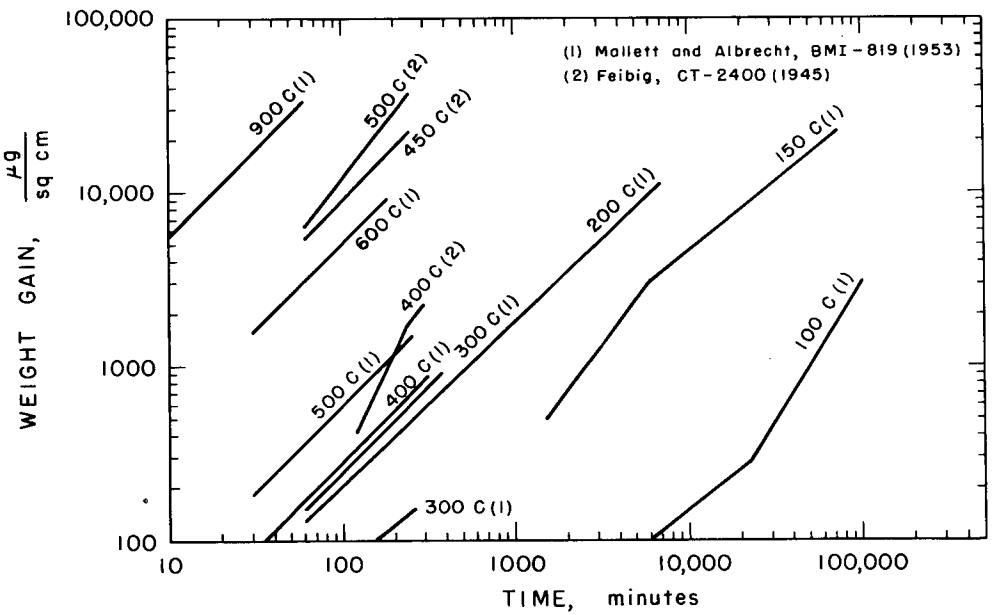

Table 32

CORROSION OF THORIUM AND A THORIUM-BERYLLIUM ALLOY IN AIR AT VARIOUS TEMPERATURES

	Wt gain after 4 hr (mg/sq cm)	
Temperature, C	Th	Th-Be (2 w/o)
400	1.72	2.53
425	9.48	3.43
450	21.40	5.82
500	34.75	9.43

B. Determination of Alpha, The Ratio of Capture to Fission Cross Sections, in EBR-I
(P. Kafalas, M. Levenson, R. R. Heinrich, M. I. Homa, A. A. Madson)

The determination of alpha of uranium-235 and plutonium-239 in EBR-I has been completed. A paper describing this study has been submitted to "Nuclear Science and Engineering" for publication. A similar study of the variation of alpha as a function of position in EBR-I has been made for uranium-238 and uranium-233.

The samples of uranium-238 and uranium-233 were sealed in aluminum pins and exposed along with the uranium-235 and plutonium-239 samples in the core and the blankets of EBR-I. The samples were then analyzed radiochemically to determine the number of fission events and the number of capture events per unit weight of fissile material. In the case of uranium-233 the capture events were not determined because the initial uranium-234 content was too high to make the results significant (0.2 per cent).

The number of capture events that occurred in each uranium-238 sample was determined by separating plutonium-239 and assaying its alpha activity on a calibrated $2\pi\alpha$ counter. The plutonium-239 was separated by TTA extraction, using plutonium-236 spiking tracer to determine the chemical yield of each extraction. The plutonium-236 was made at the cyclotron by means of the reaction $U^{235}(d,n)Np^{236} \xrightarrow[22h]{\beta^-} Pu^{236}$.

The fission patterns of uranium-233 and uranium-238 were determined by separating the fission product cesium-137 and assaying its beta activity using an end window proportional flow counter which was calibrated against a $4\pi\ \beta$ counter. The uranium content of each sample was determined by X-ray spectrometric analysis.

The fission patterns are shown here as cesium-137 activity per mg of uranium. These disintegration rates may be converted to the equivalent

number of fissions when the fission yields are known. The absolute yield of cesium-137 in fast neutron fission of uranium-233 and uranium-238 is now being determined in our laboratory.

The arrangement of the samples in the reactor is shown in Figure 22. The horizontal and vertical fission patterns of uranium-233 are shown in Figures 23 and 24. Sample No. 8 is shown with the vertical data, even though it is not on the same vertical line as the other samples (see Figure 22). Figure 24 also shows the vertical fission pattern of uranium-238.

The horizontal fission pattern of uranium-238 is shown in Figure 25. The capture patterns of uranium-238 are shown in Figures 26 and 27. In the vertical patterns the dashed lines are drawn merely as a visual aid and are not intended to imply that intermediate points would lie on the lines as drawn here. There are not enough points to yield a detailed pattern. In Figure 24 the peak value of the uranium-238 curve is obtained from the extrapolated portion of the curve in Figure 25.

In the case of uranium-233 (as well as uranium-235 and plutonium-239) the burn-up in the core is about 10 times greater than in the outer blanket region. In the case of uranium-238 the burn-up in the core is about 300 times greater than in the outer blanket region. The difference in behavior of uranium-238 is due to its high threshold energy for neutron fission ($\sim$1 Mev). The flux of neutrons of energy greater than the threshold energy decreases sharply with distance from the reactor center; this decrease is greater horizontally than vertically.

The uranium-233 fission patterns are similar to those of uranium-235 and plutonium-239, as would be expected. The uranium-238 capture patterns have the same general shape as the capture patterns of the other nuclides.

FIGURE 22.

SCHEMATIC DIAGRAM OF EBR-I SHOWING SAMPLE POSITIONS.

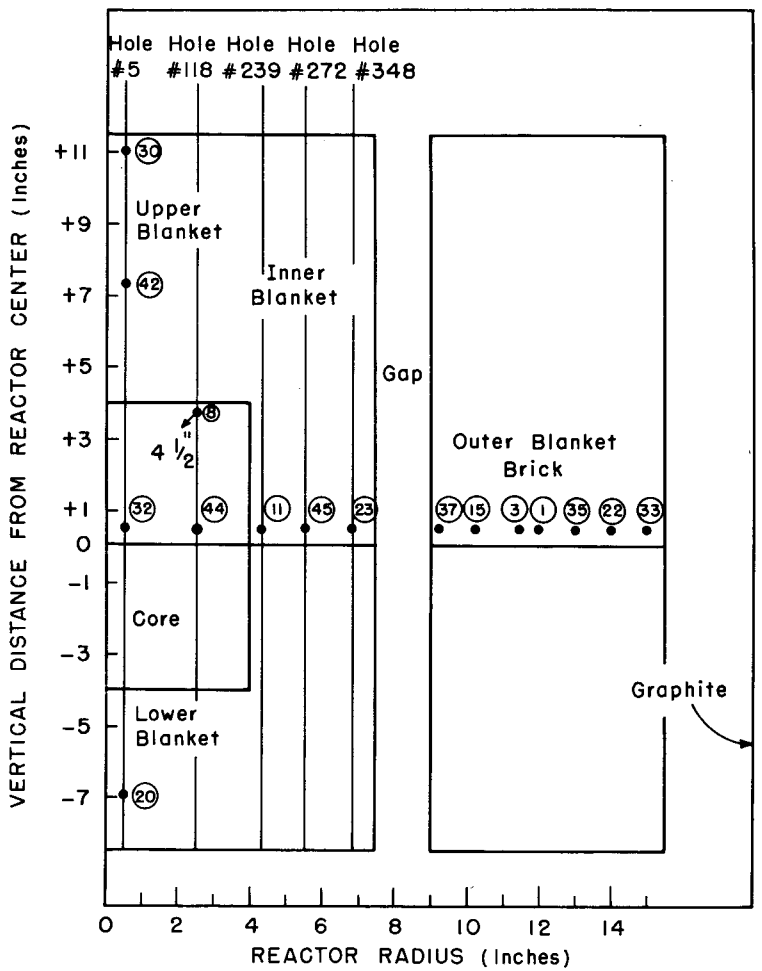

FIGURE 23.

HORIZONTAL FISSION PATTERN OF U^{233} AT MIDPLANE OF EBR-I.

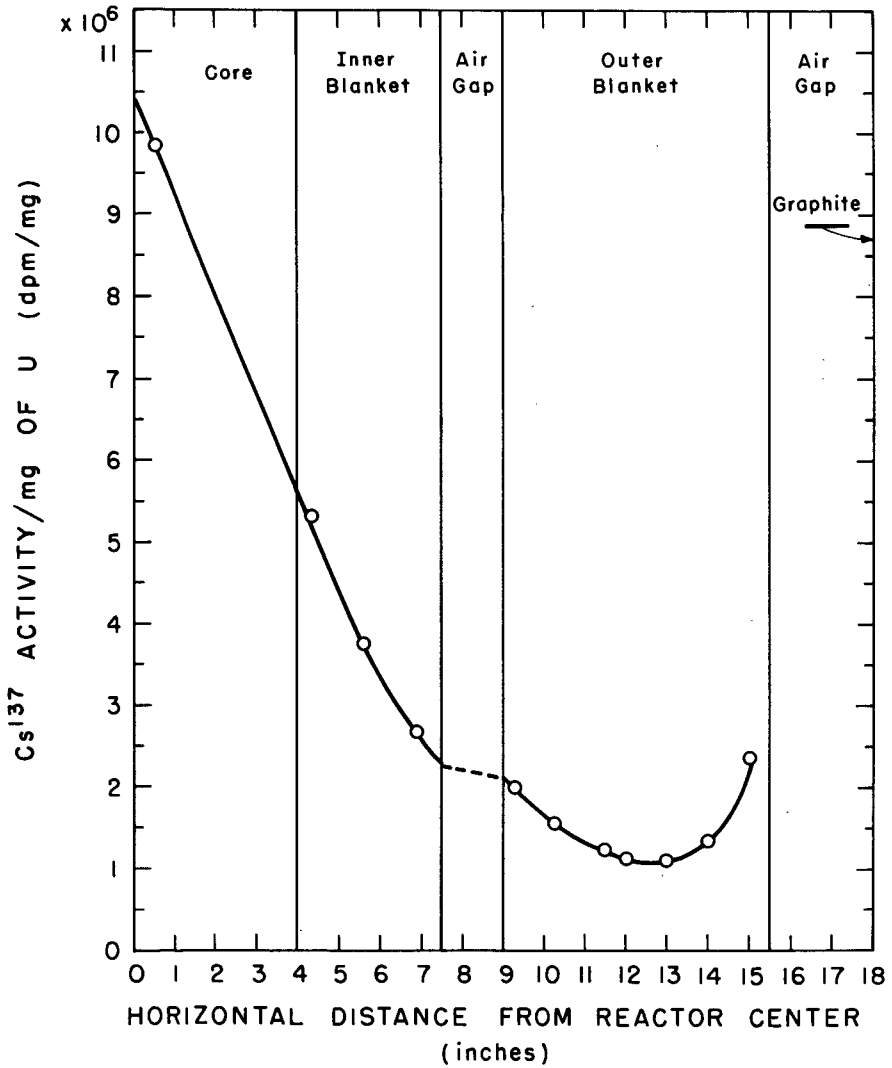

FIGURE 24.

VERTICAL FISSION PATTERNS OF U^{233} AND U^{238} IN CENTRAL ROD OF EBR-I.

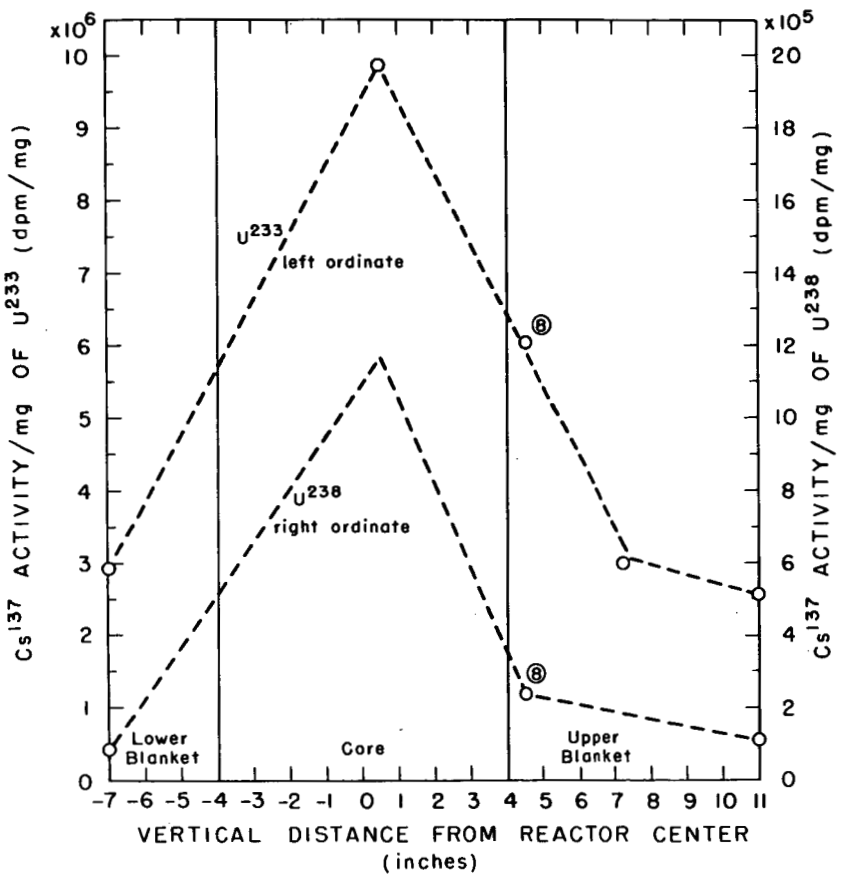

FIGURE 25.

HORIZONTAL FISSION PATTERN OF U^{238} AT MIDPLANE OF EBR-I.

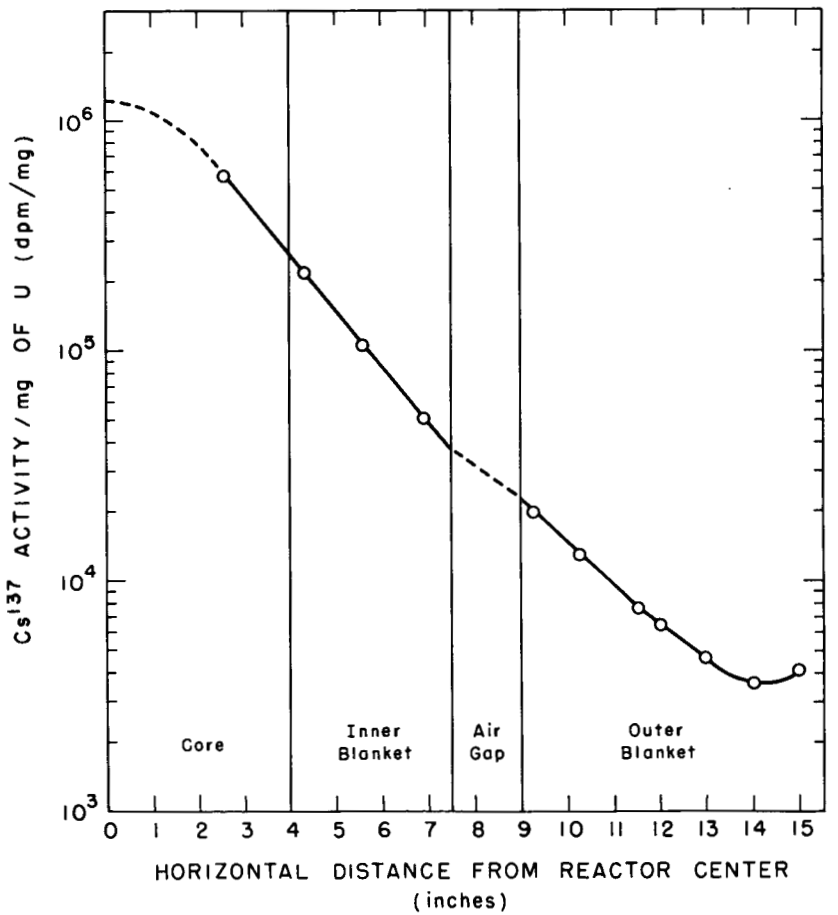

FIGURE 26.

HORIZONTAL CAPTURE PATTERN OF U^{238} AT MIDPLANE OF EBR-I.

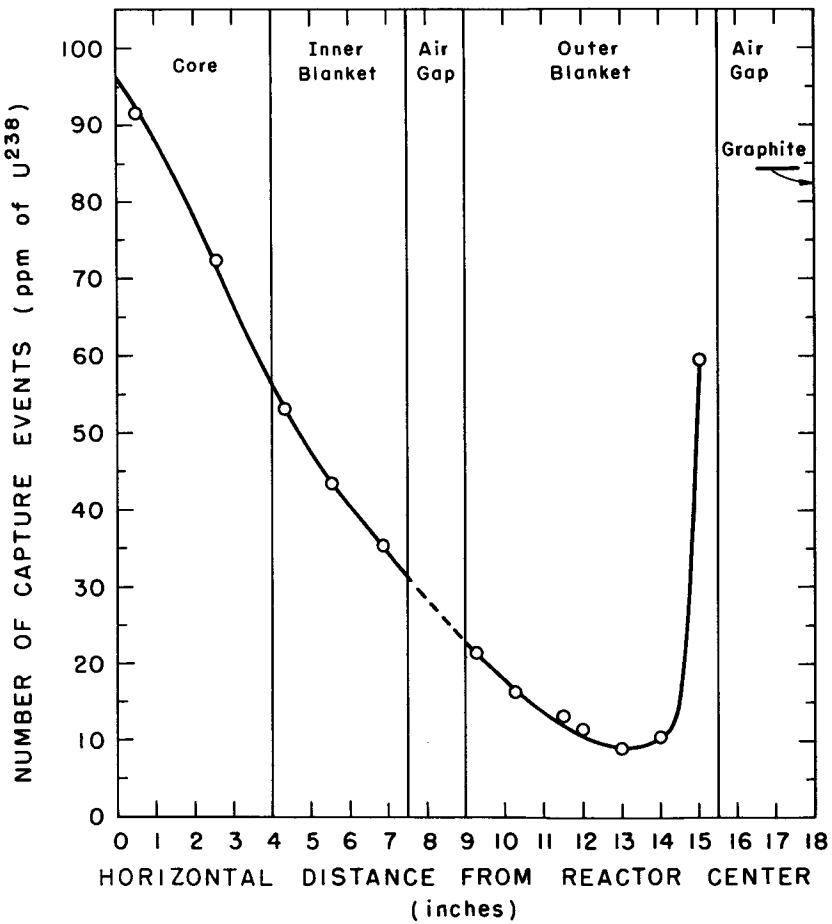

FIGURE 27.

VERTICAL CAPTURE PATTERN OF U^{238} IN CENTRAL ROD OF EBR-I.

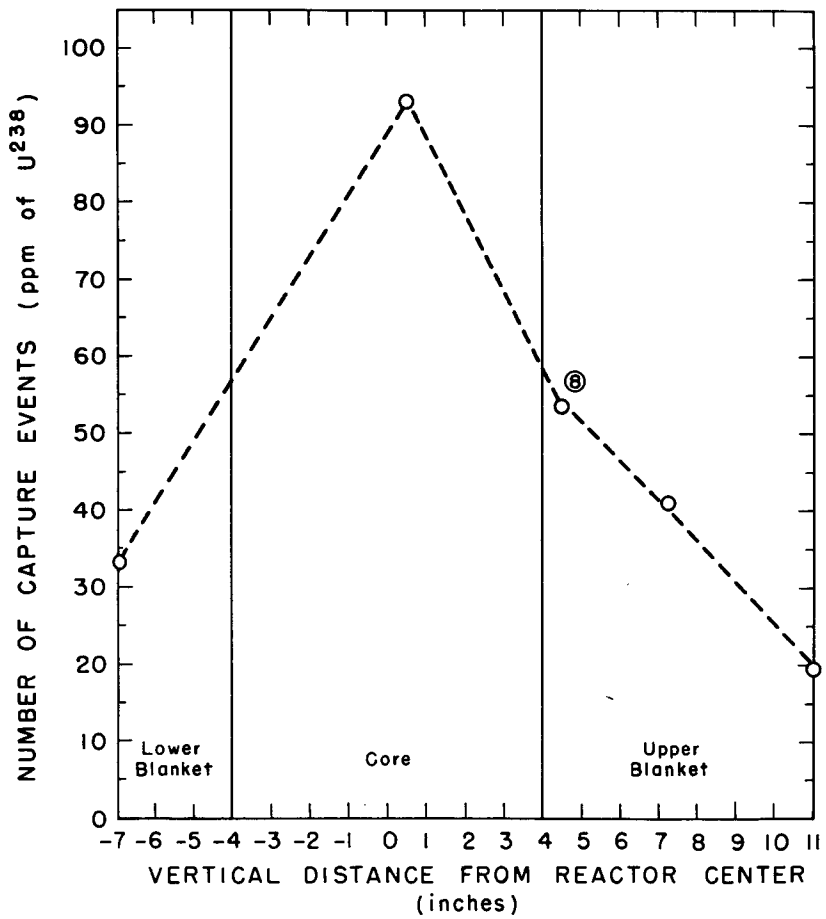

IV. CHEMICAL-METALLURGICAL SEPARATIONS PROCESSES

Pyrometallurgical methods of processing discharged reactor fuels are being developed. A melt-refining process has shown considerable promise for decontamination of metallic fuel elements.

The suitability of the Stokes furnace (described in ANL-5466, pages 32 to 39) for the melt refining and casting of plutonium-bearing materials has been tested in an experiment employing uranium alloyed with approximately 1 w/o plutonium. Alpha contamination was confined to the interior of the furnace and the plastic bag used as a plutonium dust box for unloading the furnace after the melting operation. A preferential concentration of alpha activity in the dross was found in this experiment. A 3500-g master "fissium" alloy containing 20 w/o plutonium is being prepared.

Studies have been made of the amount of radioactive iodine volatilized in melt refining of discharged reactor fuel. Under the conditions proposed for EBR-II fuel processing (inert atmosphere at 1200 to 1300 C) negligible iodine was volatilized (less than one per cent).

X-ray analysis has shown tantalum monoboride is the most stable boride formed in the ternary system uranium-boron-tantalum.

Equipment is being assembled and tested that will enable vapor pressures to be measured by an effusion method in the range 400 K to 2500 K.

Re-examination of the analytical method for determination of beryllia and lime ratios in mixtures showed the analysis to be satisfactory for beryllia but poor for lime.

Determinations of the distribution coefficient of plutonium between magnesium and uranium on uranium-chromium alloys have been made over a range 930 to 1190 C. Both forward and reverse extractions were studied. The distribution coefficient of plutonium is 0.19 (+0.01, - 0.005 at 1190 C) and 0.37 at 930 C. The heat of transfer of plutonium from the uranium-chromium phase (4.5 w/o chromium alloy) to the magnesium phase is $\Delta H = -9.2 \pm 1.6$ kcal/g atom.

Additional runs have been made to study the extraction of plutonium from powdered uranium-1 w/o plutonium alloy by liquid magnesium. The partition of zirconium, niobium, molybdenum, ruthenium, rhodium, palladium, silver, and cadmium between uranium-iron alloys (5 and 10 weight per cent iron) or uranium-5 w/o chromium alloy and magnesium has been studied.

Solubilities in the zinc-plutonium-uranium system are being obtained.

Experiments to determine the extent of cerium removal from irradiated fuel material by dross refining (3 hr at 1200 C) showed poor removal of cerium (20 to 45 per cent) in slip-cast magnesia crucibles. Effective removal (greater than 98 per cent) of cerium was obtained by the addition of zirconia chips.

The adsorption of metals volatilized during melt refining of discharged fuel material by the surface-active materials, "Molecular Sieves," activated carbon, and activated alumina, was further examined to determine the capacity and efficiency of the adsorbents under various flow and temperature conditions. Volatilized metals included the fission products, cesium, strontium, cadmium and possibly barium, sodium which adheres to the discharged fuel pins, and magnesium resulting from reaction of uranium and fission products with a magnesia crucible. Sodium has been used to test removal efficiency; high removal capacity (20 to 40 wt per cent of adsorber) and efficiency were shown by all three adsorbents (at rates up to 145 ml/(min)(sq cm) calculated for room temperature and atmospheric pressure).

Fractional crystallization of uranium with zinc or other low-melting metals provides a pyrometallurgical process for the removal of fission products from spent reactor fuels. A preliminary flowsheet for noble metal removal by this method has been developed and demonstrated on a small scale. Individual and multicomponent fission product solubilities in zinc and zinc-magnesium alloys have been determined for the following systems: (a) uranium-ruthenium-zinc, (b) uranium-ruthenium-(zinc-3 w/o magnesium), (c) barium-zinc and barium-uranium-zinc, and (d) cerium-zinc and cerium-uranium-zinc. The reduction of uranium compounds with magnesium in zinc-magnesium alloy has been demonstrated; this may have important applications in pyrometallurgical processing of nuclear fuel materials and in the preparation of uranium feed materials. Apparatus has been designed and demonstrated for (a) the separation of zinc from UZn_9 and (b) the recovery of uranium from UZn_9.

Semi-works studies on the extraction of plutonium from uranium-5 w/o chromium alloys with molten magnesium and the subsequent magnesium distillation have shown good plutonium extraction (98 per cent), but distillation runs to date have shown poor recovery of plutonium from the magnesium phase. Corrosion testing of materials for handling molten magnesium has shown tantalum to be the only metal to show promise as a container material.

An electrolytic water analyzer under consideration for continuous monitoring of EBR-II fuel processing cell gas for oxygen has been tested for accuracy and response times over a wide range of water content (up to 840 ppm).

A. Laboratory Studies
(H. M. Feder)

1. Control of Dross in Melt Refining
(N. Chellew, C. Cushing, J. Schilb, D. Finucane)

a. Melt Refining of Plutonium-Bearing Material

(1) Uranium Alloys

A melt-refining experiment employing uranium alloyed with approximately 1 w/o plutonium has been performed to determine the suitability of the Stokes melting and casting furnace for handling plutonium-bearing material. Alpha contamination was found only in the interior of the furnace and in the plastic bag used for packaging. A detailed description of this furnace, previously used for dross control studies with unirradiated material, is included in ANL-5466, pages 32 to 39.

Minor modifications of the furnace were made to adapt the system for use with plutonium. Figure 28 shows the assembly designed for induction heating and casting the alloy.

FIGURE 28
ASSEMBLY FOR MELTING AND CASTING PLUTONIUM ALLOYS

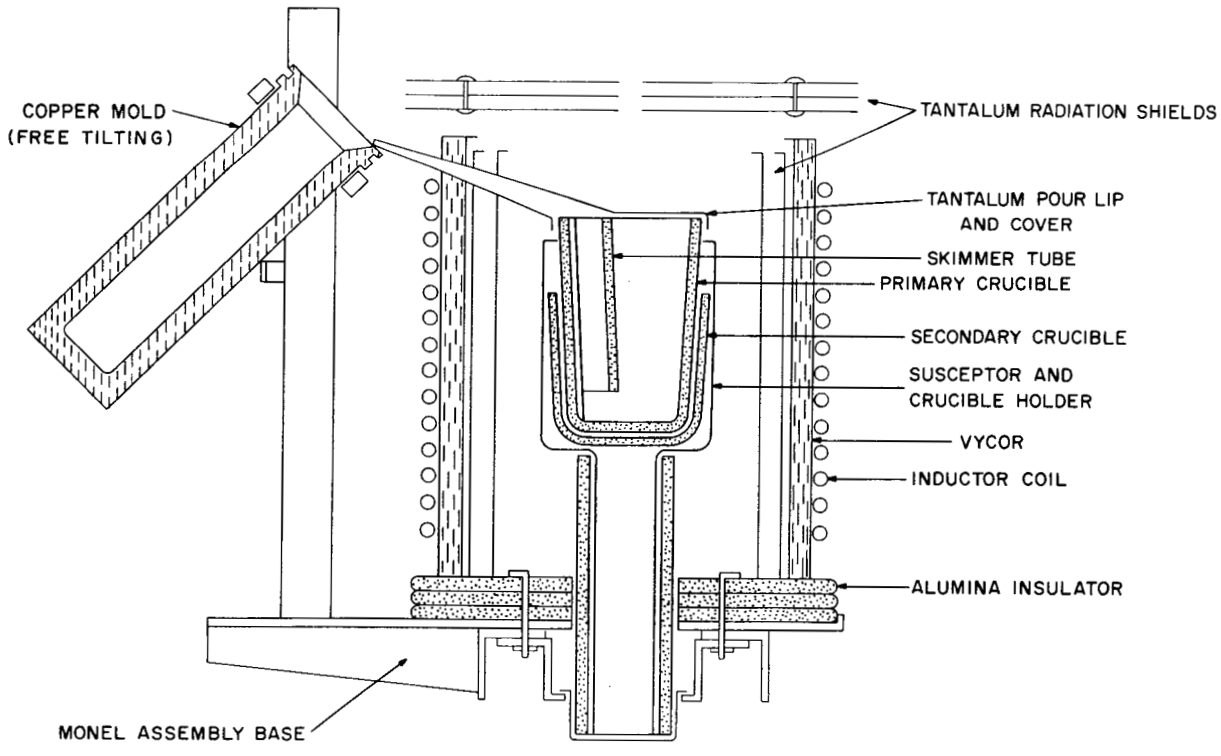

The plutonium charge was placed in a hollowed-out uranium ingot. Melting was performed in a slip-cast magnesia crucible under a purified helium atmosphere. An alumina skimmer tube was used to retain floating dross during the top pour. After the metal was poured and the furnace had cooled to room temperature, a cylindrically shaped vinyl bag was clamped over the upper portion of the furnace. Ingot, mold, crucible and top radiation shields were placed in metal packaging containers. Packaged items were then transferred to a plutonium glove box facility for inspection, weighing, sample cutting, and dissolution of dross and ingot sections for analysis.

At the completion of the packaging operations a rigid survey of the furnace, plastic bag, and laboratory floor was made. In addition, air counts were made during the experimental and decontamination procedures. Alpha contamination was found only in the interior of the furnace and plastic bag. Contamination, presumably due to fine particulate matter carried in magnesium vapor, was found to be concentrated in the top section of the furnace. Location and degree of this contamination were as follows: bottom surface of top heat shield, >40 M (1 M = 1000 dpm/100 sq cm); furnace cover, <25 M; furnace sides, <2 M; copper wool filter in the vacuum furnace outlet duct, <0.2 M; and melting assembly with mold, crucible, and top heat shields removed, <4 M. The interior of the bag was found to be free from contamination with the exception of the fingers of the neoprene gloves and the area upon which the furnace lid rested during the packaging operation. One bead of active metal, possibly dislodged during removal of the crucible cover, was found on the bottom of the furnace.

Prior to the plutonium alloy melt a dummy run was carried out in which a uranium charge was put through the same sequence of operations. Both the plutonium alloy and uranium runs yielded sound ingots which were easily removed from the mold and appeared to discolor at the same rate when handled in air. The drosses formed were typical of drosses produced when high-purity uranium is melted in slip-cast magnesia. Islands of shiny metallic oxide were found to be dislodged from the crucible-metal contact area. Weights of fractions separated by pouring are given in Table 33.

Sections from the top and bottom of the plutonium-bearing ingot were dissolved in aqua regia for determination of total alpha activity. A similar dissolution and analysis was made of the dross leached from the crucible. Alpha concentrations in top and bottom ingot sections were both 7.3×10^8 cpm/g of uranium, and alpha concentration in the dross was 24.3×10^8 cpm/g of uranium. The preferential concentration of total alpha in the dross is being investigated.

Table 33

MELT REFINING OF PLUTONIUM-URANIUM ALLOY

Crucible - slip-cast magnesia (top pour)
Atmosphere - purified helium
Stokes Melting Furnace (described in ANL-5466, pages 32 to 39)
See Figure 28 for crucible assembly.

	Uranium Alloy Run	Plutonium Alloy Run
Nominal Melt Temp (C)	1250	1250
Pour Temp (C)	1250	1300
Melt Time (min)	155	300
Charge		
Uranium (g)	494.7	511.5
Plutonium (g)	-	5.1
Ingot		
Weight (g)	456.5	491.9
w/o Charge	92.3	95.2
Button[a]		
Weight (g)	32.0	16.2
w/o Charge	6.5	3.1
Dross		
Weight (g)	5.9	9.2
w/o Charge	1.2	1.8
Total Product		
Weight (g)	494.4	517.3
w/o Charge	100.0	100.1

[a]Single buttons of unpoured metal formed at the base of the alumina skimmer tube used to retain floating dross during the top pour.

(2) "Fissium"* Alloys

Work with "fissium" alloys containing 20 w/o plutonium has been started. The purpose of these plutonium alloy melts will be to determine (a) the melt conditions necessary for high cerium removal, (b) the effect of carbon on zirconium removal, and (c) the distribution of plutonium in dross and ingot for established melt conditions. Preparations have been made to produce a 3500-g master "fissium" alloy containing 20 w/o plutonium. This alloy will serve as a source of charge material for approximately eight experimental melts.

*"Fissium" alloys were defined in ANL-5668, page 64, as uranium alloys containing cerium, ruthenium, molybdenum, palladium and zirconium in various combinations.

A preliminary check has been made of the atmospheric purity necessary for efficient separation of "fissium" metal from dross under conditions contemplated for the plutonium alloy melts. Argon and helium were compared. Results from single experiments in these atmospheres are reported in Table 34.

Table 34

EFFECT OF INERT ATMOSPHERE ON DROSS FORMATION

Crucible: Dry press magnesia; bulk density, 75 per cent of theoretical (d_{th} = 3.58).
Conditions: Nominal Temp - 1250 C; total melt time - 4.5 hr; top pour, flowing atmosphere - 50 ml/min.
Alloy Charge: Composition in w/o - Ru, 3.4; Mo, 4.4; Zr, 2.0; Pd, 0.4; Ce, ~ 0.6; balance uranium.

	Atmosphere							
		Impurities[a] (ppm)			Weight (g)			
Run	Type	H_2O	N_2	O_2	Charge	Ingot	Button[b]	Dross
I-14E	Helium[c]	7	50	80	283.7	274.0	4.9	3.9 (1.4%)
I-15E	Argon[d]	3	730	120	258.9	236.6	16.9	4.5 (1.7%)

[a]Nitrogen and oxygen values determined by mass spectrometer. Moisture values obtained by dew point technique.

[b]Unpoured metal buttons retained at the base of the magnesia skimmer tube.

[c]Bureau of Mines Grade helium purified by passage through activated charcoal at -190 C.

[d]Welding Grade argon purified by passage through activated charcoal at -80 C.

Although the nitrogen concentration in the argon (730 ppm) was roughly 15 times the amount found in helium, the increase in dross retention is not necessarily significant. A shiny, black, adhering dross weighing less than two per cent of charged material was formed. For both melts undercutting of the crucible at the melt line was found to be about 140 microns.

2. Iodine Distribution in Melt Refining (M. Ader)

An important factor in the design of equipment for disposal of radioactive gases released during melt refining is the amount of radioiodine, particularly 8.05-d iodine-131, which may volatilize. Uranium tetraiodide is thermally unstable, decomposing to uranium triiodide and iodine on heating, but it can be maintained and volatilized above 350 C if the partial pressure of iodine in the system is relatively high. Uranium triiodide may be prepared under vacuum, but little is known about its volatility except that it is reported to be relatively non-volatile.[12] Melt refining of EBR-II-type fuel is normally performed in an inert atmosphere at 1200 to 1300 C. These conditions do not favor the volatilization of either uranium tetra- or triiodide. One can attempt to predict the extent of formation and volatilization of the iodides of zirconium, molybdenum, and other fission elements from existing thermodynamic and vapor pressure data for the pure compounds. However, this would be little more than guess work in our present state of knowledge of the activities and kinetics in this complex system.

A systematic investigation of the fate of fission elements whose behavior is not well known (e.g., iodine, bromine, selenium, antimony) is being considered. It was felt that prior to such an investigation a crude experiment using trace concentrations of radioiodine would give qualitative and rough quantitative evidence of iodine behavior in melt refining. The data would be particularly meaningful from the standpoint of off-gas system design if the iodine was largely concentrated in either the melt, on the furnace walls, or in the flowing inert atmosphere.

a. Experimental

Three pieces of 1/8-in. diameter natural uranium rod, weighing 0.615, 2.81, and 0.656 g, were placed consecutively inside a length of 7-mm quartz glass tubing sealed at one end. The tubing was evacuated and flushed with helium several times, finally being filled to 1/3-atm pressure and sealed off at about $2\frac{1}{2}$ in. of length. The smaller pieces of uranium served as controls for iodine-131 analysis. After wrapping the quartz tightly with aluminum foil, it was pressed into an aluminum capsule and irradiated for about two weeks in the CP-5 reactor in a flux (thermal) of about 10^{12} neutrons/(sq cm)(sec). The irradiated metal was cooled 14 days before the experiment.

The 2.81-g piece of uranium was placed inside a hole drilled into a 102.7-g chunk of "fissium" metal which, in turn, was placed inside an outgassed magnesia crucible. The "fissium" metal composition was zirconium,

[12] Katz, J. J. and Rabinowitch, E., The Chemistry of Uranium, Part I, 536 (1951).

1.28 w/o; molybdenum, 3.04 w/o; ruthenium, 2.62 w/o; palladium, 0.18 w/o; cerium, 0.18 w/o, and uranium, 92.7 w/o. Crucible and contents were heated at 1250 C for 4 hr in a flowing, purified helium atmosphere (ca 100 ml/min) and then allowed to cool overnight in a static helium atmosphere. Quartz discs, 1/2-in. dia x 1/32-in. thick, were suspended by a tantalum wire above the melt crucible at various levels in the furnace tube (2¾ in. dia x 29 in. long). The discs, which were located at 100 C temperature intervals, were used to determine the nature of the activities sublimed from the melt and to measure the temperatures of the sublimates. The helium gas passed from the furnace tube through (1) a glass tube at room temperature containing 0.5 g of inactive iodine crystals (exchange with radioiodine), (2) a cold trap maintained at 0 C to condense iodine vapor, and (3) a bubbler containing 75 ml of 1 M sodium hydroxide to absorb any iodine vapor which was not caught in the cold trap.

The various fractions were analyzed for gamma activities by means of the 256-channel scintillation spectrometer* (4-in. dia x 4-in. thick sodium iodide-thallium activated crystal). Radioiodine was determined by counting under the 368-kev iodine-131 peak. Appropriate correction factors were applied to all samples for coincidence, decay, geometry, photopeak efficiency, and chemical yield in order to obtain the iodine-131 disintegration rate at the time of the experiment.

b. Discussion of Results

The results of analyses for iodine-131 are given in Table 35. In addition, Figure 29 shows a graph of iodine-131 disintegrations per minute counted under the 368-kev peak versus temperature of the quartz discs. (There was no disc at 800 C.) Some additional observations are reported in the discussion below.

Ingot. Difficulties in the chemical analyses are believed responsible for the poor agreement between iodine content of the irradiation controls and of the ingot.

Cold Trap and Sodium Hydroxide Trap. A very small amount of iodine-131 was found in the cold trap at 0 C and none in the sodium hydroxide bubbler. However, gamma-ray scans of both traps revealed the presence of minor amounts of 80- and 32-kev activities, neither of which is associated with iodine-131. These activities are attributed to 5.3-d xenon-133, which has a gamma-ray transition of 80-kev. The 32-kev activity approximates the 30-kev characteristic radiation of xenon.

---

*Gamma scintillation spectrometry performed by C. Crouthamel and C. Gatrousis.

Table 35

DISTRIBUTION OF IODINE-131 IN MELT REFINING EXPERIMENT

Charge: 2.81 g irradiated natural uranium (cooling time, 14 days) and 102.7 g "fissium"
Crucible: Magnesia (outgassed at 1250 C)
Conditions: System outgassed at 600 C for 30 min; heated at 1250 C for 4 hr under flowing helium atm (100 ml/min); helium passed over solid iodine at room temp, cold trap at 0 C, and through 75 ml of 1 M sodium hydroxide; 0.5-in. dia quartz discs suspended over melt at 100 C intervals.

Fraction	Disintegration Rate[a] (dpm)	Per Cent of Original Charge
(1) Charge[b]	1.13×10^{10}	100.
(2) Ingot[c]	1.77×10^{10}	157.
(3) Cold Trap at 0 C[d]	1.62×10^{3}	1.4×10^{-5}
(4) 1 M NaOH Trap[e]	0	0
(5) Quartz Discs, total[e]	7.71×10^{4}	6.8×10^{-4}
(6) Furnace Tube Wall[f]	3.9×10^{7}	0.34

[a]Corrected for coincidence, decay, geometry, photopeak efficiency, and chemical yield.

[b]Average of 2 control analyses (±2.5 per cent) after HNO_3 dissolution and iodine separation.

[c]Dissolution in 10 M HNO_3-0.25 M HF-0.12 M $Al(NO_3)_3$ left residue which was dissolved in aqua regia. After iodine separation, supernatant liquid and residue found to contain 1 and 156 per cent, respectively, of original iodine.

[d]0.5 g iodine dissolved in 40 ml CCl_4 and counted without chemical separation.

[e]Counted without chemical separation.

[f]Calculated by assigning an average dpm/sq in for each inch of length of furnace tube.

FIGURE 29
IODINE-131 DISINTEGRATION RATE
VERSUS TEMPERATURE OF QUARTZ DISCS

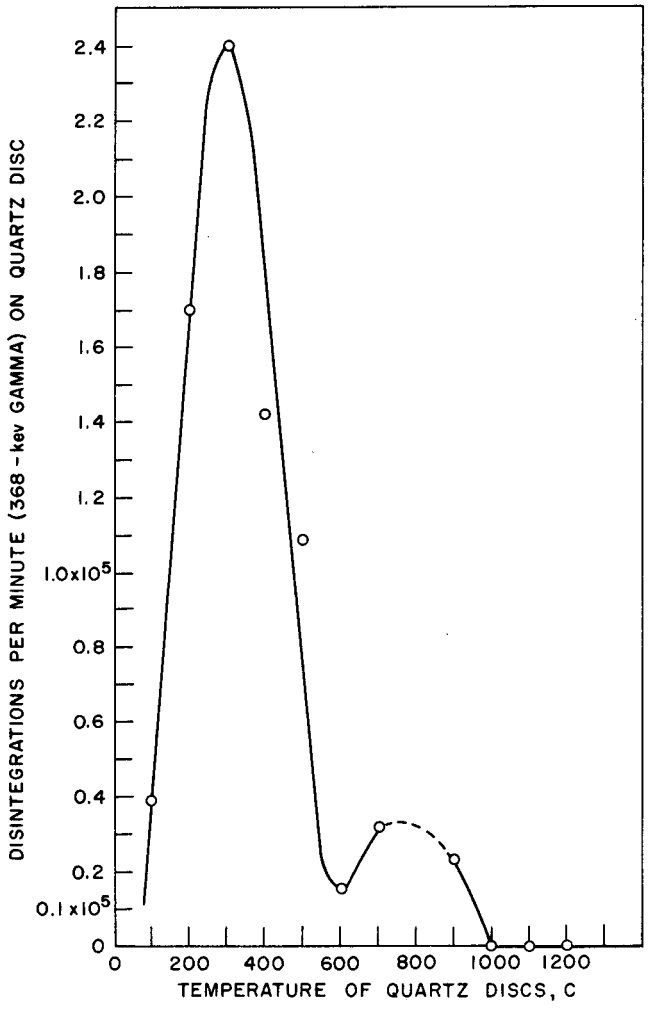

Quartz Discs. Figure 29 shows that iodine-131 activity deposited on discs whose temperatures were in the range of 100 to 900 C but did not deposit at 1000 C or above. Most of the activity deposited in the region of 150 to 500 C, with the maximum occurring at about 300 C. The smaller peak found at 700 to 800 C may be spurious, since its presence depends entirely upon the position of the 600 C point on the curve. If real, however, the second maximum may be explained by an iodine compound different from that attributable to the 300 C maximum. Furthermore, this iodine compound need not have volatilized as such from the melt but may have been formed by reaction or decomposition of a volatile iodine species, e.g., uranium tetraiodide decomposing to uranium triiodide plus iodine. Since the amount of iodine activity deposited on the quartz discs and furnace wall was small (see Table 35), it is reasonable to conclude that iodine activity is essentially non-volatile under the conditions of melt refining proposed for processing spent EBR-II fuel.

In addition to the 368-, 280-, 184-, and 80-kev activities associated with iodine-131, gamma-ray scans of the quartz discs showed the presence of small amounts of 550- and 240-kev activities. Half-life determinations of the latter activities were not conclusive (less than 2 days), loss of activity from the discs due to a volatile species being suspected. The presence of 21-hr iodine-133 decaying to 2.1-d xenon-133m and 5.3-d xenon-133 accounts for the observations.

A significant fact concerning the iodine activity found on the quartz discs and in the cold trap is the absence of any other radioactive fission product. Barring the presence of inactive impurities which could form volatile compounds with iodine, it may be concluded that the small amounts of iodine that were removed from the melt volatilized as uranium tetraiodide or triiodide or both.

3. Reactions of Uranium Container Materials
(C. L. Rosen, H. H. Turner)

Tantalum borides have been found to be a satisfactory container material for molten uranium (ANL-5660, page 88). The equilibrium phases in the ternary system boron-tantalum-uranium are important in determining the precise tantalum-boron compound responsible for corrosion resistance. X-ray analysis of the products of the reactions between the following starting materials indicates that tantalum monoboride is the most stable boride formed in the ternary system uranium-boron-tantalum.

Starting Materials	Found by X-ray Analysis After Heating to 1800 C
$TaB + UH_3$	TaB
$UB_2 + Ta$	TaB, UB_2
$TaB_2 + UH_3$	TaB

4. Vapor Pressure Studies
(C. L. Rosen, H. H. Turner)

(a) Equipment that will enable vapor pressures to be measured by an effusion method in the range 400 K to 2500 K is being assembled and tested.

The major effort of the investigation at present is being directed toward finding suitable materials for use as effusion cells. The materials that indicate the most promise are (1) graphite for the vaporization of TaB_2, Ta_3B_4 and TaB, (2) flame-sprayed alumina for the reaction $U + Al_2O_3$, and (3) sintered tungsten for the vaporization of UZn_9.

(b) In a Knudsen effusion experiment the partial pressure of a volatile species effusing through a small orifice is given by

$$P_i = \frac{W_i}{CSt}\left(\frac{2\pi RT}{M_i}\right)^{1/2}\left(\frac{d^2 + r^2}{r^2}\right) = \frac{W_i A}{C\,M_i^{1/2}} \quad ,$$

where

P_i = partial pressure of species i

W_i = weight in grams of species i deposited on a collector

S = orifice size in sq cm

t = time in seconds

T = temperature

R = gas constant in ergs

M_i = molecular weight of species i

d = distance from orifice to collector

r = radius of collector in the same units as d

C = Clausing factor (the transmission coefficient of a tube, the ratio of the quantity of gas leaving a tube to that entering it)

$$A = \frac{(2\pi RT)^{1/2}}{St}\left(\frac{d^2 + r^2}{r^2}\right) .$$

Effusion data have been obtained for the reaction of alumina with uranium. The general net reaction may be written as:

$$\left(\frac{\alpha}{2} + \beta + \frac{\gamma}{2}\right) Al_2O_3 + \left(\frac{\alpha}{4} + \beta + \frac{3\gamma}{4}\right) U = \alpha AlO + \beta Al_2O + \gamma Al + \left(\frac{\alpha}{4} + \beta + \frac{3\gamma}{4}\right) UO_2 .$$

The observations must be consistent with the equations

$$W = W_{AlO} + W_{Al_2O} + W_{Al} = \alpha_1 M_{AlO}^{1/2} + \beta_1 M_{Al_2O}^{1/2} + \gamma_1 M_{Al}^{1/2}$$

$$K_p = P_{AlO}^{\alpha}\, P_{Al_2O}^{\beta}\, P_{Al}^{\gamma}$$

$$\Delta F = -RT \ln K_p \quad ,$$

where

W = total weight deposited in collector ,

K_p = equilibrium constant ,

and

ΔF = free energy change for the reaction .

Using estimated free energies of formation for AlO and Al_2O[13] the data for the alumina-uranium reaction can be analyzed to determine the coefficients α, β and γ.

Preliminary analysis indicates that at 1500 K, Al_2O is the only volatile species ($\beta = 1$, $\gamma = \alpha = 0$), while at 2000 K an equal molar ratio of Al_2O and AlO are the volatile species ($\alpha = \beta = 1$, $\gamma = 0$).

5. Phase Diagram Studies of Oxide Systems
(M. Ader, D. Fredrickson)

Work on the preparation and properties of 2 CaO·3 BeO was temporarily halted in order to re-examine the analytical methods used in determining beryllia to lime ratios in various preparations. This was prompted by the need for a higher degree of accuracy to establish the exact composition of the compounds formed in the lime-beryllia system. Low material balances were encountered in analyses of solidified melts. Gravimetric methods of analysis were satisfactory for beryllium determination but poor for calcium. Ammonium salts present in the calcium determination tended to give low results. Tests of a volumetric ethylenediaminetetracetate method indicated it to be satisfactory.

Briefly, gravimetric analyses for beryllium and calcium were made on solutions prepared by dissolving 0.4- to 0.6-g samples in refluxing 12 M hydrochloric acid in quartz glassware for about 8 hr. Beryllium hydroxide was precipitated from solution by ammonia gas, ignited to the oxide at about 1100 C, and weighed. Calcium, in the filtrate, was precipitated as calcium oxalate, and ignited to calcium carbonate at 500 C. Brush Beryllium Co, GC grade beryllia and Mallinckrodt primary standard calcium carbonate, both dried at 475 C, were assayed at 100.0 and 99.9 per cent beryllia and calcium carbonate, respectively. Negligible blank corrections of 0.1 mg for beryllia and 0.2 mg for calcium carbonate were found. To test the recoveries of beryllium and calcium from solution, mixtures of these reagents were dissolved in 12 M hydrochloric acid and analyzed by the above procedures. The results indicate that the beryllia, but not the calcium carbonate determinations, were within analytical tolerance, the latter being low by about 0.6 per cent.

Solutions derived by filtration of beryllium hydroxide precipitates differ from those prepared by direct dissolution of calcium carbonate in dilute acid by the presence of large amounts of ammonium chloride and nitrate. These salts are added by the neutralization of concentrated hydrochloric acid with ammonia gas and washing of the precipitated beryllia with 2 per cent ammonium nitrate solution. Tests of the effect of ammonium salts on calcium recovery were made.

---

[13] Brewer, L. and Searcy, S. W., J. Amer. Chem. Soc. 73, 5308 (1951).

Ammonium chloride (18.4 g) and ammonium nitrate (8.0 g), the amounts calculated to be present in a typical sample solution, were added to primary standard calcium carbonate dissolved in dilute hydrochloric acid and diluted to about 400 ml. The presence of the ammonium salts caused the calcium analyses to be low by about 0.3 per cent. Although the effect is not large enough to account for the low calcium analyses in samples where no ammonium salts were added, it appears to be significant.

Determination of calcium by ethylenediaminetetracetate (EDTA) titration has been tested. The volumetric method appears to be highly satisfactory. The titration is also advantageous because it substantially reduces the time required for a calcium analysis and permits replicate analyses to be made on suitable aliquots.

6. Magnesium Extraction Studies

a. Extraction of Plutonium from Liquid Uranium or Its Alloys (E. Greenberg, M. W. Nathans, K. E. Anderson)

This project has now been completed. Since a terminal report is in preparation, only the final results and conclusions are given.

The distribution coefficient of plutonium between magnesium and uranium at 1190 C and in the concentration range of 0.5 - 1 w/o plutonium is $K_{Mg/U} = 0.19$ (+ 0.01. -0.005) (mol fraction basis). This value is based on experiments in which equilibrium was approached from both directions.

In the extraction of plutonium from liquid uranium-chromium (4.5 w/o) alloy the results, obtained from equilibrations from both directions at different temperatures and contact times, are shown in Figure 30 as log K vs 1/T. The data were insufficient to determine K at each temperature within the same limits as for the uranium-plutonium-magnesium system. Therefore, a least squares straight line was calculated whereby it was assumed, for lack of a better assumption, that the points were to be weighed in proportion to the contact times.

The result is:

$$\log K = 2010/T - 2.134 = b/T - a$$

$$\sigma_a = 0.136$$

$$\sigma_b = 176$$

$$\sigma_{K,\ 1/T} = 0.0578 \quad .$$

The heat of transfer of plutonium from the uranium-chromium phase to the magnesium phase was calculated from the slope as

$$\Delta H = -9.2 \pm 1.6 \text{ kcal/g atom} \quad .$$

The data show that at 1200 C the addition of chromium to uranium has little effect on K, and that at 900 C the expected equilibrium value is about 0.38.

FIGURE 30
DISTRIBUTION RATIO OF PLUTONIUM BETWEEN URANIUM-CHROMIUM (4.5 w/o) AND MAGNESIUM

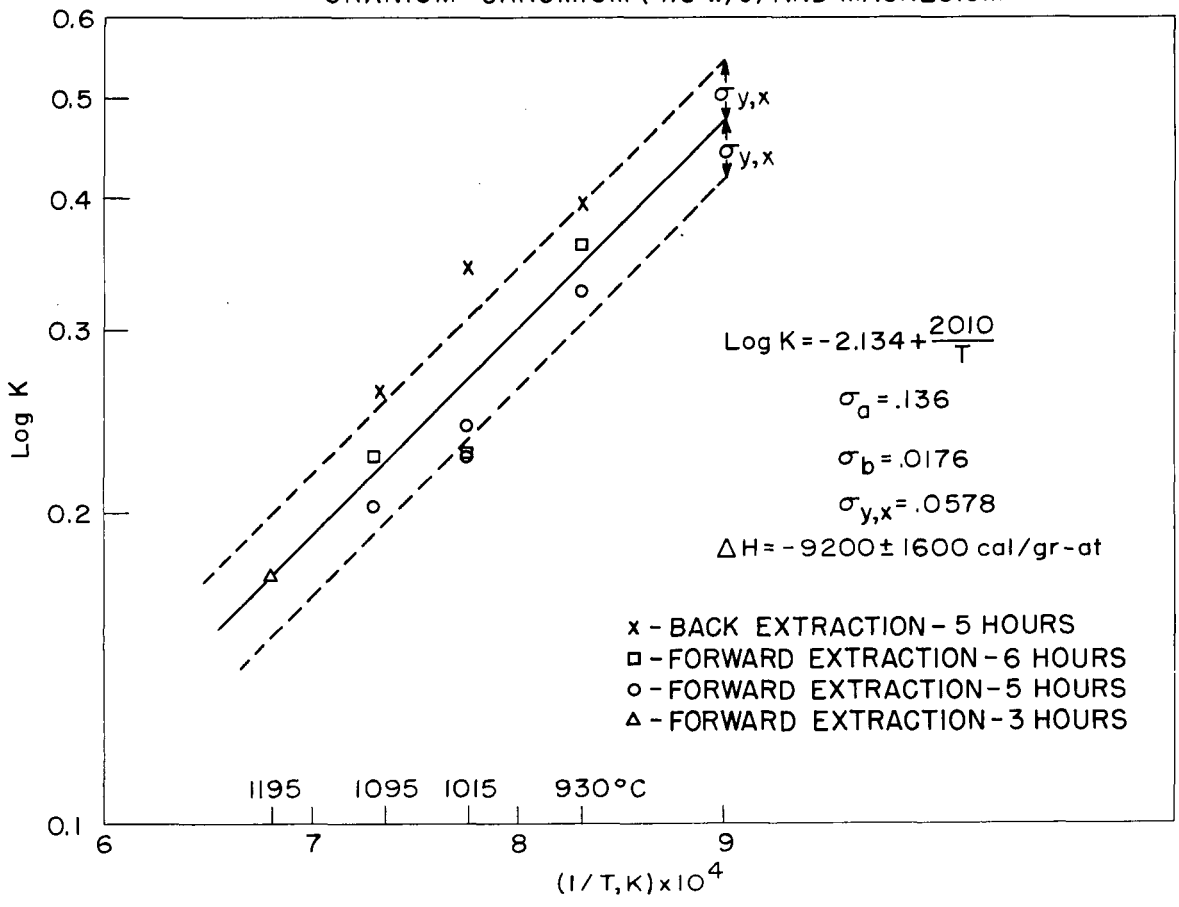

b. Extraction of Plutonium from Powdered Uranium
(R. Nuttall, J. Settle)

Several more runs have been made to study the extraction of plutonium from powdered uranium - 1 w/o plutonium alloy by liquid magnesium. These runs have included a two-stage extraction in which the powdered alloy was extracted with liquid magnesium, which was then removed through a filter and replaced with fresh magnesium.

Complete analytical results have not been obtained on any of these runs so discussion will be deferred.

c. Extraction of Fission Products from Uranium Alloys
(G. R. B. Elliott, R. U. Sweezer)

(1) Uranium, Chromium, and Iron Solubilities

Solubility data from the equilibration of uranium-5 weight per cent chromium and of uranium-10.5 weight per cent iron alloys with magnesium are presented in Table 36. The two liquid phases were shaken together in inert atmosphere capsules as described in ANL-5633, page 111.

A scatter exists in these data which is believed to result from an insufficient rate of cooling in some cases. Such a cooling would result in segregation of solid metal and a solubility corresponding to some lower temperature. For this reason the higher values of Table 36, as presented below, are considered to represent the true solubility (weight per cent):

U in Mg at 940 C in equilibrium with U-Cr alloy[a]	0.05
U in Mg at 920 C in equilibrium with U-Fe alloy[a]	0.06[b]
U in Mg at 800 C in equilibrium with U-Fe alloy[a]	0.03
Cr in Mg at 940 C in equilibrium with U-Cr alloy[a]	0.06
Fe in Mg at 800 C in equilibrium with U-Fe alloy[a]	0.008

The smoothed values of the work of Chiotti and Shoemaker[14] indicate:

U in Mg at 940 C in equilibrium with Solid U	0.065
U in Mg at 800 C in equilibrium with Solid U	0.024
U in Mg at 900 C in equilibrium with U-Cr alloy[a]	0.052[b]

Other literature values of interest[15] include:

Fe in Mg at 800 C from Solid Fe	0.12, 0.08
Cr in Mg at 734 C from Solid Cr	0.008

[a]Alloys contained small amounts of other components.

[b]Based on single measurements

---

[14]Chiotti, P., and Shoemaker, H. E., "Pyrometallurgical Separation of Uranium from Thorium," American Chemical Society Meeting, Miami, Florida, April 1957.

[15]Burris, L. and Dillon, I. G. et al., "Properties and Handling Procedures for Magnesium - a Literature Survey," ANL-5749 (1957)

Table 36

THE SOLUBILITY OF URANIUM ALLOYS IN MAGNESIUM

(Equipment and procedure described in ANL-5633, page 111.)

Run No.	Temp (C)	Time Heated (hr)	Other Components	Solubility (w/o) U	Cr	Fe[a]	Fe[b]
SERIES A	URANIUM - 10.5 w/o IRON - MAGNESIUM						
10-2-E	810	1	Ta, Ru	0.020		0.005	-
11-1-E	800	8	Ta, Ru	0.026		0.005	
11-2-E	800	8	Ta, Ru	0.014		0.005	
15-2-E	920	1.5	Ru	0.062		0.005	0.011
16-1-E	860	1	Ru	0.088[c]		0.008	0.0105
16-2-E	860	1	Ru	0.029		0.005	0.082
19-1-E	800	0.5	Ru	0.027		0.005	
20-2-E	790	4	Pd[d]	0.032		0.003	
SERIES B	URANIUM - 5 w/o CHROMIUM - MAGNESIUM						
21-1-E	940	3	Pd[d]	0.038	0.079		
21-2-E	940	3	Mo	0.019	0.058		
22-1-E	940	3	Ru	0.023	0.023		
22-2-E	940	3	Zr	0.033	0.039		
23-1-E	930	4	Zr	0.08[c]	0.061		
23-2-E	930	4	Zr	0.05	0.054		
24-2-E	950	3	Mo	0.049	0.058		
25-2-E	940	3	Ru	0.022	0.033		
27-1-E	940	3	Ru	0.045	0.040		
27-2-E	940	3	Zr	0.035	0.044		
30 B-1-E	950	3	-	0.054	0.061		

[a]Relative solubility spectroscopically.

[b]Absolute solubility colorimetrically.

[c]Questionable value.

[d]Because of high solubility of Pd in Mg, the other solubilities may be affected

(2) Distribution of Other Elements

Table 37 completes the earlier Table 25 in ANL-5668, page 78.

Table 37

THE DISTRIBUTION OF FISSION PRODUCT ELEMENTS BETWEEN MAGNESIUM AND URANIUM - 5 w/o CHROMIUM

(This table completes Table 25, ANL-5668, page 78.)

Run No.	Element Tested	Conc. (Atom Fraction)[a]	Partition Ratio[b]
23-1-E	Zr	0.015	3.6×10^{-3}
23-2-E	Zr	0.0052	$<3.0 \times 10^{-3}$
27-2-E	Zr	0.017[c]	$< 6 \times 10^{-4}$ [a]
28-2-E	Nb	0.044	$< 1 \times 10^{-4}$
26-2-E	Mo	0.035	$<4.8 \times 10^{-5}$
25-2-E	Ru	0.052	$<3.3 \times 10^{-4}$
27-1-E	Ru	0.114	5.6×10^{-4}
24-1-E	Pd	0.0071	>100

[a]Concentration in the preferred phase; each phase weighed ~ 25 g.

[b]Ratio of atom fraction in magnesium to atom fraction in uranium-chromium.

[c]Suspect incomplete dissolution of Zr into melt.

B. Semi-Works Studies of High-Temperature Processes
(L. Burris, Jr.)

1. Removal of Cerium by Dross Refining
(L. Burris, Jr., V. Thelen)

Analytical results on removal of cerium from fission alloys by dross refining (3 hr at 1200 C) in slip-cast magnesia crucibles are presented in Table 38. It is evident that, under the conditions employed, poor removal of cerium was effected in slip-cast magnesia crucibles (20 to 45 per cent - Runs 56, 57, and 63). This is in agreement with laboratory

work which has indicated that more extreme conditions (1300 C for five hours) are required for good cerium removal. A series of runs at 1300 C is planned. These runs will be made in a new furnace recently received from the National Research Corp.

Table 38

CERIUM REMOVAL IN MAGNESIA CRUCIBLES

Scale: 2 kg
Material: Equilibrium "fissium"
Conditions: Liquation time of 3 hr at 1200 C in slip-cast MgO crucibles

Run	Liquation Temp (C)	Cerium Conc. in Charge (w/o)	Cerium Conc. (w/o) after: 15 min	1 hr	2 hr	3 hr	Cerium Conc. in Poured Ingot (w/o)
56	1200	0.53	0.56	0.54	0.51	0.44	0.46
57	1200	0.55	0.62	0.46	0.46	0.43	0.47
63	1200	0.89	0.76	0.54	0.52	0.42	0.40
62[a]	1200	0.97	0.55	0.07	<0.02	<0.01	-[b]

[a]Added 108 g of small pieces of slip-cast zirconia to crucible.

[b]No ingot sample taken.

Effective removal of cerium by the addition of zirconia chips occurred in Run 62. The cerium concentration was reduced to less than 0.01 per cent in 3 hr at 1200 C. However, the low pour yield (88 per cent) in this run resulted from wetting of the zirconia chips and resultant bridging of metal between the chips causing high retention of uranium metal in the crucible. It is planned to procure pressed zirconia crucibles in order to conduct drossing runs in this type of crucible.

In future runs, it is also planned to attempt to dissolve the dross reaction layers and uranium metal in zinc or zinc-magnesium alloys (see page 105). If necessary, hydriding and dehydriding of the material remaining in the crucible will be carried out to provide greater surface area for dissolving.

2. Control of Volatile Fission Products
(J. Wolkoff, P. Kelsheimer)

Work continued on the adsorption of metals volatilized during melt refining of discharged fuel material. The metals volatilized are the fission products, cesium and possibly barium, strontium and cadmium, sodium which adheres to the discharged fuel pins, and magnesium resulting from reaction of uranium and fission products with a magnesia crucible. As indicated in the last quarterly report (ANL-5668, page 89), several surface-active materials were efficacious in the adsorption of vaporized sodium. Three, activated alumina, activated carbon, and "Molecular Sieves," were selected for further testing with regard to capacity and efficiency under various flow and temperature conditions.

A flow system has been put into operation for determining the capacity and breakthrough point of the three selected bed materials under controlled conditions of bed temperature, carrier gas rate and metal vapor concentration in the carrier gas. A schematic drawing of the equipment is shown in Figure 31. The new apparatus consists of a resistance-heated, 2-in. stainless steel furnace tube containing a gas saturator and a bed of the adsorbent material. The gas saturator consists of a nickel crucible so arranged that an argon stream can pick up alkali metal vapor by bubbling through the shallow pool of metal contained in the crucible. The bed is composed of discrete stages, each of which can be handled and analyzed separately. Vapor-laden gas travels successively through each stage from top to bottom. The bed temperature can be controlled at a temperature different from that of the saturator. Thermocouples are located within the bubbler and below the bottom bed.

Argon gas can be recirculated in a closed cycle with the Sigmamotor pump or used "once through" by venting. Closed-cycle argon circulation is being used only during heating and attainment of steady-state conditions. The oxygen that is provided underneath the bottom bed forms a white fume with the alkali metal visible in the sight glass as soon as breakthrough occurs. At this point the run is generally discontinued.

Runs to date are summarized in Table 39. All were made with the bed at 800 C and with metallic sodium as the vapor to be retained by the bed. In Runs 2, 3a, 4a, and 4b the time of breakthrough was not known, since a method of breakthrough detection had not been evolved. Subsequent runs using oxygen to indicate breakthrough were concluded immediately after breakthrough. The first runs carried beyond breakthrough provide good information on the capacities of the materials for sodium, which at 800 C are surprisingly high. Activated alumina and "Molecular Sieves" are capable of retaining about 20 weight per cent sodium of adsorbent charged material (Runs 2 and 4a). Activated carbon can adsorb sodium up to 40 per cent of its weight at 800 C (Run 3a).

FIGURE 31

FLOW SYSTEM FOR METAL RETENTION STUDY ON SORBENT BED

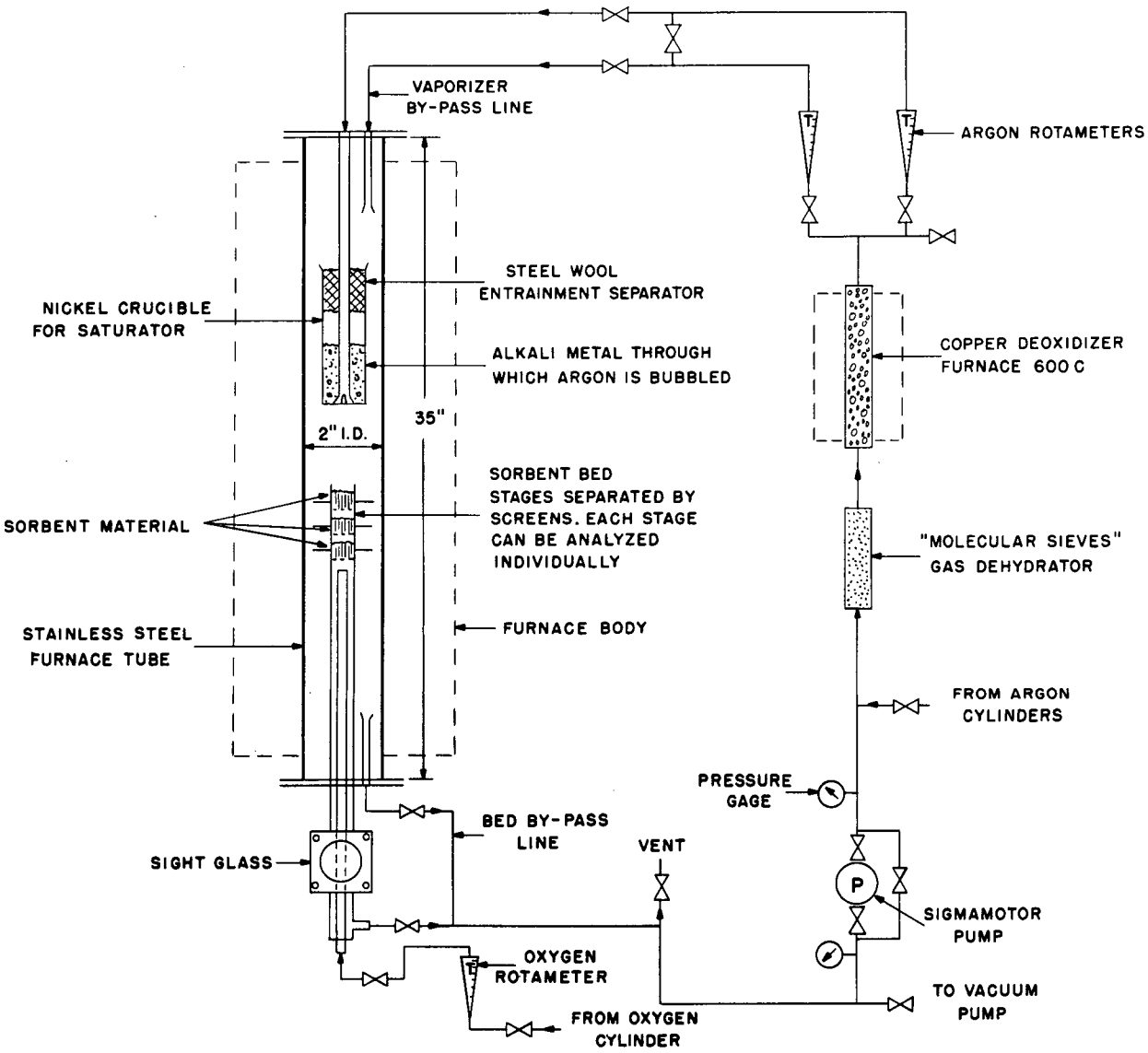

Table 39

REMOVAL OF METAL VAPOR FROM CARRIER GAS WITH SURFACE ACTIVE MATERIALS

(Vaporization of metallic sodium and removal by 3 beds in series, each 13/16 in. dia x 1 in. deep; gas flow through beds from top to bottom. See Figure 31, page 103 for equipment description.)

Run No.	Bed Material	Bed Temp (C)	Metal Vaporizer Temp (C)	Argon Flow Rate (ml/min (STP))	Argon Flow Time (min)	Location	Initial Wt (g)	Gain in Wt (g)	Wt Gain / Initial Wt
2	Activated alumina F10	785	810	50	505[a]	Top	6.29	1.30	0.21
						Middle	6.20	1.44	0.23
						Bottom	6.16	1.21	0.20
5	Activated alumina F10	807	805	50	258[b]	Top	5.97	1.50	0.25
						Middle	6.05	1.48	0.24
						Bottom	6.41	0.45	0.07
3a	Activated carbon CXA	795	805	50	207[a]	Top	3.43	1.50	0.44
						Middle	3.28	1.36	0.42
						Bottom	3.51	1.19	0.34
3b	Activated carbon CXA	808	800	50	245[b]	Top	3.32	1.43	0.43
						Middle	3.39	1.43	0.42
						Bottom	3.24	1.31	0.40
4a	"Molecular Sieves" 4A	795	802	50	260[a]	Top	5.40	0.98	0.18
						Middle	5.02	0.93	0.18
						Bottom	5.36	0.76	0.14
4b	"Molecular Sieves" 4A	795	798	50	200[a]	Top	5.11	1.10	0.22
						Middle	5.05	1.06	0.21
						Bottom	5.54	0.79	0.14
4c	"Molecular Sieves" 4A	798	802	50	175[b]	Top	5.23	0.97	0.19
						Middle	4.99	1.01	0.20
						Bottom	5.51	0.88	0.16
6	Activated carbon CXA	810	795	500[c]	16[b]	Top	3.34	0.94	0.28
						Middle	3.62	0.74	0.20
						Bottom	3.32	0.35	0.11
7	"Molecular Sieves" 4A	820	802	500[c]	25[b]	Top	5.34	0.80	0.15
						Middle	5.69	0.88	0.15
						Bottom	5.60	0.79	0.14

[a] Breakthrough time not known accurately

[b] Run concluded at breakthrough

[c] Equivalent to 145 ml/(min)(sq cm)

Subsequent runs carried only to breakthrough show the adsorption of sodium to be efficient at low flow rates (50 ml/min) since the first two of the three inches of bed material were saturated before breakthrough occurred (Runs 3b, 4c and 5). With activated carbon (Run 3b), saturation throughout was reached before breakthrough. As expected, efficiency of adsorption is lower at high argon flow rates (500 ml/min = 145 ml/(min)(sq cm)) at room temperature and atmospheric pressure, but is still very good (Runs 6 and 7).

3. Uranium Purification by Fractional Crystallization from Liquid Metal Solution

(J. B. Knighton,* A. Chilenskas, J. Pavlik, L. Dorsey, F. Mertes**)

Fractional crystallization of uranium in zinc or other low-melting metals provides a possible pyrometallurgical process for the removal of fission products from spent reactor fuels. Experimental work to date has been carried out with zinc. It is presently envisioned to use fractional crystallization from zinc solution in conjunction with the oxide drossing process which removes elements such as cesium, barium, strontium and the rare earths, but does not remove noble elements such as molybdenum, ruthenium, rhodium, and palladium.

In addition to processing of the drag-out material, fractional crystallization methods might afford a complete method of processing uranium-base irradiated reactor fuels. The basis of separation by fractional crystallization is the difference in the solubility of zinc intermetallic compounds of uranium and the fission product elements in zinc. The discharged reactor fuel might be first dissolved in zinc at a temperature of around 800 C. Concentrations could be adjusted so that upon cooling the noble metal fission products remain in solution while the bulk of the uranium is crystallized. In the case of zinc the crystallized phase is UZn_9. Separation may be effected by filtration. Subsequent uranium recovery is effected by the decomposition of UZn_9 at 945 C to gamma uranium and zinc vapor. Additional heating will coalesce the uranium which is then available for refabrication and use in reactor fuel elements.

a. Preliminary Flowsheet for Drag-Out Processing

The noble metal fission products, ruthenium, rhodium, palladium, molybdenum, and presumably technetium, silver, cadmium, indium, and tin are not removed by the oxide drossing process. The concentrations of these metals can be controlled in recycled fuel by replacement of a portion of the fuel with fresh fissionable material. The equilibrium

---

*Special Scientific employee on loan from American Smelting and Refining Co.

**Student aide from Northwestern University.

concentrations of these elements are therefore dependent on the percentage of replacement or "drag-out." The resulting fuel materials have been termed "fissium," and differentiation of these fuels with respect to composition is made on the basis of the per cent drag-out. Thus, 5 per cent "fissium" indicates the equilibrium composition resulting from 5 per cent drag-out in an oxide slagging operation. This corresponds to 3.4 w/o molybdenum, 2.6 w/o ruthenium, 0.47 w/o rhodium, 0.30 w/o palladium, and 0.10 w/o zirconium.* Irradiation tests by the Metallurgy Division have shown such fissium alloys to be highly resistant to radiation damage.

The drag-out material must be specially processed to remove the noble metals so that the fissionable material may be recovered and reconstituted to new fuel. A preliminary flowsheet for drag-out processing, based on solubility data obtained to date, is given in Figure 32. The major operations of this flowsheet have been demonstrated on a small scale.

b. Determination of Uranium and Fission Product Element Solubilities in Zinc and Zinc-Magnesium Alloys

Work during this period has been directed toward determining the individual and multicomponent fission product element solubilities in zinc and zinc-magnesium alloys. Magnesium has been added to zinc in an attempt to increase the ruthenium solubility.

(1) Uranium-Ruthenium-Zinc System

The mutual solubilities of uranium and ruthenium in zinc have been determined as a function of temperature (Figure 33). The solubilities shown are applicable only to the starting concentrations. A well-defined shift exists in the ruthenium solubility. Since in any process the ruthenium in solution (controlled by initial uranium concentration) should not exceed the solubility at the filtration temperature, the sharp decrease in the solubility of ruthenium at 500 C indicates 500 C or slightly above as the filtration temperature.

(2) Uranium-Ruthenium-(Zinc-3 w/o Magnesium) System

The addition of magnesium to form the eutectic at 97 w/o zinc-3 w/o magnesium increases the ruthenium solubility slightly at lower temperatures (see Figure 34) when compared to the zinc system. This increase of ruthenium solubility may alloy a better separation between uranium and ruthenium. The uranium solubility in this system is not appreciably influenced by the magnesium present in a 3 w/o concentration.

---

*Values are based on no chemical separation of molybdenum, ruthenium, rhodium, palladium, and 70 per cent removal of zirconium.

Figure 32

PRELIMINARY FLOWSHEET FOR PROCESSING FIVE PER CENT DRAG-OUT FUEL MATERIAL

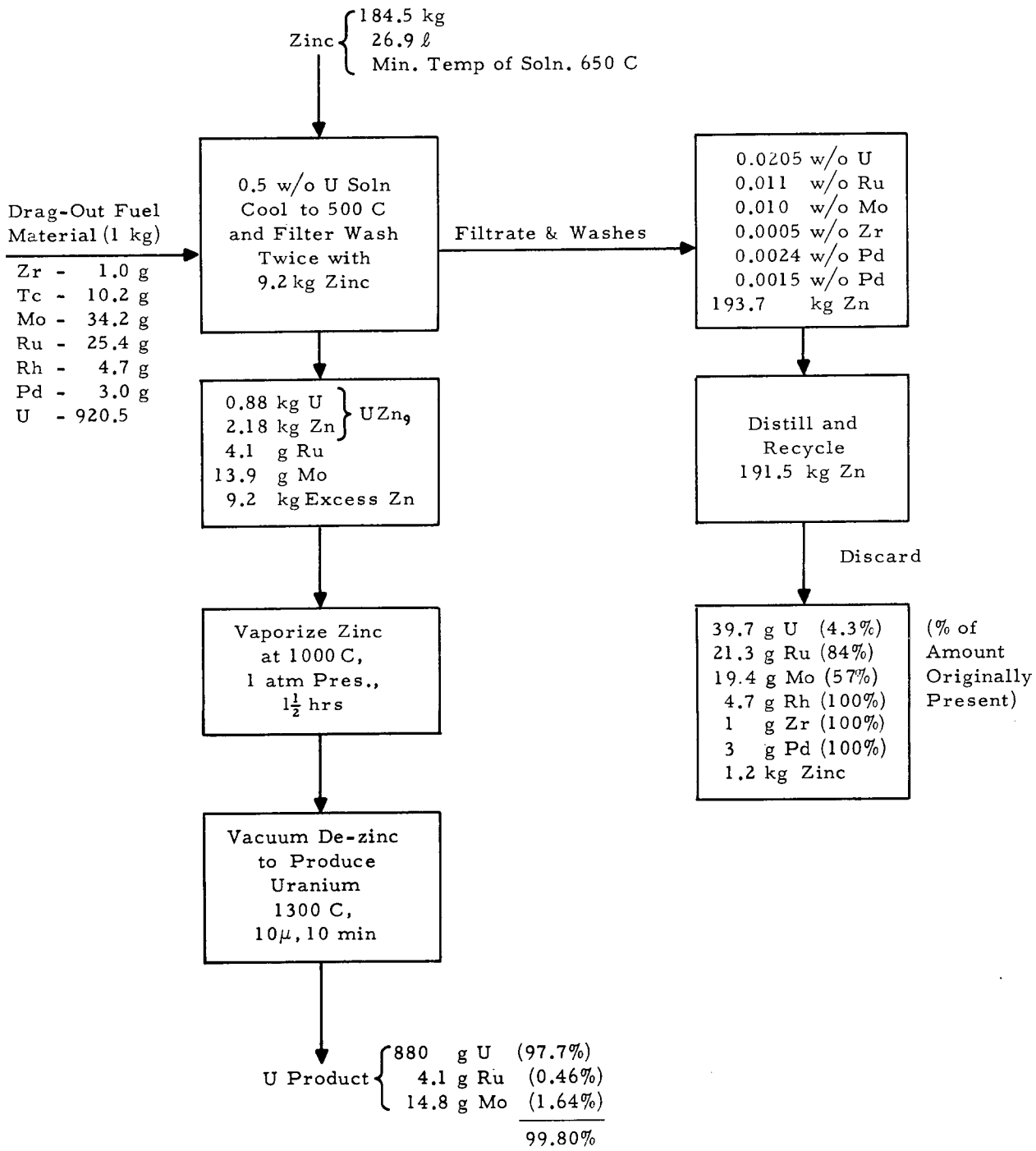

FIGURE 33

MUTUAL EQUILIBRIUM SOLUBILITIES OF RUTHENIUM AND URANIUM IN THE SYSTEM RUTHENIUM - URANIUM - ZINC

(Data from Two Runs)

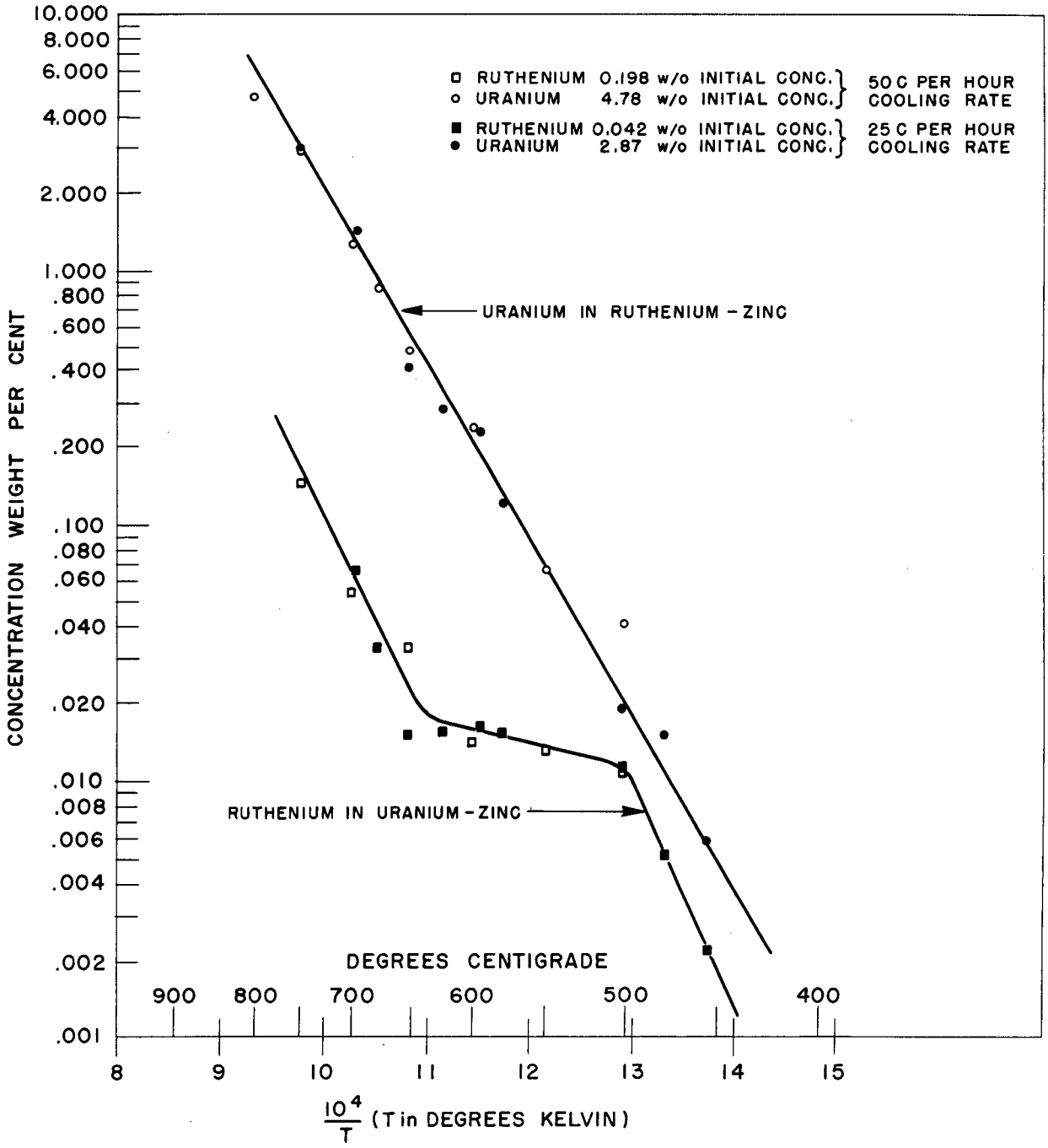

FIGURE 34

MUTUAL EQUILIBRIUM SOLUBILITIES OF URANIUM AND RUTHENIUM IN THE SYSTEM RUTHENIUM - URANIUM - [ZINC - 3 w/o MAGNESIUM]

(Data from Two Runs)

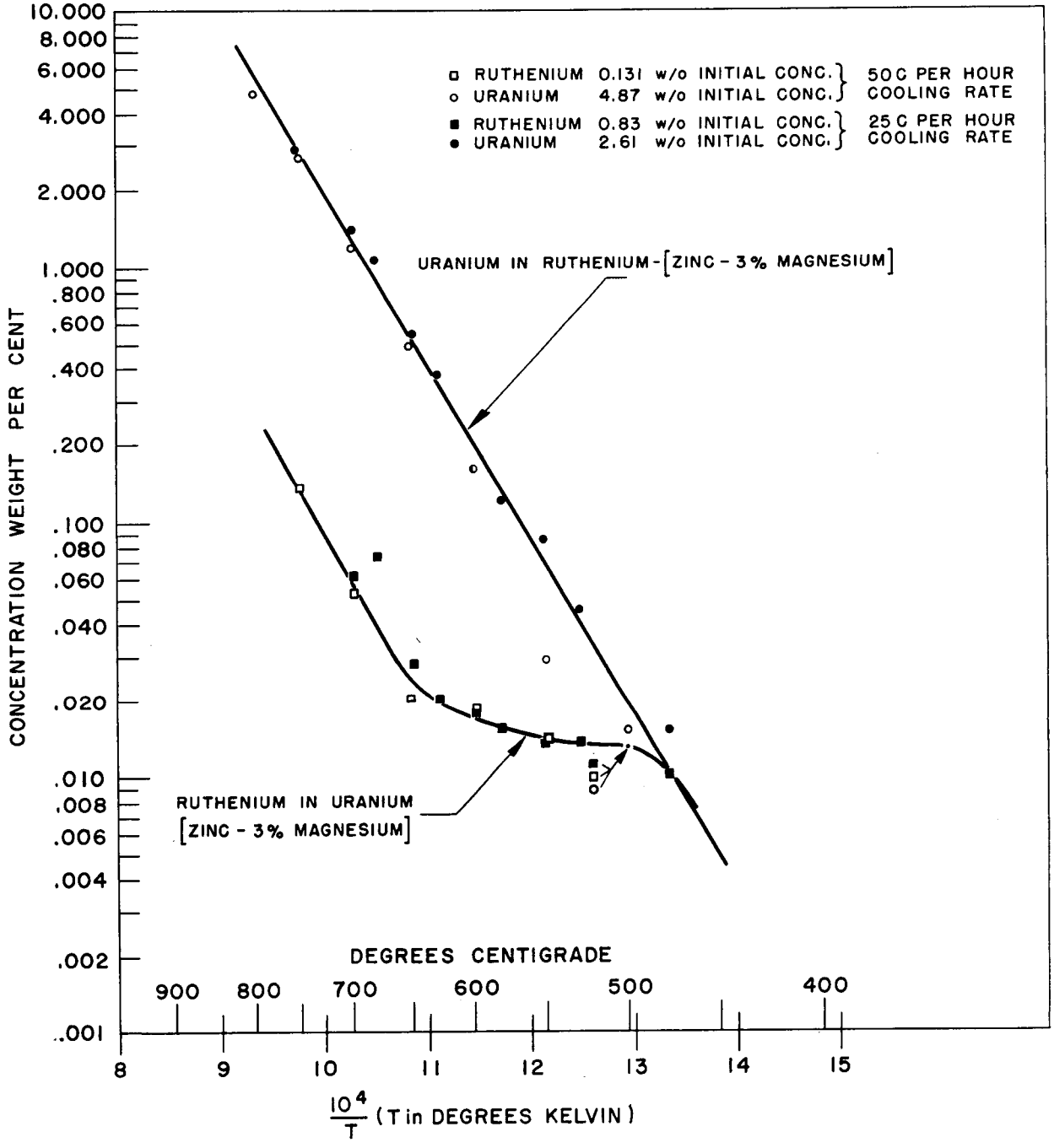

(3) Barium-Zinc and Barium-Uranium-Zinc Systems

The single component solubility of barium in zinc shows barium to be less soluble than uranium (Figure 35). The solubility of uranium in the system barium-uranium-zinc is unaffected by the presence of barium. In the presence of uranium the barium solubility shifted to higher values at high temperatures and lower values at low temperatures than the single component barium solubility in zinc (Figure 36).

(4) Cerium-Zinc and Cerium-Uranium-Zinc Systems

Cerium, like barium, is less soluble than uranium in zinc (Figure 35). For the three-component system cerium-uranium-zinc (Figure 37), the presence of uranium does not appreciably affect the solubility of cerium in zinc. The uranium solubility is depressed by the presence of cerium.

(5) Multicomponent Runs

Runs have been made using "fissium" (see page 87 for definition) to determine the separation of uranium from noble metal fission products. Analytical data are not available. Runs using irradiated uranium are planned for the next quarter.

c. Reduction of Uranium Compounds with Magnesium in Zinc Solvent

The possibility of reducing uranium compounds in liquid metal media may have important applications in pyrometallurgical processing of nuclear fuel materials and in the preparation of uranium feed materials. Experiments have been made which indicate that magnesium in zinc-magnesium alloys will reduce uranium compounds.

Specifically, the following chemical reactions have been effected in a zinc-6 w/o magnesium alloy:

(1) $UO_2 + 2\ Mg + 9\ Zn \longrightarrow 2\ MgO + UZn_9$

(2) $UO_3 + 3\ Mg + 9\ Zn \longrightarrow 3\ MgO + UZn_9$

(3) $UF_4 + 2\ Mg + 9\ Zn \longrightarrow 2\ MgF_2 + UZn_9$

These reactions are verified by the presence of UZn_9 in resulting ingots. Similarly, the uranium in oxide drosses (metallic and oxide) has been reduced to UZn_9 by the action of zinc-6 w/o magnesium alloys. Studies are being made to determine the degree of completion of the reactions.

FIGURE 35

CERIUM, BARIUM AND URANIUM SOLUBILITIES AS SINGLE COMPONENTS IN ZINC

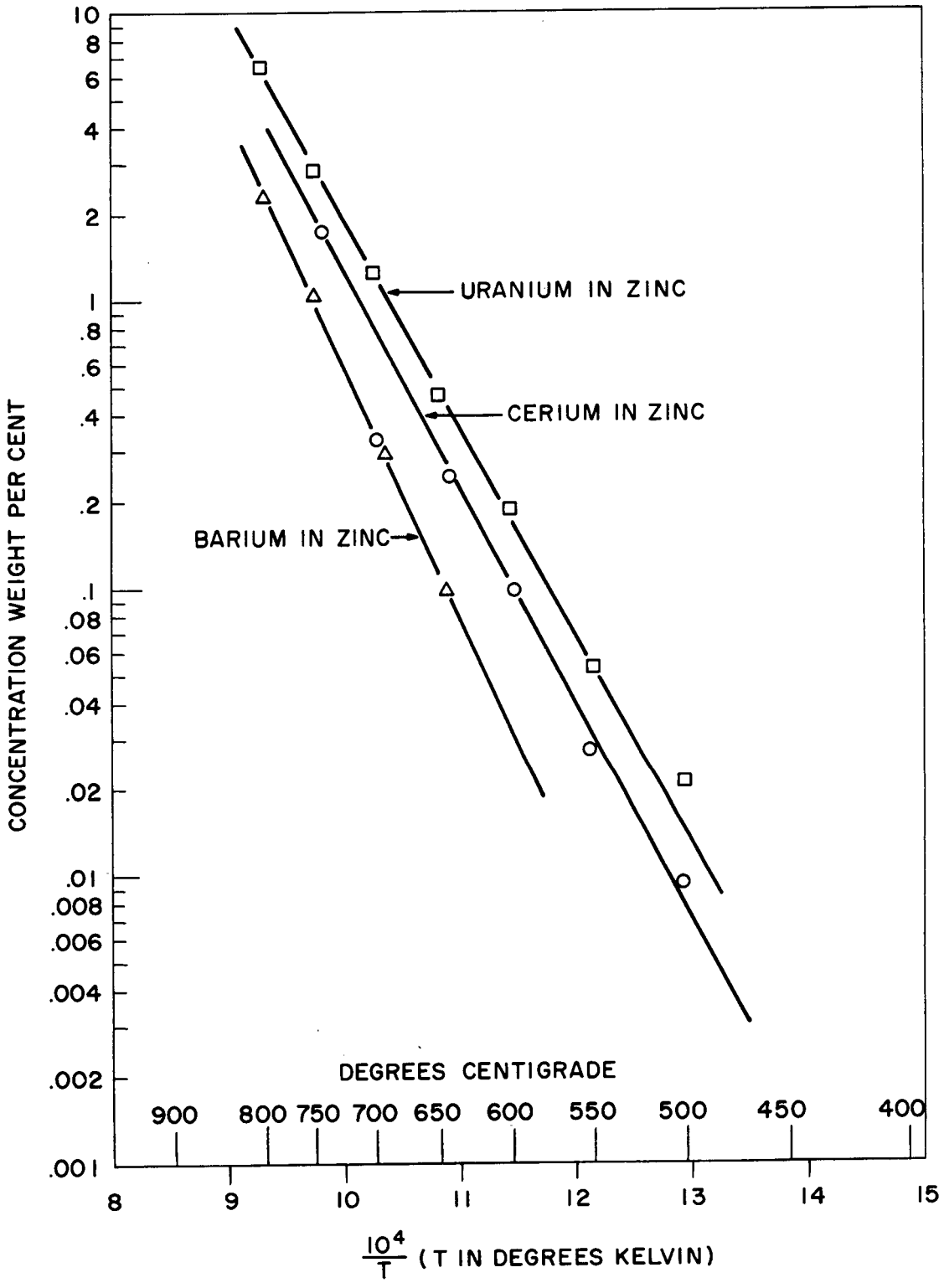

FIGURE 36

MUTUAL SOLUBILITIES OF BARIUM AND URANIUM IN THE SYSTEM BARIUM — URANIUM — ZINC

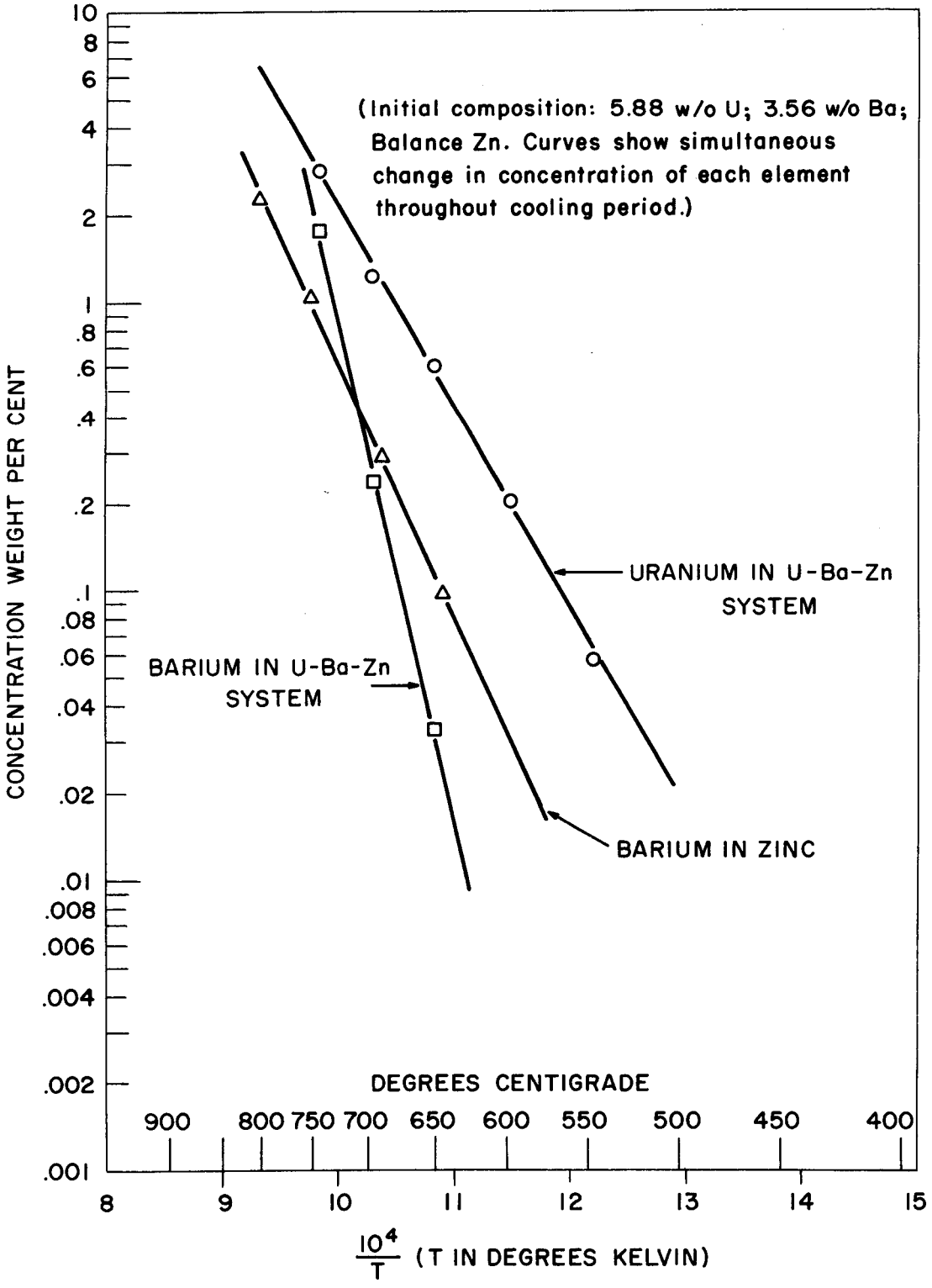

FIGURE 37

MUTUAL SOLUBILITIES OF CERIUM AND URANIUM IN THE SYSTEM CERIUM - URANIUM - ZINC

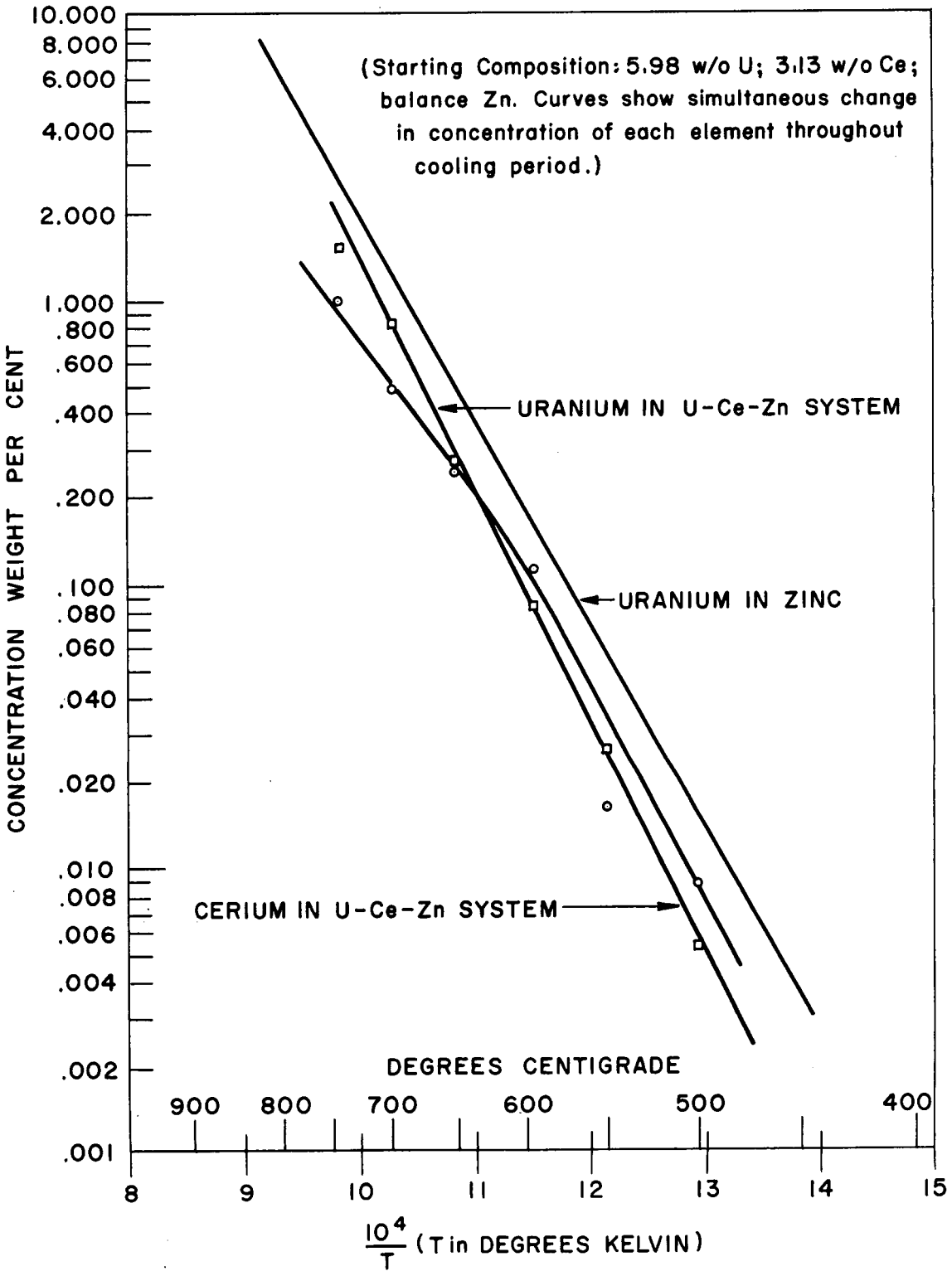

d. Engineering Development

Apparatus has been designed and preliminary experiments completed for the purpose of demonstrating (1) the separation of zinc from UZn_9 and (2) the recovery of uranium from UZn_9. This work is summarized below.

(1) Separation of Zinc from UZn_9

A necessary operation in the process is the separation of the molten zinc containing the dissolved fission elements from the solid crystalline UZn_9 at about 550 C. The apparatus shown in Figure 38 has been used to demonstrate this separation.

FIGURE 38
ZINC FILTRATION APPARATUS

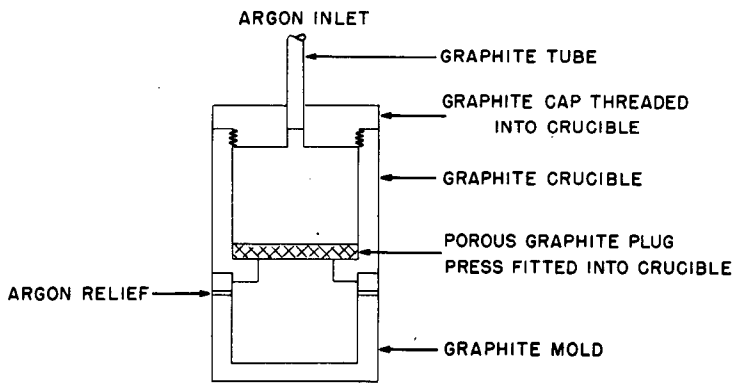

Several experiments were performed in this apparatus. A typical experiment consisted of charging a zinc-uranium ingot to the crucible, heating and stirring at 800 C for one hour, cooling to 550 C, and separating the molten zinc from the UZn_9 by applying 12 psi pressure differential across a porous graphite filter of 180-micron average pore size with argon for two minutes.

The filter cake obtained from a charge of 19 g of uranium and 477 g of zinc weighed 97 g and contained an estimated 66 g of UZn_9 and 31 g of zinc. It was crystalline in appearance and oxidation-resistant at room conditions. The zinc filtrate (346 g) represented an estimated 92 per cent of the total uncombined zinc present in the zinc-uranium ingot.

(2) Recovery of Uranium from UZn_9

At present consideration is being given to the recovery of uranium from UZn_9 by the vaporization of zinc from the UZn_9 under vacuum or under an inert atmosphere such as helium. The feasibility of this separation was demonstrated in the apparatus shown in Figure 39.

FIGURE 39
URANIUM RECOVERY FROM UZn_9

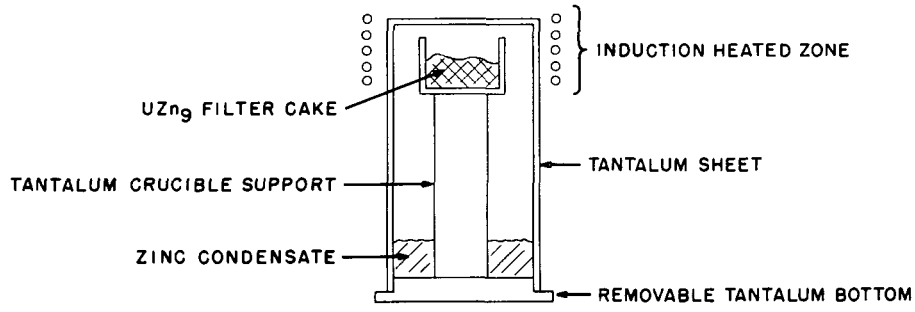

Preliminary experiments on a small scale were performed in which a tantalum, magnesia or alumina crucible was charged with small amounts of filter cake (ca 30 g) heated to about 1000 C for $1\frac{1}{2}$ hr under an argon atmosphere to vaporize the zinc. The uranium was then heated to 1300 C to permit coalescence and cooled under argon. When a tantalum crucible was used, globules of uranium metal were produced along with some non-metallic residue, whereas the uranium residue remaining when oxide refractory crucibles were used appeared as spongy semi-metallic buttons. The residues contained an average of 60 ppm of zinc as determined by emission spectrographic analysis.

In order to continue this study on a larger scale, the preparation of UZn_9 from essentially stoichiometric quantities of uranium and zinc was accomplished to provide a source of UZn_9. The apparatus shown in Figure 40 has been used for this purpose.

FIGURE 40
PRODUCTION OF UZn_9

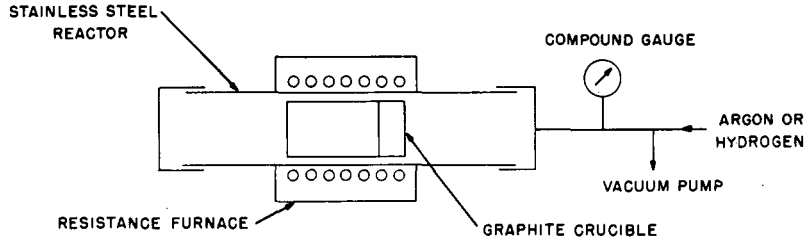

The uranium (weighing 454 g and charged as small segments of 5/16-in. rod) and zinc bar slightly in excess of the stoichiometric quantity required are enclosed within the graphite crucible by means of a threaded graphite cap. The graphite (CS type) is sufficiently porous to permit gases to pass through but retains molten zinc. Powdering the uranium rod is accomplished by hydriding the uranium at 1 atm and 240 C and dehydriding at 360 C under vacuum. The powdered uranium and zinc charge are then held at 800 C for five hours with occasional agitation provided by rocking the reactor.

Metallographic examination of segments of the product ingot showed crystals assumed to be UZn_9 with some unreacted zinc constituting a second phase. No evidence of unreacted powdered uranium has been found, although several large lumps of uranium which apparently had not hydrided were discovered in sectioning the ingot.

4. Extraction of Plutonium by Liquid Magnesium

Semi-works studies on the extraction of plutonium from uranium-5 w/o chromium alloys with molten magnesium and on the subsequent magnesium distillation step have been continued. Two runs of four successive batch extractions have been made in the small-scale batch extraction unit described in ANL-5602, page 122. In the first run, which was made in an alumina-coated graphite crucible, a total of 83 per cent of the plutonium was extracted. A decreasing distribution coefficient on successive extractions was noted and is taken as evidence of loss to the crucible or of formation of inextractible plutonium compounds such as the carbide. In the second run, which was made in a tantalum crucible, 98 per cent of the plutonium was extracted. Distribution ratios (mol fraction basis) in favor of the magnesium varied between 0.022 and 0.177, which are lower than those measured in the laboratory (see page 96). Distillation of magnesium from a concentrated plutonium-in-magnesium phase has, in small-scale runs made to date, resulted in poor transfer of plutonium to a uranium-chromium phase.

Development of various components suitable for handling molten magnesium in a plutonium extraction process has continued. Data have been obtained on the corrosion resistance of various metals in molten magnesium. Of the metals tested only tantalum has shown any promise as a container material.

a. Magnesium Extraction Studies
(I. O. Winsch, A. R. Cole, W. Walters, W. Spicer, K. Olsen)

Two magnesium extraction runs of four successive extractions each have been completed in the small-scale extraction unit (see ANL-5668, page 98). In each of these runs the uranium-chromium-plutonium alloy was contacted with magnesium in a 1 to 1 weight ratio. In the first run,

Run VI, an alumina-coated graphite crucible was used to contain the molten metal and agitation of the two phases was continued for 1/2 hr at 950 C; in the second run, Run VII, a tantalum crucible was used and agitation time was increased to $1\frac{1}{2}$ hr. Following cessation of mixing, the two phases were cooled to 800 C, thereby freezing the uranium-chromium phase and allowing the magnesium phase, containing extracted plutonium, to be poured off into a receiving mold.

In Run VI, about 84 per cent of the plutonium originally present in the U-Cr was extracted during the four extractions (see Table 40). The overall plutonium material balance amounted to 88 per cent, with the graphite crucible probably accounting for the remainder. A steady decrease in the value of the plutonium distribution ratio was noted, decreasing from 0.170 to 0.022. The distribution ratio for each extraction is based on the calculated amount of plutonium remaining in the uranium. A decrease in the distribution ratio is indicative of unavailable plutonium, such as loss to the graphite crucible or the formation of plutonium compounds, such as plutonium carbide.

Table 40

SUCCESSIVE BATCH EXTRACTIONS OF PLUTONIUM IN SMALL-SCALE BATCH EXTRACTION UNIT

Run VI

Uranium Alloy:	5% chromium; 1.23% plutonium
Charge:	497.8 g alloy; 6.115 g plutonium
Agitation Time:	1/2 hr
Temperature:	900 C
Crucible:	alumina-coated graphite

Run VII

Uranium Alloy:	5% chromium; 1.03% plutonium
Charge:	503.5 g alloy; 5.22 g plutonium
Agitation Time:	$1\frac{1}{2}$ hr
Temperature:	900 C
Crucible:	tantalum

Run No.	Extraction No.	Charge Wt (g)		Plutonium Extracted		Available Pu Extracted (per cent)	Distribution Coefficient (K)
		Mg	Pu	(g)	(cumulative per cent)		
VI	1	503.9	6.125	3.87	63.2	63.2	0.170
	2	-	-	0.76	75.7	33.9	0.068
	3	-	-	0.35	81.4	23.8	0.037
	4	-	-	0.18	84.4	15.5	0.022
	Plutonium Material Balance				88.1		
VII	1	499.3	5.22	3.32	63.5	63.6	0.177
	2	-	-	1.03	83.2	54.4	0.131
	3	-	-	0.34	89.7	39.0	0.070
	4	-	-	0.097	91.6	18.5	0.026
	Plutonium Material Balance				94.3		

In order to eliminate as much as possible these suspected losses of plutonium, Run VII, was made in a tantalum crucible. As indicated in Table 40, 92 per cent of the plutonium was recovered in the four magnesium extracts, the overall plutonium material balance was 94 per cent. The distribution ratio again decreased (from 0.177 to 0.026). These coefficients are, however, much lower than measured in single laboratory extractions (see page 96).

An attempt was made to carry out three successive, 1/2-hr batch extractions in the 5-kg scale extraction unit (ANL-5633, page 129) using a 5-kg charge of a uranium-5 w/o chromium alloy which initially contained 0.5 g of plutonium. The agitator shaft became disengaged after the first extraction. This is being repaired in preparation for further runs at higher plutonium concentrations.

About 55 per cent of the plutonium was extracted in the first extraction for an effective distribution coefficient of 0.15 (mol fraction basis).

b. Magnesium Distillation
(I. O. Winsch, A. R. Cole, W. Walters, W. Spicer, K. Olsen)

A check of the plutonium concentration in the magnesium heel from distillation Run 22 (1585 g of magnesium and 2.5 g of plutonium - see ANL-5668, page 102) confirmed that only 50 per cent of the plutonium remained in the magnesium heel. Analyses of a pie-shaped sample cut out of the heel agreed with analyses of previous samples, which were drillings taken in each of the four quadrants of the cylinder. It is suspected that the graphite crucible which contained the molten magnesium absorbed the remaining plutonium. Future runs will be made using a tantalum crucible in an attempt to decrease the plutonium losses.

A small-scale distillation was conducted during the past quarter in which an attempt was made to transfer plutonium from a concentrated plutonium-in-magnesium phase to a uranium-chromium phase. The experiment was conducted in a stainless steel tube furnace which was inductively heated. The still pot charge was contained in a Morganite recrystallized alumina crucible supported in a tantalum secondary. The still pot charge consisted of 121.3 g of uranium-5 w/o chromium alloy and 30.9 g of magnesium containing 123 mg of plutonium. The magnesium was distilled at a temperature of about 920 C in order to maintain the uranium-chromium alloy in the molten state during the distillation.

A clean uranium-chromium button resulted, and this was sampled for plutonium analyses. An etching of the button was made initially, followed by complete dissolution of the button for a separate sample. Only 35 per cent of the plutonium originally charged could be accounted for in the

uranium-chromium "getter." The surface etching of the button indicated a ratio of 1 mg Pu/g U-Cr as compared to a ratio of 0.35 mg Pu/g U-Cr in the main portion of the button.

Future distillations will be made using a tantalum crucible to contain the molten magnesium and a sieve-type baffle arrangement over the mouth of the crucible. Some consideration is being given to using a uranium liner in the tantalum still pot crucible to contain the plutonium heel after distillation of the magnesium.

c. Development of Components for Magnesium Handling (G. Bennett, W. Kline)

The development of various components suitable for handling molten magnesium in a plutonium extraction process has continued. These components include:

(1) a valve for sealing molten magnesium;

(2) a liquid level indicator;

(3) a sampling apparatus.

Data have also been obtained on the corrosion resistance of various metals to molten magnesium.

These developments may be summarized as follows:

(1) Inasmuch as the "pipe-trap" type of freeze valve described in ANL-5668, page 103, has been demonstrated to seal satisfactorily on a static system, equipment is now being set up to check its reliability. In these tests, it is planned to circulate molten magnesium by inert gas pressure between two storage tanks through the freeze valve. The magnesium trapped in the valve will then be frozen, while maintaining the rest of the magnesium in the system in a molten condition. The reliability of the valve as a seal will be checked over a number of cycles.

(2) In the development of a liquid level indicator, accent has been on designing a coil which will withstand the operating temperature of 950 C. Tests have been made with coils consisting of single layers of platinum, tungsten, and palladium wound on a magnesia core. In order to compensate for the loss of signal due to the decreased number of turns, an additional amplification stage was added to the balance circuit.

As with the copper wire, excellent results were obtained in locating the magnesium-argon interface in the cold. However, mechanical weaknesses in the probe design have prevented operation for longer than about one hour under molten conditions. This was sufficient time, however, to show that the balance circuit is affected by the change

of electrical resistivity of the coil with temperature. Although plant operation will be essentially isothermal, Mr. Gerhardt Weiss of the Electronics Division is redesigning a portion of the circuit to compensate for this effect.

Another major problem is the development of a satisfactory coating material to protect the coil from external abrasion and internal shorting. At the present time Sauereisen is being used; however, this tends to crack upon extended exposure to heat. Other cements are being investigated for this application by Mr. Robert Lied of the Metallurgy Division.

(3) The problem of developing a suitable sampling apparatus consists of two parts: (a) materials for sampling and (b) methods for sampling. A suitable material is considered as one which will neither react with nor be wet by magnesium or uranium and from which the solidified sample can be easily removed. A suitable method is one which can be depended upon to give uniform samples from any desired level.

Accordingly, sampling tubes of the materials listed in Table 41 were tested by dipping into molten magnesium and withdrawing a sample by means of a Leco sampling gun, a device by means of which samples are drawn into a tube by a preset vacuum.

Table 41

MATERIALS TESTED AS SAMPLING TUBE

Uncoated	Outside Coated with Aqua-dag	Both Sides Coated with Aqua-dag
Vycor[a]	Vycor	Vycor
Cold Rolled Steel	Cold Rolled Steel	Type 446 SS
Porcelain	Graphite	Type 304 SS
Graphite		Graphite

[a]Alumina-coated vycor also tested.

The cleanest samples were obtained using the uncoated graphite. The magnesium did not wet the graphite and removal of the sample was accomplished easily by breaking the graphite tube. Aqua-dag coating of graphite was superfluous. All other materials were wet by or reacted with the magnesium.

Difficulty was experienced in obtaining samples at every attempt and in obtaining equal amounts of sample with a Leco sampling "gun." A more satisfactory sampling technique has been the use of graphite dip tubes closed at the lower end and with an entrance hole in the side 3/4 in. from the bottom. The next step in this program will involve the use of a slip-fit graphite plug inside the graphite dipping tube. By means of this movable plug it is expected to be able to control the level at which the sample is taken.

d. Corrosion Resistance of Various Metals to Molten Magnesium

One of the major problems in handling molten magnesium at the temperatures of interest (~950 C) is that of finding suitable container materials. Several materials considered most likely to withstand molten magnesium under flow conditions at 950 C were tested in the last quarter under the impetus of finding a material suitable for use in an electromagnetic pump. The materials selected were Type 446 SS,* 1018 mild steel, black iron, tantalum and Croloy $2\frac{1}{4}$,** the latter tested primarily because of its high-temperature strength. These coupons were suspended from iron wires attached to steel rods inside a steel tank. Sufficient magnesium was added so that the coupons at the uppermost level were subjected to interfacial corrosion. The magnesium was maintained at 950 ± 5 C by means of a 30-kw, 10,000-cps induction heating unit. Throughout the run a pressure of five pounds of argon was maintained.

The run was continued at temperature for a period of 65 hr, at which time the thermocouple failed. The average temperature was 947 C. Adhering magnesium was leached away from the sample with dilute (2 per cent) acetic acid. Blanks showed negligible effect of the leaching operation on the samples.

Visual observation showed very strong interfacial and vapor phase attack on both the steel tank and thermocouple protection tube (Figure 41), and on the steel rod used to support the samples. Attention is also called to large deposits of iron phase in the bottom of the melt.

Visual examination of the sample coupons (Figure 42) showed that tantalum was essentially unaffected, the 446 and Croloy $2\frac{1}{4}$ were somewhat attacked, and the 1018 steel and black iron were very badly attacked. For Croloy $2\frac{1}{4}$, 1018 steel and black iron, interfacial corrosion was far more severe than liquid-phase corrosion; however, tantalum was unaffected in either case.

---

*~26 w/o chromium

**$2\frac{1}{4}$ w/o chromium, 1 w/o molybdenum.

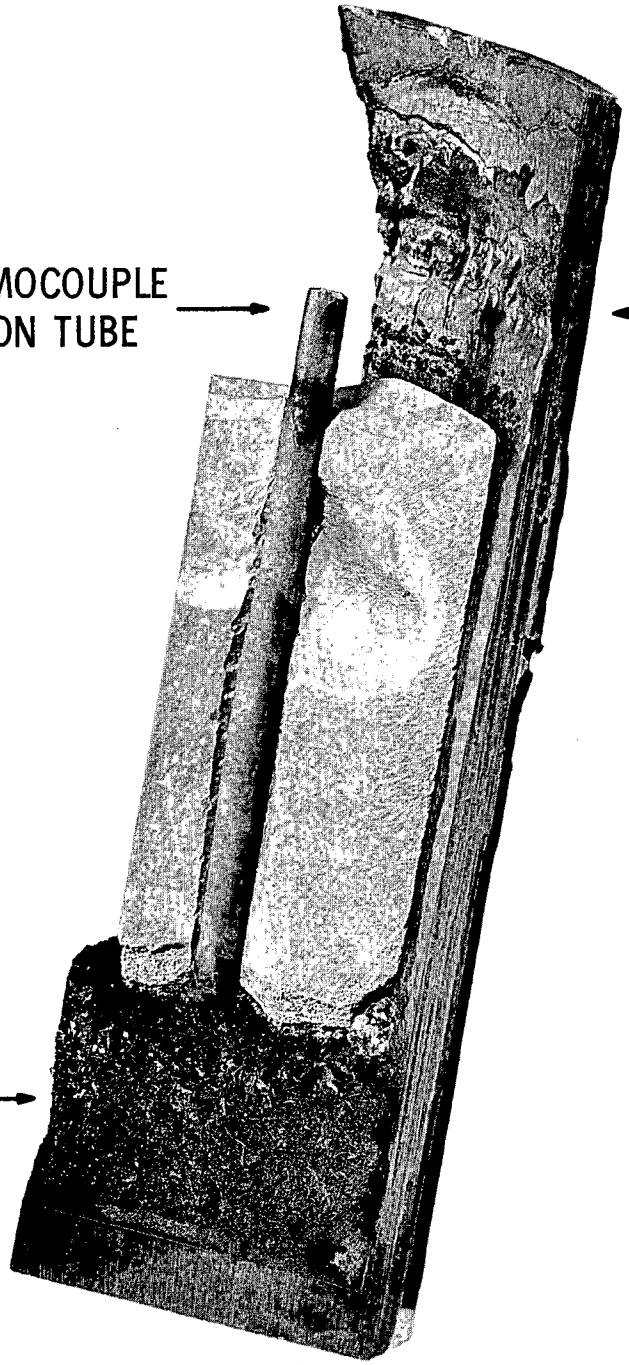

FIGURE 41
MAGNESIUM CORROSION TEST:
SECTION OF STEEL TANK CONTAINING MAGNESIUM

FIGURE 42
MAGNESIUM CORROSION TEST: SAMPLE COUPONS - SIDE VIEW

These observations are confirmed quantitatively in Table 42, which lists the corrosion rate of the samples in mils per day based upon measurement of weight difference. For comparison purposes, the results of an earlier test made on 446 SS and Croloy $2\frac{1}{4}$ are included.

Table 42

CORROSION RATE OF METAL SAMPLES IN 950 C MAGNESIUM

	Corrosion Rate - Mils per day[a]			
	65-Hour Test		6-Hour Test	
Sample No.	1	2	1	2
Material				
Tantalum	0	0[b]	-	-
446 SS	3.3	5.9	8.4	13.2
Croloy $2\frac{1}{4}$	6.8[b]	0.4	10.4	5.6
1018 Steel	7.78	-[c]	-	-
Black Iron	-[c]	21.6	-	-

[a]Assuming linear corrosion rate with time.

[b]Interfacial corrosion.

[c]Interfacial corrosion resulting in sample dissolution.

A comparison of the corrosion rates obtained in the 65-hr test with those obtained in the 6-hr test shows the corrosion rate tends to decrease with time. A rough flexure test made with both treated and untreated tantalum indicated no embrittlement had occurred during the test period. A metallographic examination is being carried out on the tantalum samples; results were not yet available.

5. Inert Gas Purification
(I. G. Dillon, K. Bremer, V. N. Thelen)

Tests have been made on the Manufacturers Engineering and Equipment Corporation Model W Electrolytic Water Analyzer which is being considered for continuous monitoring of EBR-II fuel processing cell gas for oxygen. The oxygen is first converted to water by passing the gas and added hydrogen over a palladium catalyst (not part of instrument). In the instrument, the water is absorbed and electrolyzed in a cell. The

current which flows in an electrical circuit is a measure of the water content of the gas. The Model W Analyzer is less expensive ($575 vs $5000) and much smaller (25 lb vs 700 lb) than the GE Dewpoint meter, which has been previously tested (ANL-5494, page 76).

The Model W Analyzer was checked for accuracy and response time for water contents from 8 to 840 ppm by parallel operation with the General Electric Dewpoint Recorder. Present EBR-II design envisions a maximum oxygen content of the cell gas in the order of 100 ppm. This corresponds to 200 ppm water when using the proposed water monitoring system. Water content in the argon gas was controlled by means of the system shown in Figure 43.

FIGURE 43
APPARATUS USED FOR TESTING MODEL W ELECTROLYTIC WATER ANALYZER

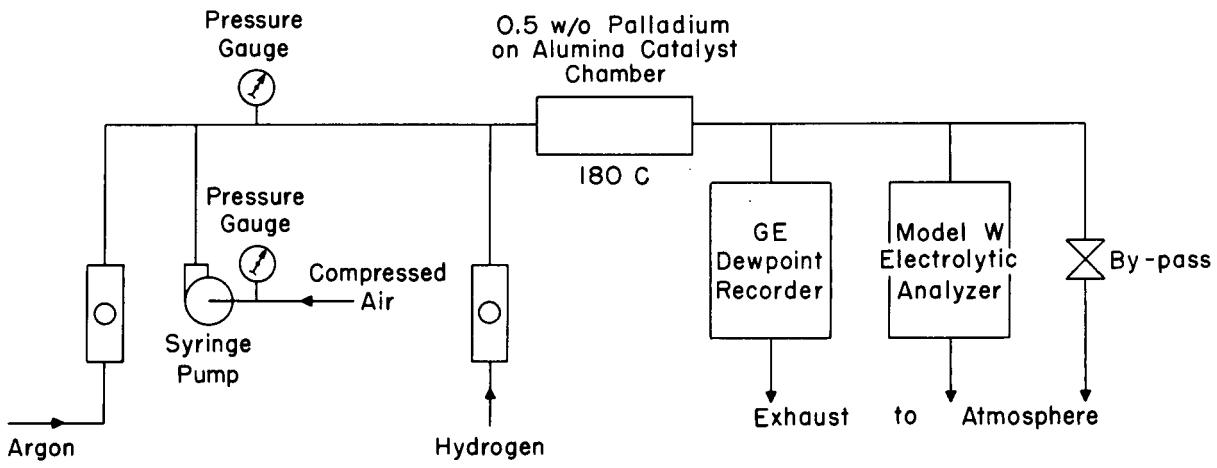

Run data are summarized in Table 43. The Model W consistently gave values slightly lower than the GE recorder but usually within the limit of error of the GE instrument (± 2 F). Response time was very rapid, with an almost instantaneous change in reading with change in water content.

Table 43

CALIBRATION TESTS ON MODEL W ELECTROLYTIC WATER ANALYZER

(Manufacturers Engineering and Equipment Corporation)

Argon Flow[a] (cc/min)	System Press (in. H_2O)	Water Content, ppm	
		GE Recorder	Model W Electrolytic Analyzer
2460[b]	69	8	8
440[b]	42	15	17
1033	44	840	812
1300	47	685	623
1372	46	582	573
1735	66	529	476
2030	43	407	398
2050	43	407	387
2380	64	407	346
2840	45	310	287
3400	41	294	253
3510	63	328	248
4560	69	223	189
6590	43	132	126
6650	68	140	128
8340	38	104	100

[a]Total argon flow through GE Dewpoint Recorder, Model W Electrolytic Water Analyzer and by-pass, and through auxiliary by-pass.

[b]No hydrogen and oxygen (water) addition = tank argon.

6. High-Activity Level Demonstrations of Dross Refining (V. G. Trice)

It has been deemed advisable to demonstrate the melt-refining process under conditions approximating those anticipated in the EBR-II recovery plant. These conditions require the melting and pouring of 60 per cent enriched "fissium" irradiated to two per cent burn-up in 180 days.

The equipment necessary for melt refining will be installed in the Chemical Engineering Division Senior Cave facility. This installation is expected to be available for process studies by October 1958.

A water-cooled irradiation facility is being designed for installation in the CP-5 research reactor. A specially designed thimble, immediately adjacent to the fuel elements, will be employed for this purpose. The heat dissipation capacity of the facility will be about 30 kw. At the current CP-5 operating level of 2 Mw, one per cent burn-up of 30 per cent enriched fission rod has been realized in about 200 days. With the expected increase in pile operating level to 4 Mw it will be possible to handle in the water-cooled facility the irradiation of 300-g rods of 10 to 20 per cent enriched fission. About one per cent burn-up would be realized in 120 days.

V. ANALYTICAL RESEARCH

A. An X-ray Spectrometric Method for Determining Plutonium in Solution (D. S. Flikkema, R. V. Schablaske)

It has been shown by a preliminary account that the method of X-ray emission spectrometry could be extended advantageously to the determination of plutonium in solution (ANL-5633, pages 137 to 140). Since K and L X-ray emission is not measurably affected by the valence state of the emitting atom or ion, this physical method is especially attractive for elements such as plutonium whose chemistry is intricate and whose chemical analysis is complicated by several valence states existing in solution. Further, the method is independent of isotopic content which must be known for the radiochemical assay of plutonium.

From the outset the sensitivity and simplicity inherent in the X-ray emission method[16] gave promise that reliable results should be obtainable with much less plutonium than required for methods in use, thus minimizing the personal hazard from this alpha emitter. With a total amount of plutonium between 0.3 and 0.8 mg the standard deviation of a single result has been found to be about 1 per cent.

The detailed study is being presented in a topical report.

B. Ascending Paper Chromatographic Analysis of Irradiated Uranium and Thorium in a Hydrofluoric Acid Medium (C. E. Crouthamel, C. Gatrousis)

A summary of the results of the chromatographic analysis of irradiated uranium and thorium targets is shown in Table 44 and Figures 44 and 45. Chromatograms are prepared by immersing one end of a strip of Whatman 3-mm paper to a depth of about one inch in the developing medium (for example, 20 g 49 per cent hydrogen fluoride in 100 ml methyl ethyl ketone); by capillary action the medium flows up the paper contacting the radioactive sample which is located just above the lower black line on the chromatograms shown in Figures 44 and 45. The ions dissolved by the medium continue to travel up the paper, each ion traveling at a rate shown in Figures 44 and 45. The developed chromatogram is then contacted with photographic film to produce the radioautograph. The identifications of various fractions have been obtained by gamma-pulse analysis by a sodium iodide crystal and with beta counting. Half-life determinations on the various fractions were also obtained. In each case the identification was also confirmed by a chemical isolation and a chromatogram of the purified material. The chromatograms are being used in the analysis of uranium and thorium targets for the determination of various reactor cross sections.

[16] Flikkema, D.S., Larsen, R.P., and Schablaske, R.V., The X-ray Spectrometric Determination of Uranium in Solution, ANL-5641 (November 1956)

Table 44

SUMMARY OF THE BEHAVIOR OF RADIOACTIVE NUCLIDES WITH HYDROGEN FLUORIDE AND HYDROGEN FLUORIDE-METHYL ETHYL KETONE MEDIUM IN ASCENDING PAPER CHROMATOGRAMS

	R_f[a]			
	Developing Solvent			
Nuclide	20 gm 49% HF per 100 ml MEK	60 gm 49% HF per 100 ml MEK	49% HF	Remarks
Cs^{137},Cs^{134}	0.3	0.6	1.0	Other alkali and alkali earths behave similarly. Results may be difficult to reproduce as there is a tendency for a fraction to remain fixed in paper.
Ba^{140}	0.0	0.0	0.8	
Sr^{90}	0.0	0.0	0.8	
Ce^{141}, La^{140}, Y^{90}, Th^{234}	0.0	0.0	0.0	
Nb^{95}, Nb^{97}	1.0	1.0	0.7	
Ta^{181}	1.0	1.0	0.7	
Zr^{95}, Zr^{97}	0.0	0.05	0.2	
$Sb(V)^{125}$	1.0	1.0	0.8	
Ru^{106}	-	0.2	0.8	Species unpredictable, variable R_f values.
$Te(VI)^{132}$	0.5	0.6	0.8	
Mo^{99}	0.1	0.25	0.1	
Tc^{99m}	0.5	0.6	0.7	
Pa^{233}	0.0	0.05	0.9	
UO_2^{++}	0.0	0.05	0.2	Considerable tailing
Np^{239}	0.0	0.0	0.2	Considerable tailing
Pu^{239}	0.0	0.0	0.2	Considerable tailing
Am^{241}	0.0	0.0	0.0	

[a] $R_f = \frac{\text{distance traveled by species*}}{\text{distance traveled by solvent boundary}}$

*Measured from the sample point

FIGURE 44

CHROMATOGRAMS OF ONE-DAY AND ONE-WEEK OLD URANIUM

(Contact Prints)

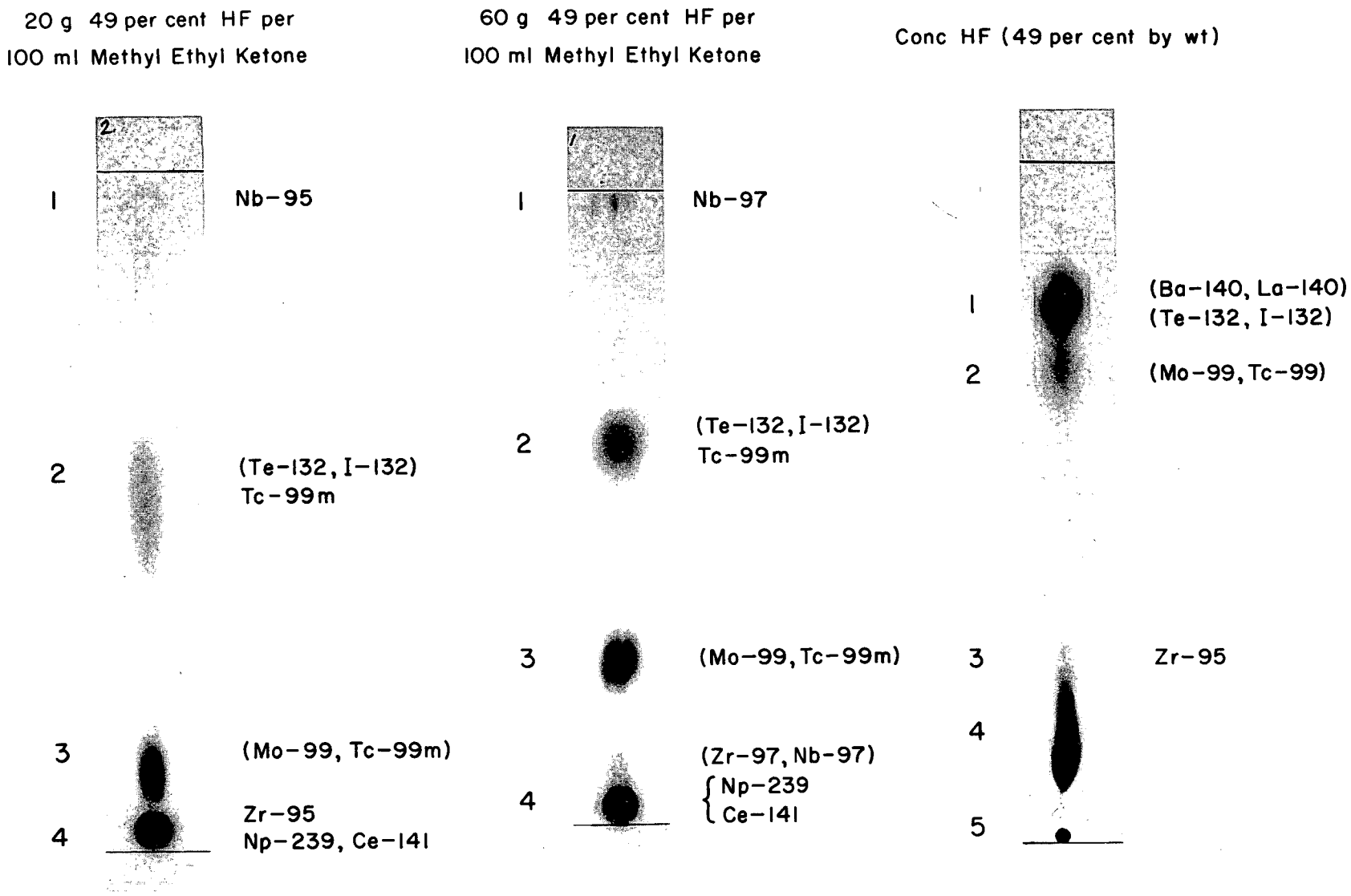

FIGURE 45

CHROMATOGRAMS OF CHALK RIVER URANIUM IRRADIATED TO APPROXIMATELY TEN PER CENT TOTAL ATOM BURN-UP AND COOLED THREE YEARS

(Contact Prints)

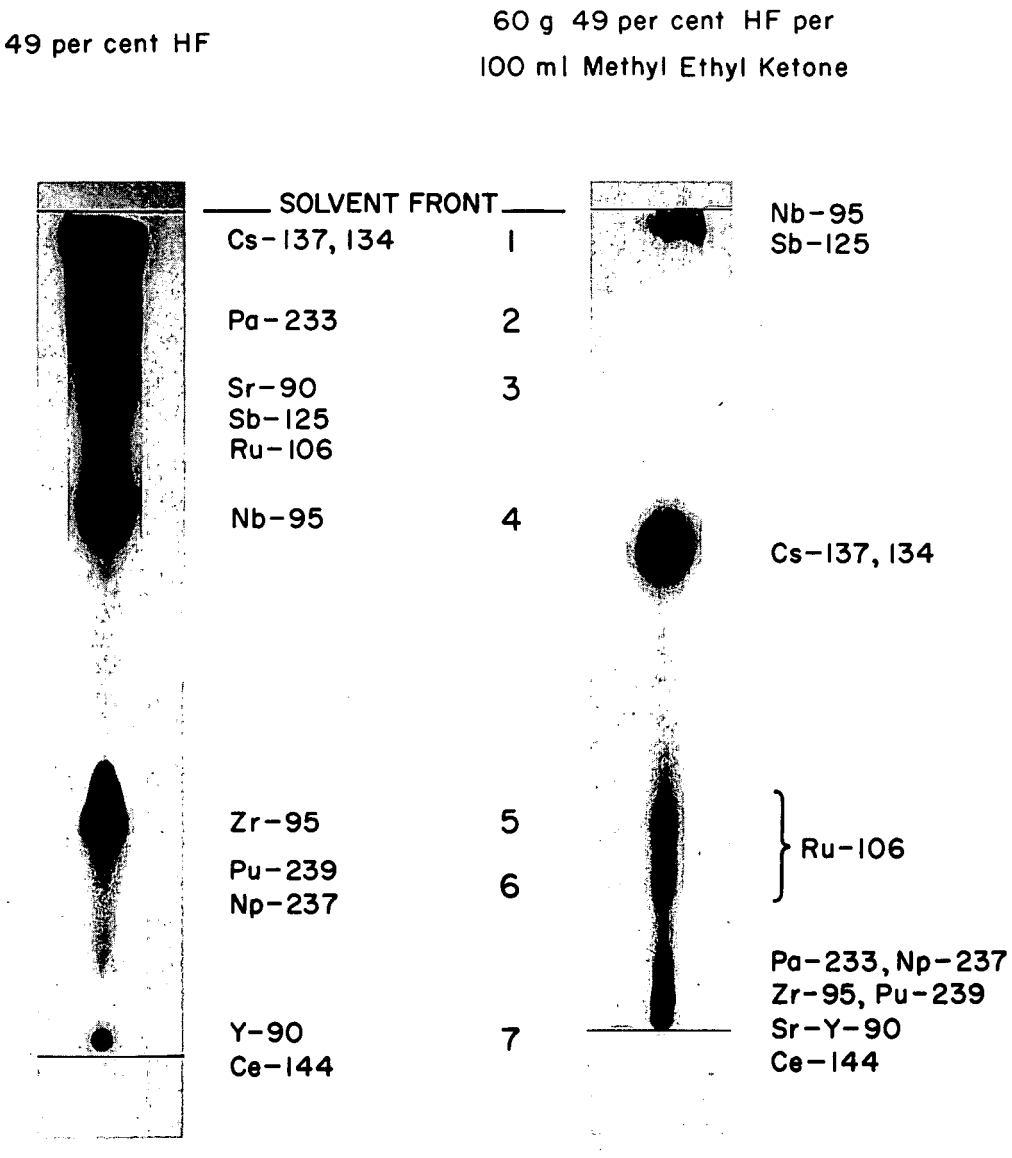

VI. ROUTINE OPERATIONS

A. Waste Processing

(J. Harast, A. Rashinskas, E. Johnston, J. Pavlik)

A total of 46,500 gal of liquid radioactive wastes were processed in this quarter. Of this amount 41,100 gal were processed by evaporation, 4,700 gal by flocculation and 700 gal by adsorption into vermiculite.

B. Gamma-Irradiation Facility

(H. G. Swope, J. Harast, D. Turner, J. Gates, R. Juvinall, N. Ondracek)

The number of samples irradiated during each of the three months and the total urn units are shown in Table 45.

Table 45

SAMPLES IRRADIATED DURING PERIOD JANUARY-MARCH, 1957

Month	No. of Samples[a]	Total Units[b]
January	886	2099
February	966	1957
March	849	2193
	2701	6249

[a]Equivalent to No. 2 can.

[b]Unit = 2×10^6 rep.

In addition to the above irradiations, three groups of samples were irradiated in the new rack which is 20 in. in diameter and 30 in. high (see ANL-5668, page 109, for a detailed description).